LBL-25834 c.2

Lawrence Berkeley Laboratory

UNIVERSITY OF CALIFORNIA

LIBRARY AND DOCUMENTS SECTION
BERKELEY LABORATORY
DEC 6 1988

Materials & Chemical Sciences Division

Electron Transfer in Bis([8]annulene)f-element Systems

D.C. Eisenberg
(Ph.D. Thesis)

August 1988

TWO-WEEK LOAN COPY

This is a Library Circulating Copy which may be borrowed for two weeks.

Prepared for the U.S. Department of Energy under Contract Number DE-AC03-76SF00098.

LBL-25834 c.2

DISCLAIMER

This document was prepared as an account of work sponsored by the United States Government. While this document is believed to contain correct information, neither the United States Government nor any agency thereof, nor the Regents of the University of California, nor any of their employees, makes any warranty, express or implied, or assumes any legal responsibility for the accuracy, completeness, or usefulness of any information, apparatus, product, or process disclosed, or represents that its use would not infringe privately owned rights. Reference herein to any specific commercial product, process, or service by its trade name, trademark, manufacturer, or otherwise, does not necessarily constitute or imply its endorsement, recommendation, or favoring by the United States Government or any agency thereof, or the Regents of the University of California. The views and opinions of authors expressed herein do not necessarily state or reflect those of the United States Government or any agency thereof or the Regents of the University of California.

LBL-25834

Electron Transfer in Bis([8]annulene)f-element Systems

David Charles Eisenberg
(Ph.D. Thesis)

Materials and Chemical Sciences Division
Lawrence Berkeley Laboratory
1 Cyclotron Road
Berkeley, California 94720

August 1988

This work was supported by the U.S. Department of Energy under Contract Number DE-AC03-76SF00098.

Electron Transfer in Bis([8]annulene)f-element Systems

David Charles Eisenberg

Abstract

The rate of electron exchange between potassium bis(*t*-butyl[8]-annulene)ytterbate(II) and potassium bis(*t*-butyl[8]annulene)-ytterbate(III) has been measured by NMR line broadening techniques: typical second order rate constants are 5×10^7 at 19.3 °C in tetrahydrofuran (THF), and 1×10^7 in THF containing diglyme. From the activation parameters a mechanism is proposed that involves change in coordination of diglyme from η^3 to η^1 type coordination.

Electron exchange studies have been extended to uranium, neptunium, and plutonium systems. This involved the first isolation and thorough characterization of the reduction product of uranocene. Bis(*t*-butyl[8]annulene) compounds were prepared for neptunium III and IV and for plutonium III and IV. The ^{1}H NMR spectra of all of these compounds are reported; bis([8]annulene)plutonium(IV) exhibits temperature independent paramagnetism, while all of the other compounds exhibit temperature dependent paramagnetism. In all of these systems electron exchange occurs on the ^{1}H NMR time scale. The ability or inability to freeze out the exchange in the different systems is consistent with the rate and mechanism observed in the ytterbium system.

The reduction of biuranocenylene is reported. Partial reduction

leads to preparation of a mixed valent (III-IV) compound which undergoes intermolecular exchange on the NMR time scale with biuranocenylene. Complete reduction produces a thermally unstable compound which has equivalent uranium atoms (III½-III½) on the NMR and electronic time scale.

X-ray crystal structures are reported for potassium bis([8]annulene)ytterbate(III) and potassium bis(methyl[8]annulene)uranate(III). Comparison of these structures with previously solved ytterbium(II) and uranium(IV) bis([8]annulene) structures allows for determination of the effect of oxidation state of the central metal on structure. Also, along with other recent structures of [8]annulene-f-element compounds, it is now possible to reexamine an ionic model, which was proposed by Raymond et. al. to explain bond lengths in organo-f-element compounds. It is proposed that the model must be modified in order to accurately predict metal carbon bond lengths in these structures.

Acknowledgements

I would first like to thank the many members of the Streitwieser group for their help and for their stimulating discussions about chemistry and various other topics. I would also like to thank the Actinide Group on the Hill, in particular Wing Kot and Rob Rosen.

Over the years I have had the help of many teachers to whom I am grateful, in particular my general chemistry teacher, Thomas Dunn, who inspired me to go on in chemistry, and my undergraduate research director, M. David Curtis, who put up with all the trials and tribulations of my undergraduate research. As for my teachers at Berkeley, I would particularly like to acknowledge the helpful discussions I have had with Professors Connick, Bergman, and Andersen, and of course Professor Streitwieser, for giving me the freedom to pursue areas that I thought were of interest, and for the guidance to understand the meaning of the results. I would also like to thank my committee for signing this thesis.

Most of all I would like to thank my parents for their love, support, and for the inspiration to learn.

Table of Contents

CHAPTER 1: INTRODUCTION

Perspective.....1

Early History of Electron Transfer.....4

Electron Transfer between Ferrocene and.....10
Ferricenium Cation

Biferrocene and Biferrocenylene.....13

Electron Transfer in f-Element Systems.....14

Divalent Organolanthanides.....15

Trivalent Uranium Compounds.....18

Transuranium Chemistry.....19

References.....22

CHAPTER 2: ELECTRON EXCHANGE BETWEEN POTASSIUM BIS([8]ANNULENE)YTTERBATE(II) AND POTASSIUM BIS([8]ANNULENE)YTTERBATE(III)

Introduction.....28

Electron Exchange.....31

Preparation of *t*-Butyl Analogues of.....34
Ytterbate(II) and (III)

Determination of the Rates and Mechanisms for.....35
Electron Exchange

Ion Pair Electron Transfer.....43

Experimental Section.....46

References.....49

Appendix.....50

CHAPTER 3: ELECTRON TRANSFER IN URANIUM AND TRANSURANIUM SYSTEMS

Introduction.....52

Preparation of Compounds.....55

Electron Exchange.....63

Magnetic Properties of Plutonium(IV) and Neptunium(III).....65

The Unidentified Uranocene Reduction Product.....68

Comments on Extension of Electron Transfer Work to Other Systems.....70

Experimental.....71

References.....75

CHAPTER 4: REDUCTION OF BIURANOCENYLENE

Introduction.....78

Synthesis of Compounds.....79

Reduction of Biuranocenylene.....81

Perspective on Biuranocenylene.....85

Experimental.....87

References.....91

CHAPTER 5: STRUCTURES OF ORGANO-F-ELEMENT COMPOUNDS DIFFERING IN THE OXIDATION STATE OF THE F-ELEMENT: CRYSTAL STRUCTURES OF BIS([8]ANNULENE) COMPLEXES OF YTTERBIUM(III) AND URANIUM(III)

Introduction.....92

Comparison of Structures.....95

Discussion of Ionic Bonding Model.....97

Experimental Section.....103

Appendix.....107

Chapter 1: Introduction

Perspective

In the twenty years since uranocene was first made[1] (Figure 1.1) a wide variety of bis([8]annulene) complexes of the lanthanides and actinides have been synthesized. These are the divalent complex of ytterbium;[2] trivalent complexes of uranium,[3] neptunium,[4] plutonium,[4] americium,[5] and all the lanthanides[6] except promethium, europium, and thulium; and tetravalent complexes of cerium,[7] thorium,[8] protactinium,[9] uranium,[1] neptunium,[10] and plutonium.[10] Substituted bis([8]annulene) complexes of many of theses metals have also been prepared such as alkyl, benzo, alkoxycarbonyl, dimethyl amino, cyclooctatetraenyl, and others.[11]

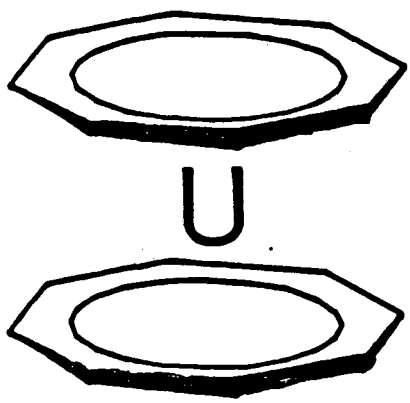

Figure 1.1: Uranocene

Extensive studies of the physical properties of these compounds (including NMR,[11] uv-vis, magnetic susceptibility, Mössbauer spectroscopy,[4,10] UV-photoelectron spectroscopy,[12] X-ray photoelectron spectroscopy (XPS),[13] X-ray crystallography,[14] and semiempirical

calculations)[15] have been performed, aided by the high symmetry of the molecules. In the case of uranocene itself, these studies have focussed on determining the degree of covalency in the metal ligand bonding. The Mössbauer studies of neptunocene and its reduction product and the XPS studies of uranocene have been the best evidence thus far of extensive covalent interaction in these systems with the actinide (IV) compounds being significantly more covalent than the actinide (III) systems.

Although these bis([8]annulene)f-element systems have been amenable to extensive study of their physical properties, investigation of the reaction chemistry have been much more limited, due to both the thermodynamic stability of these compounds (in the absence of oxygen) and to the steric constraints involved in getting an incoming ligand between the bulky COT rings. The primary reactions that had been studied are the hydrolysis of uranocene, studied by Bob Moore,[16] and the reaction of uranocene with alkyl and aryl nitro compounds producing their respective azo compounds.[17] In both of these reactions the uranium product is uranium oxide.

Several of the lanthanides and perhaps all of the actinides (*vide infra*) have more than one oxidation state available and in principle one mode of reaction that might occur with these compounds which would not be prevented by steric constraints is electron transfer. This mode of reaction was indeed found to occur in these systems and it is the central topic of this thesis. The initial example discovered is the exchange between potassium bis([8]annulene)ytterbate(II) and potassium bis([8]annulene)ytterbate(III), first investigated by Steve Kinsley.[3b] He was able to prove that the observed exchange was electron exchange

rather than ligand exchange.

My problem was then to determined the rate and mechanism of the reaction; this work is described in the second chapter of this thesis. Attempts were then made to extend this work to actinide systems by preparing the uranocene reduction product as well as bis([8]annulene) complexes of neptunium (III) and (IV) and plutonium (III) and (IV) to determine if electron transfer occurred in these systems; this work is described in the third chapter of this thesis, while the fourth chapter describes the extension of this work to a dimetallic system capable of intramolecular electron transfer, biuranocenylene. The fifth chapter compares the structures of some of these compounds with an attempt to see what changes in structure occur when the oxidation state changes and whether the structures fit an ionic bonding model.

This introduction continues with a brief history of studies of electron transfer reactions highlighting the work of Taube, Marcus and Hush. Wahl's NMR studies on electron transfer in the ferrocene-ferricenium ion system, which were the initial basis for the analysis for electron transfer in the ytterbium system, are next described, followed by studies of electron exchange in dimeric ferrocene systems.

As the study of electron transfer in these f-element systems has necessitated the use of metals in uncommon oxidation states and uncommon metals this chapter concludes with a review of organo-f-element chemistry of divalent lanthanides, trivalent uranium compounds, and transuranium systems.

Early History of Electron Transfer

The systematic study of electron transfer probably began with Henry Taube's classic studies in the early 1950's.[18] Before his work it was known that there are systems in which outer sphere electron transfer occurs but it was only hypothesized that inner sphere electron transfer, "in which oxidant and reductant metal centers are linked through primary bonds to a bridging group," occurs. In pioneering studies which were aided by the then recent advent of synthetic radioactive tracers and which he did by himself (he was unable to convince his graduate students to work on the project) he was able to demonstrate that transfer between pentaamminecobalt(III) chloride and hexaaquachromium(II) occurs through a bridging chloride ligand.[19] The significance in the difference between innersphere and outer sphere electron transfer was later demonstrated by huge rate differences. For example, the transfer from hexaaquochromium(II) to pentaamine-cobalt(III) chloride, which takes place through an inner sphere mechanism is eight orders of magnitude faster than the outer sphere transfer from chromium(II) to hexaaminecobalt(III).[20] Years later Taube revived the interest in intramolecular electron transfer with the preparation of the Creutz-Taube compound (figure 1.2).[21] This

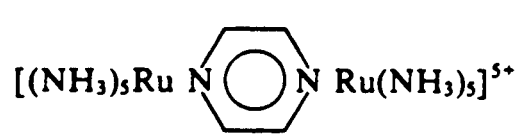

Figure 1.2

was the first stable mixed valence compound and has been the subject of extensive study to determine if it is valence localized or delocalized on the electronic time scale.

The systematic study of outer sphere electron transfer was spurred by Marcus' articles[22] beginning in 1956 on the theory of electron transfer "involving no rupture or formation of chemical bonds in the elementary electron transfer step." Up until that time it had been assumed that the limited electronic interaction between donor and acceptor would be the rate limiting step, but Marcus assumed instead that "only a slight electronic interaction may be sufficient to electronically couple the two molecules and permit the electron transfer." Marcus stated that there are two barriers to electron transfer: a thermodynamic part arising from the overall free energy change in the reaction and a kinetic part resulting from solvent and bond reorganization, and he assumed that transfer was adiabatic; that is, given the correct solvent and bonding configuration transfer would always occur. An expression was derived that related the rate of exchange to the free energy change of the reaction as well as the solvent dielectric properties, the size of donor and acceptor, the work necessary to bring reactants and products together and the change in bond distances between reactants and products (Equation 1-9)

1. $k = \rho\kappa Z \exp-(G^{*}/RT)$
2. $G^{*} = w + m^{2}\lambda$
3. $\lambda = \lambda_{o} + \lambda_{i}$
4. $m = -\{1/2 + (\Delta G^{o} + w_{p} - w)/2\lambda\}$
5. $m = -1/2$

6. $\lambda_0 = \{1/(2a_1) + 1/(2a_2) - 1/r\}(1/D_{op} - 1/D_s)(n_e)^2$

7. $\lambda_i = \Sigma(k_j k_{jp})/(k_j + K_{jp})(\Delta q_j)^2$

8. $k_{12} \approx (k_{11}k_{22}K_{12}f)^{1/2}$

9. $\ln f = (\ln K_{12})^2/\{4\ln(k_{11}k_{22}/Z^2)\}$

Equation 1 relates the rate constant k to the product of ρ, the nuclear tunneling factor generally assumed to be near unity, κ, the adiabadicity factor also assumed to be near unity, Z, the collision number which is generally taken to be about 10^{11}, and the last term where G^* is defined by equation 2. In equation 2, w is the work needed to bring the reactants together, λ is the reorganization term defined in equation 3 as the sum of the solvent reorganization term, λ_o, and the innersphere bond reorganization term, λ_i, and m is defined in equation 4. In equation 4, ΔG^o is the free energy change in the reaction and w_p is the work needed to bring the products together. In the case of homogenous electron transfer equation 4 simplifies to equation 5. In Equation 6, a_1 and a_2 are the radii of the spherical reactants and their sum equals the distance between reacting metal centers r, D_{op} is the square of the refractive index, D_s is the static dielectric constant, and n_e is the number of electrons transferred. Equation 7 defines the innersphere reorganizational factor in terms of the force constants of the appropriate vibrational coordinates for the reactants, k_j, and the products, k_{jp}, and the bond length change Δq_j. Equations 8 and 9 relate the rate of a cross reaction k_{12} to the rates of the homogenous reactions k_{11} and k_{22} and to the equilibrium constant for the cross reaction K_{12}. These equations predict that the rate of exchange will increase with thermodynamic driving force up to

a point when the inverted region is reached and the rate of exchange gets slower with increasing thermodynamic driving force.

This can be seen in Figure 1.3. This is a diagram of atomic configuration vs energy, where the atomic configuration represents all changes in bond distances and angles involved in conversion of reactants to the products, as for example metal ligand distances, solvent positions, and counterion positions. As the bond lengths and angles of the reactants change so that they more closely resemble those of the products they can be thought of as moving up the R curve toward the P curve. If there is sufficient overlap between the reactants, when the intersection region of the curves is reached, that is, when the bond lengths, angles, solvent position etc. become more like those of the products than those of the reactants, electron transfer will occur, and the reaction is adiabatic. If there is insufficient overlap, the reactants will stay on the R curve and no transfer will occur.

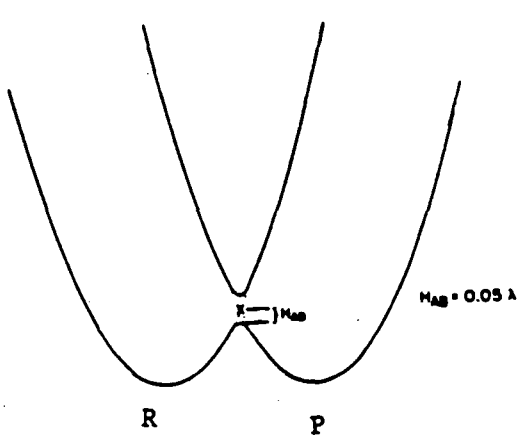

Figure 1.3

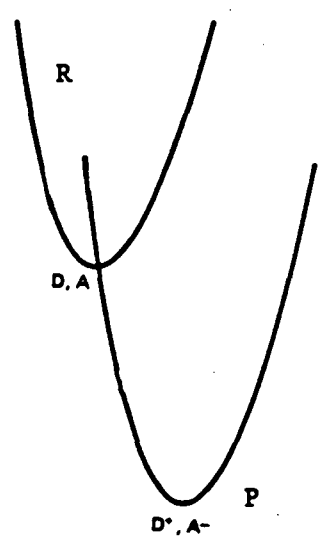

Figure 1.4

As the R curve is raised with respect to the P curve (as the thermodynamic driving force increases) the rate of transfer will increase until the curves become as they are shown in Figure 1.4. At this stage the rate of reaction will get slower for increasing thermodynamic driving force, the so-called inverted region. The prediction of the inverted region was the most unexpected aspect of Marcus theory. Numerous attempts have been made to detect this region experimentally with as yet minimal success. With respect to other predictions of Marcus theory, absolute rates are generally predicted within an order of magnitude of the experimental findings which Marcus believes is reasonably successful given the huge span in rates found in electron transfer reactions,[23] although this degree of accuracy does argue against using some of the recent "improvements" in the theory which make it more complicated, for example dropping the assumption of spherical reactants. The predictions of relative rates and the use of the cross reaction equation have been more successful.

Systematic studies of intramolecular electron transfer began with reviews by Robin and Day,[24] and Allen and Hush[25] of the physical properties of mixed valent compounds. Robin and Day categorized these compounds into three types. In class I compounds only a weak interaction occurs between the two centers in different oxidation states and the properties of the molecule essentially equal the sum of the properties of these centers. In class II systems there is a moderate interaction and new properties emerge which are not simply the sum of the two centers. In class III molecules there is a strong interaction and the two centers are equivalent on any time scale.

At the same time Hush[26] provided a theoretical framework for mixed

valent compounds and derived equations from which the relation between optical and thermal electron transfer could be predicted as well as the effects of solvent and the linewidth of the intervalence transfer band.

$$11.\ E_{op} \approx 4\Delta G^{*}_{th}$$

$$12.\ \Delta\upsilon_{\frac{1}{2}} = (2310\ \upsilon_{max})^{\frac{1}{2}} cm^{-1}$$

Equation 11 is illustrated in Figure 1.5 which shows how the energy of optical intermolecular electron transfer relates to thermal electron transfer. The halfwidth of the optical resonance, also called the intervalence transfer band, is related to its energy in equation 12.

Soon after the publication of the papers of Robin and Day and Hush the Creutz-Taube ion was isolated and its electronic properties were explained by using Hush's equations. The mixed valence biferrocenium salt was isolated shortly thereafter and its properties as well as the intermolecular exchange between ferrocene and ferricenium cation are described in the next two sections.

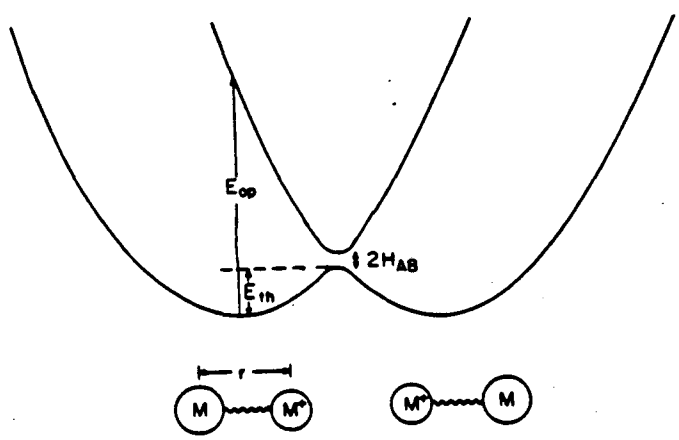

Figure 1.5: Potential energy versus nuclear configuration for a symmetric mixed valence complex

Electron Transfer between Ferrocene and Ferricenium Cation

The most thoroughly studied system involving electron transfer of organometallic sandwich compounds is the ferrocene-ferricenium ion system, studied by Wahl, Chan, and others in Wahl's group.[27] The work began with the idea of looking at electron transfer in systems in which the structure of the compounds are the same in both oxidation states to minimize Franck-Condon factors, and in which there would be no coulombic repulsion between the compounds. Also with the large, polarizable counter ions and the polar solvents that were used, the ferricenium cations were expected to exist as free ions in solution (this assumption was later found to be primarily correct in all solvents except CH_2Cl_2, CH_2ClCH_2Cl, and to a small degree CH_3OH). Taken together these facts should facilitate the testing of Marcus theory in these systems with solvent reorganization being the main barrier to electron transfer.

Rates of exchange were determined by the NMR line broadening using the following formula:

$$W_{dp} = f_p W_p + f_d W_d + f_p f_d 4\pi(\delta\nu)^2/kc$$

where W_{dp}, W_p, and W_d represent the linewidth of the exchanging species and W_p and W_d represent the natural linewidths of the paramagnetic and diamagnetic species respectively, f_p and f_d are the mole fractions of the paramagnetic and diamagnetic species, $\delta\nu$ is the separation in Hz between the diamagnetic resonance and the paramagnetic resonance, k is the second order rate constant, and c is the

concentration in moles per liter.

This equation is a simplification of the general line shape equation derived by Gutowski, McCall, and Slichter,[28] and McConnell[29] (the derivation is well described in Pople, Schneider, and Bernstein)[30] which is appropriate for studying two site exchange with no overall free energy change in the near fast exchange region. Different simplifications are used in the fast and slow exchange regions, with the full equation being necessary in the intermediate exchange region.

A variety of substituted ferrocenes were measured with the solvents, counterions, and ionic strengths also varying. It was found that the reaction is second order and typical rates are on the order of $5 \times 10^6\ M^{-1}\ s^{-1}$. Several trends were found to go against Marcus theory predictions: for example, it was found that excess KPF_6 or $KClO_4$ has only a small effect on the rate and no effect on the rate of the positively charged trimethylammonium substituted ferrocene in contrast to predictions of Marcus theory. Also, the rate constant did not vary with dielectric concentration, in contrast to predictions, and the rate for transfer involving the trimethylammonium substituted ferrocene was only about 5 times slower than the rate of the unsubstituted system compared with a factor of 60 predicted by Marcus theory. Temperature effects were also found to be smaller than predicted.

In Table 1.1 rates of exchange are listed for different substitutions; notice that the fastest exchanging ferrocene is permethylferrocene and the slowest is the trimethylammonium substituted ferrocene. Although slow it is over an order of magnitude faster than

predicted by Marcus equation. Rates of exchange are also listed for different solvents in Table 1.2 along with theoretical predictions. They do not match.

Table 1.1

Rate of Electron Exchange in CD_3CN at 25 °C

	10^{-6} k sec^{-1}
Fe $(Cp)_2$	5.3 ± 0.8
Fe $(Cp\text{-}CH_3)_2$	8.3 ± 0.8
Fe $(Cp\text{-}(CH_2)_3\text{-}Cp)$	14.6 ± 10.7
Fe $(Cp\text{-}(CH_3)_5)_2$	38 ± 4
Fe $(Cp,\ Cp\text{-}CH_2N(CH_3)_3^+)$	1.8 ± 0.16

Table 1.2

Effect of Solvent on Rates of Exchange

	k expt x 10^{-6}	k theory[a] x 10^{-6}
CH_3OH	6.0 ± 0.5	3.5
CH_3CN	5.3 ± 0.8	3
CH_3NO_3	5.8 ± 0.5	5
$(CH_3)_2CO$	4.6 ± 0.3	4.5
$(CH_3)_2SO$	1.6 ± 0.6	15
$C_6H_5NO_2$	2.3 ± 0.2	45
$(CH_2Cl)_2$	4.3 ± 0.4	50
CH_2Cl_2	4.3 ± 0.3	50
CH_3COOH	7.0 ± 2.5	60

(a) k theory calculated from listed free energy of activation[27c]

Wahl and Chan proposed as an explanation for the lack of rate dependence on solvent properties that their assumption of solvent reorganization as the main barrier to exchange was wrong;[27d] if the activation energy for solvent reorganization is near zero there would be little expected solvent dependence on the rate. This however leaves

the question of what the barrier to electron exchange actually is. Their theory is that "the necessity for redistribution of charge during electron exchange .... because of the different orders of molecular orbitals, could be a deterrent to electron exchange and might account for the observed negative values of S, an indication that the transmission coefficient, κ, is less than unity."

Biferrocene and Biferrocenylene

Studies of exchange in the ferrocene system were extended to dimetallic systems by Cowan and coworkers in 1970 when they prepared biferrocenium cation[31] (Figure 1.6), which was also the second mixed valent compound isolated (after the Creutz-Taube ion). It was found to be valence delocalized on the NMR time scale but valence localized on the Mössbauer time scale, or, using the terminology of Robin and Day, it was a class II compound. Two years later, biferrocenylene (figure 1.7) cation was isolated[32] and it was found to be valence delocalized, or a class III compound.

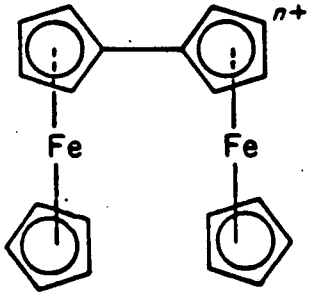

Figure 1.6

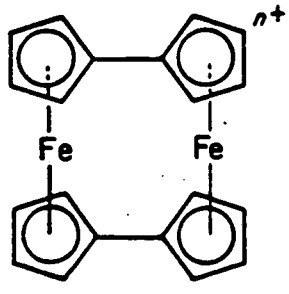

Figure 1.7

These compounds were made in the hopes that they would have interesting electrical properties and serve as models for studying biological mixed valent compounds. Many similar compounds have been prepared, such as ferrocenophanes, and substituted forms of biferrocene. A particularly interesting one is 1′,6′-diiodobiferrocene[33] which is valence delocalized in solution but is sometimes valence localized in the solid state depending on temperature and counterion.

Electron Transfer in f-Element Systems

There are not many studies of electron transfer in f-element systems and very few in organo-f-element systems. Tendler and Farragi studied the pulse radiolysis stimulated electron transfer of all of the lanthanides in water and were able to correlate the rates with thermodynamic driving force.[34] Espenson *et. al.* measured rates of electron transfer between divalent complexes of ytterbium and samarium and some transition metal systems also in water.[35]

The main studies of organo-f-element electron transfer are the studies of innersphere electron transfer involving cyclopentadienyl and tris(trimethylsilyl)amido complexes of ytterbium and uranium studied by Andersen and coworkers.[36] They have also prepared mixed valent compounds by treating tris(cyclopentadienyl)uranium(III) with tris(cyclopentadienyl)uranium(IV) fluoride to prepare the mixed valent (III-IV) fluorine bridged compound;[37] a mixed valent bridging methyl compound has also been prepared[38] as well as a mixed valent fluorine bridging ytterbium(II-III) compound.[39]

Our electron transfer studies have necessitated the use of f-

elements in uncommon oxidation states, in particular divalent lanthanides and trivalent uranium, and the use of some transuranium compounds. Therefore it is appropriate at this time to briefly summarize the organometallic chemistry of these compounds with an emphasis on previous bis([8]annulene) studies.

Divalent Organo-Lanthanides

The preferred oxidation state of the lanthanides is the trivalent state, although there are many tetravalent cerium and divalent samarium, europium, and ytterbium compounds. The standard reduction potentials for all the trivalent lanthanide are listed below (Table 1.3).[40] The two most stable divalent ions are the half filled f-shell europium and filled f-shell (and hence diamagnetic) ytterbium.

Table 1.3

Lanthanide III/II E^o

	E^o		E^o
Ce	-2.92	Tb	-2.83
Pr	-2.84	Dy	-2.56
Nd	-2.62	Ho	-2.79
Pm	-2.44	Er	-2.87
Sm	-1.50	Tm	-2.22
Eu	-0.34	Yb	-1.18
Gd	-2.85	Lu	unknown

Trends in the potential are best interpreted in terms of the tetraad effect.[41]

The divalent lanthanides particularly of europium and ytterbium

strongly resemble the alkaline earth compounds in that they form only ionic compounds (for example, the Mössbauer shift of $EuCp_2$ is -1.32 compared to -1.34 for $EuCl_2$),[42] the metals are soluble in liquid ammonia, and europium and strontium and ytterbium and calcium have similar ionic radii. Some data are summarized in Table 1.4.

Table 1.4

Metal	Ionic Radius[a] Å	Ionization Potential,[b] eV 1st	2nd	M/MII E^o
Eu	1.39	5.67	11.25	-3.44[c]
Sr	1.40	5.70	11.03	-2.91
Yb	1.28	6.25	12.17	-2.80[c]
Ca	1.26	6.11	11.87	-2.86

(a) ref. 43. (b) ref. 44. (c) calculated from M(III)/M(II) and M/M(III) couples from reference 45.

Although divalent lanthanides have found extensive use as reducing agents, there has been limited work on their organometallic chemistry. The primary studies of divalent organolanthanide compounds involves the Cp compounds. Originally synthesized by Fischer[42] in liquid ammonia, the bis Cp compounds of europium and ytterbium were found to be isostructural with the bis Cp compounds of strontium and calcium. More recently, extensive work has been done by Andersen's group[46] and Evans' group[47] on compounds of the divalent lanthanides with bulkier cyclopentadienyl compounds; in particular, the bis pentamethyl Cp compounds of samarium, europium, ytterbium, calcium, strontium, and barium have been made. Surprisingly, the rings in these compounds are not in parallel planes (Figure 1.8). The large opening afforded by the

bent rings greatly facilitates coordination of weak ligands. Thus, a wide variety of Lewis bases have been coordinated to these compounds including various phosphines, isocyanides, acetylene, and even methane. These compounds also polymerize ethylene and isomerize allenes to acetylenes.[39]

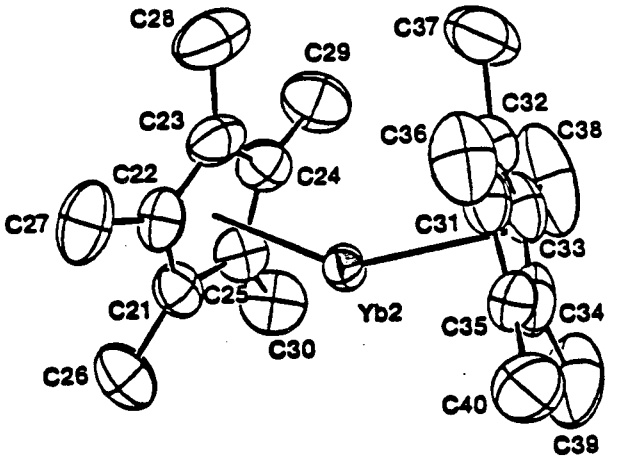

Figure 1.8: ORTEP Diagram of $(Me_5C_5)_2Yb$[39]

Synthesis of divalent COT lanthanides began with work by Hayes and Thomas[48]:

$$COT + M \longrightarrow MCOT \qquad M = Eu, Yb.$$

These compounds are pyrophoric powders which are insoluble in hydrocarbon solvent but soluble in ether solvents. The synthesis of a divalent cerium compound was reported by Greco *et. al.*[7a] The preparation involved potassium reduction in DME of the cerate (III). The characterization was less than unambiguous and attempts by our group to repeat this preparation, either by the reported method or in the presence of catalytic naphthalene produced only cerium metal and COT dianion.

The bis([8]annulene)lanthanide(III) compounds can be prepared by reaction of the lanthanide trichloride with COT dianion in THF or

glyme. Thus, all of the bis COT lanthanide III compounds except those of promethium, europium, and thulium have been made.

Trivalent Uranium Compounds

The tetravalent state is the favored oxidation state for uranium, but the trivalent state is generally also stable in the absence of an oxidizing agent, its oxidation in aqueous solution being favored by 0.6 V. Trivalent organouranium chemistry is primarily the chemistry of triscyclopentadienyl and tris{tris(trimethylsilyl)amido}uranium compounds, again primarily studied by Andersen's group.[49]

The tris-amido compound can be prepared by reaction of uranium trichloride with an alkali metal salt of the amide, or by reducing the tetravalent tris-amide monochloride uranium complex. It forms adducts with such Lewis bases as pyridines, isocyanides, phosphine oxides, and nitriles. The amido compounds can also be alkylated or fluorinated with silver fluoride to form uranium(IV) compounds or reacted with organic azides to form uranium(V) imides.[50]

The tris-Cp compounds are prepared from UCl_3 and an alkali metal cyclopentadienyl salt. These compounds have been prepared for a variety of Cp's including methyl, trimethylsilyl, and bis-trimethylsilyl. Base adducts have been formed using such bases as cyanides, isocyanides, pyridines, phosphines, phosphites, and carbon monoxide. The relative coordination strengths of many of these bases have been determined and from a comparison of these relative values to those obtained from a similar study involving tris Cp cerium (III) evidence was obtained indicating that back donation from the trivalent metal to

π-accepting ligands does occur with uranium but not with cerium.[51]

Transuranium chemistry

Whereas in the lanthanides the most important trend is the lanthanide contraction, the most important trend in the chemistry of actinides is probably the increasing stability of the lower oxidation states along the series, with the exception of berkelium (due to the half filled effect). Thorium exists almost entirely in the tetravalent state; the oxidation state preferences for the other actinides are listed in Table 1.5.[52]

Table 1.5

	M V/IV E^o	M IV/III E^o	M III/II E^o
Protactinium	-0.1		
Uranium	disp.	-0.61	
Neptunium	1.25, 1.14	0.16	
Plutonium	disp.	0.93, 0.98	
Americium		2.18, 2.34	
Curium		3.1	
Berkelium		1.6	
Californium			-1.6
Einsteinium			-1.2
Fermium			
Mendelevium			-0.15
Nobelium			1.45

disp = disproportionates in aqueous solution

Organoactinide chemistry is primarily organo-thorium and organo-uranium chemistry, the chemistry of the other actinides being very

brief in comparison. This is because uranium-238 (half-life 4.5×10^9 yrs.) and thorium-232 (half-life 1.4×10^{10} yrs.) are the only readily available low radiation nuclei. Despite the difficulty in working with other actinides, bis([8]annulene) compounds of protactinium, neptunium,[4,10] plutonium,[4,10] and americium have been reported.

Protactinium may be the most dangerous of the actinides. The major isotope of protactinium is Pa-231 which is an alpha emitter and has a half-life of 32,500 years. Protactinium is an extreme exposure hazard due to its particularly harmful daughter nuclei which undergo the radium decay chain. Its chemistry is probably the most unusual and least tractable of the actinides bearing some resemblance to that of niobium and tantalum. Two bis([8]annulene) compounds of protactinium, bis([8]annulene)protactinium(IV) and bis(tetramethyl[8]annulene)protactinium(IV) have been made.[9,10b] Protactinocene itself was prepared in trace amounts by reaction of $PaCl_4$ and potassium or cyclooctatetraene dianion, followed by sublimation or toluene extraction, and characterized by comparison of its powder pattern and IR spectrum to those of uranocene. The bis-tetramethyl protactinocene was prepared by reaction of protactinium tetrachloride and potassium tetramethyl-COT dianion and purified by THF extraction and characterized by powder pattern and visible absorption.

Neptunium and plutonium are the easiest transuranium compounds to work with. The most common isotope of neptunium, ^{237}Np is an alpha emitter with a half-life of 2,140,000 years, and the most common isotope of plutonium is plutonium-239 which has a half-life of 24,000 years and is used in nuclear weapons and reactors. Plutonium-242, which is an alpha emitter and has a half life of 379,000 years, is

more commonly used to study reaction chemistry, although ^{244}Pu is actually the longest lived isotope of plutonium, having a half-life of 80,000,000 years, but it is extremely rare and the world's supply is approximately 1.5 grams. Being alpha emitters both ^{237}Np and ^{242}Pu are ingestion, rather than exposure hazards in small quantities. Plutonium is particularly dangerous in this regard because once inside the body plutonium(IV) mimics iron(III) and is transported by ferritin to the bone marrow where it remains and can do the most damage.[53] Bis([8]annulene) compounds of neptunium and plutonium have been prepared and will be discussed in chapter three.

[8]Annulene "half sandwich" compounds of neptunium and plutonium have been obtained with the other ligands being borohydrides by reaction of the tetrakis-borohydride with COT dianion:[54]

$$Pu(BH_4)_4 + K_2BuCOT \xrightarrow[THF]{} (BuCOT)Pu(BH_4)_2(THF)_x$$

This reaction also works for thorium, but when a cyclooctatetraene dianion is added to the uranium borohydride, uranocene is obtained. It was reported that addition of one equivalent of $BuCOT^{-2}$ to the previously mentioned plutonium half sandwich compound produced 1,1'-dibutylplutonocene; however, the reported ^1H NMR spectra strongly indicate the product was the reduction product of 1,1'-dibutylplutonocene.

Americium-241, which has a half-life of 458 years, is the only form of the element with a practical application; it is used for smoke detectors. Americium-243 is more frequently used for reaction chemistry; it has a half life of 7370 years and is a major gamma emitter which precludes using more than 10 mg of the material in a given reaction. Potassium bis([8]annulene)americium(III)[5] has been

prepared by reaction of AmI_3 with K_2COT_2 and characterized less than unambiguously by its uv-vis. It was reported that attempts at reduction to prepare the divalent americium compound failed.

References

1. Streitwieser, A., Jr.; Muller-Westerhoff, U. *J. Am. Chem. Soc.* **1968**, *90*, 7364.

2. Kinsley, S. A.; Streitwieser, A., Jr.; Zalkin, A. *Organometal.* **1985**, *4*, 52.

3. (a) Billian, F.; Folcher, G.; Marquet-Ellis, H.; Rigney, P.; Saito, E. *J. Am. Chem. Soc.* **1981**, *103*, 5603. (b) Eisenberg, D. C.; Streitwieser, A., Jr.; Kot, W. To be submitted for publication to *Organometal.*

4. Karraker, D. G.; Stone, J. A. *J. Am. Chem. Soc.* **1974**, *96*, 6885.

5. Karraker, D. G. *J. Inorg. Nucl. Chem.* **1977**, *39*, 87.

6. (a) Hodgson, K.; Mares, F.; Starks, D.; Streitwieser, A., Jr. *J. Am. Chem. Soc.* **1973**, *95*, 8450. (b)

7. (a) Greco, A.; Cesca, S.; Bertolini, G. *J. Organometal. Chem.* **1976**, *113*, 321. (b) Streitwieser, A., Jr.; Kinsley, S. A.; Rigsbee, J. T.; Fragala, I. L.; Ciliberto, E.; Rösch, N. *J. Am. Chem. Soc.* **1985**, *107*, 7786. (c) Rigsbee, J. T.; Streitwieser, A., Jr. To be submitted for publication to *J. Am. Chem. Soc.*

8. Streitwieser, A., Jr.; Yoshica, N. *J. Am. Chem. Soc.* **1969**, *91*,

7528.

9. (a) Starks, D. F.; Parsons, T. C.; Streitwieser, A., Jr.; Edelstein, N. *Inorg. Chem.* **1974**, *13*, 1307. (b) Goffart, F.; Fuger, J.; Brown, D.; Dayckaerts, G. *Inorg. Nucl. Chem. Lett.* **1974**, *10*, 413.

10 (a) Karraker, D. G.; Stone, J. A.; Jones, E. R., Jr.; Edelstein, N. *J. Am. Chem. Soc.* **1970**, *92*, 4841. (b) Solar, J. P.; Burghard, H. P. G.; Banks, R. H.; Streitwieser, A., Jr.; Brown, D. *Inorg. Chem.* **1980**, *19*, 2186.

11. Luke, W. Ph. D. Thesis, University of California, Berkeley, **1980**.

12. Green, J. C.; Payne, M. P.; Streitwieser, A., Jr. *Organometal.* **1983**, *2*, 1707.

13. 13. Beach, D. B.; Bomben, K. D.; Edelstein, N. M.; Eisenberg, D. C.; Jolly, W. L.; Shinomoto, R.; Streitwieser, A., Jr. *Inorg. Chem.* **1986**, *25*, 1735.

14. (a) Zalkin, A.; Raymond, K. N. *J. Am. Chem. Soc.* **1969**, *91*, 5667. (b) Ardeef, A.; Raymond, K. N.; Hodgson, K. O.; Zalkin, A. *Inorg. Chem.* **1972**, *11*, 1083.

15. (a) Rösch, N.; Strietwieser, A., Jr. *J. Am. Chem. Soc.* **1983**, *105*, 7237. (b) Rösch, N. *Inorg. Chim. Acta* **1984**, *94*, 297.

16. Moore, B. Ph.D. Thesis, University of California, Berkeley, **1985**.

17. Grant, C. B.; Streitwieser, A., Jr. *J. Am. Chem. Soc.* **1978**, *100*, 2435.

18. Taube, H. *Science*. **1984**, *30*, 1028.

19. (a) Taube, H.; Myers, H.; Rich, R. L. *J. Am. Chem. Soc*. **1953**, *75*, 4118. (b) Taube, H.; Myers, H. *J. Am Chem. Soc*. **1954**, *26*, 2103.

20. Zwickel, A. M.; Taube, H. *J. Am. Chem. Soc*. **1959**, *81*, 2915.

21. (a) Creutz, C.; Taube, H. *J. Am. Chem. Soc*. **1969**, *91*, 3988. (b) Creutz, C.; Taube, H. *J. Am. Chem. Soc*. **1973**, *95*, 1086.

22. (a) Marcus, R. A. *J. Chem. Phys*. **1956**, *24*, 966. (b) Marcus, R. A. *J. Chem. Phys*. **1957**, *26*, 867. (c) Marcus, R. A. *J. Phys. Chem*. **1963**, *67*, 853.

23. Marcus, R. A. *J. Chem. Phys*. **1965**, *43*, 679.

24. Robin, M. B.; Day, P. *Adv. Inorg. Chem. Radiochem*. **1967**, *10*, 247.

25. Allen, G. C.; Hush, N. S. *Prog. Inorg. Chem*. **1967**, *8*, 356.

26. Hush, N. S. *Prog. Inorg. Chem*. **1967**, *8*, 391.

27. (a) Chan, M. S.; DeRoos, J. B.; Wahl, A. C. *J. Phys. Chem*. **1973**, *77*, 2163. (b) Yang, E. S.; Chan, M. S.; Wahl, A. C. *J. Phys. Chem*. **1975**, *79*, 2049. (c) Yang, E. S.; Chan, M. S.; Wahl, A. C. *J. Phys. Chem*. **1980**, *84*, 3094. (d) Chan, M. S.; Wahl, A. C. *J. Phys. Chem*. **1982**, *86*, 126.

28. Gutowsky, H. S.; McCall, D. W.; Slichter, C. P. *J. Chem. Phys*. **1953**, *21*, 279.

29. McConnell, H. M. *J. Chem. Phys*. **1958**, *28*, 430.

30. Pople, J. A.; Schneider, W. G.; Bernstern, H. J. "High-Resolution Nuclear Magnetic Resonance." McGraw-Hill, New York, 1959.

31. Cowan, D. O.; Kaufman, F. *J. Am. Chem. Soc.* **1970**, *92*, 219.

32. Cowan, D. O.; LeVanda, C. *J. Am. Chem. Soc.* **1972**, *94*, 9271.

33. (a) Morrison, W. H., Jr.; Hendrickson, D. N. *Inorg. Chem.* **1975**, *14*, 2331. (b) Dong, T. Y.; Hendrickson, D. N.; Pierpont, C. G.; Moore, M. F. *J. Am. Chem. Soc.* **1986**, *108*, 963.

34. Christensen, R. J.; Espenson, J. H. *Chem. Comm.* **1970**, 756.

35. (a) Faraggi, M.; Tendler, Y. *J. Chem. Phys.* **1972**, *56*, 3287. (b) Tendler, Y.; Faraggi, M. *J. Chem. Phys.* **1972**, *57*, 1358.

36. Brennan, J. G.; Andersen, R. A. *J. Am. Chem. Soc.* **1985**, *107*, 514.

37. Brennan, J. G. Ph.D. Thesis, University of California, Berkeley, **1985**.

38. Stults, S. D.; Andersen, R. A.; Zalkin, A. Manuscript in preparation.

39. Burns, C. Ph.D. Thesis, University of California, Berkeley, 1987.

40. Mikheev, N. B. *Inorg. Chim. Acta.* **1984**, *94*, 241.

41. Spitsyn, V. I.; Vokhmin, V. G.; Ionova, G. V. *Inter. Rev. Phys. Chem.* **1985**, *4*, 57.

42. (a) Fischer, E. O.; Fischer, H. *Angew. Chem. Int. Ed. Eng.* **1964**, *3*, 132. (b) Fischer, E. O.; Fischer, H. *J. Organometal. Chem.*

1965, *3*, 181.

43. Shannon, R. D. Acta Crystal. 1976, A32, 751.

44. Weast, R. C. "CRC Handbook of Chemistry and Physics" 60th Ed. CRC Press, Boca Raton, Florida, 1980.

45. Huheey, J. "Inorganic Chemistry," 2nd. Ed., Harper and Row, New York, 1978.

46. (a) Burns, C. J.; Andersen R. A. *J. Am. Chem. Soc.* 1987, *109*, 915. (b) Burns, C. J.; Andersen R. A. *J. Am. Chem. Soc.* 1987, *109*, 941. (c) Burns, C. J.; Andersen R. A. *J. Am. Chem. Soc.* 1987, *109*, 5853.

47. Evans, W. S.; Hughes, L. A.; Hanusa, T. P. *Organometallics* 1986, *5*, 1285.

48. Hayes, R. G.; Thomas, J. L. *J. Am. Chem. Soc.* 1969, *91*, 6876.

49. (a) Kanellakopulos, B.; Fischer, E. O.; Dornberger, E.; Baumgartner, F. *J. Organomet. Chem.* 1970, *24*, 507. (b) Wasserman, H. J.; Zozulin, A. J.; Moody, D. C.; Ryan, R. R.; Salazar, K. V. *J. Organomet. Chem.* 1983, *254*, 305. (c) Stults, S. D.; Zalkin, A. *Acta Cryst.* 1985, *C41*, 1038. (d) Stewart, J. L. Ph.D. Thesis, University of California, Berkeley, 1988.

50. Stults, S. D. Ph.D. Thesis, University of California, Berkeley, 1988.

51. (a) Brennan, J. G.; Stults, S. D.; Andersen, R. A.; Zalkin, A. *Organometallics* 1988,*7*, 1329. (b) Brennan, J. G.; Stults, S. D.;

Andersen, R. A.; Zalkin, A. *Inorg. Chim. Acta* **1987**, *139*, 201.

52. Nugeng, L. J.; Baybarz, R. D.; Burnett, J. L.; Ryan, J. L. *J. Phys. Chem.* **1973**, *77*, 1528.

53. Personal Communication with K. N. Raymond

54. Solar, J. P.; Streitwieser, A., Jr. in "Lanthanide and Actinide Chemistry and Spectroscopy," ACS Symposium Series, Washington, D. C., **1980**.

Chapter 2: Electron Exchange between Potassium Bis([8]annulene)ytterbate(II) and Potassium Bis([8]annulene)ytterbate(III)

Introduction

Steve Kinsley prepared potassium bis([8]annulene)ytterbate(II) and potassium bis([8]annulene)calcate(II)[1] in order to compare the two compounds and determine if there was any evidence of covalency in the bonding of the ytterbate compound. The compounds were prepared in liquid ammonia in the presence of THF (the THF is needed to dissolve the COT which is a solid at liquid ammonia temperature):

$$M + 2\ COT + 2K \xrightarrow[NH_3,\ THF]{} K_2MCOT_2 \quad M = Ca, Yb$$

The products were produced in high yield and found to be quite similar, having clearly similar powder patterns (Table 2.1), the same IR spectrum (Figure 2.1), the same NMR chemical shift of 5.5 ppm (ytterbium(II) is f_{14} and diamagnetic), and similar air (both compounds are pyrophoric) and thermal stabilities (both compounds are stable in argon to at least 360 ^{o}C and in vacuum to 200 ^{o}C). Because there can be no significant covalent interactions in the calcate compound and the calcate and ytterbate(II) are so similar, there appears to be no significant covalent interactions in the ytterbate(II) compound.

It had been reported that potassium bis([8]annulene)Yb(III) could not be prepared from ytterbium trichloride[2] so Kinsley also prepared it in liquid ammonia again in the presence of THF:

$$Yb + 2COT + K \xrightarrow[NH_3,\ THF]{} K(COT)_2Yb$$

He was able to obtain pure crystals of the ytterbate(II) by slow

Table 2.1: X-ray powder diffraction data on $K_2[Yb(C_8H_8)_2]*2DME$ and $K_2[Ca(C_8H_8)_2]*2DME$[1b]

M = Yb calculated[a]		Yb found		Ca found	
d(Å)[b]	I	d(Å)[c]	I[d]	d(Å)[c]	I[d]
9.75	282	9.83(5)	w+		
8.81	140	8.80(4)	w	8.76(4)	w
7.31	747	7.31(3)	s-	7.33(3)	s-
6.76	1282	6.73(2)	s	6.74(2)	s
6.35	229	6.36(2)	w+	6.37(2)	w-
5.79	1125	5.76(2)	s-	5.76(2)	s-
5.46	77	5.45(2)	w-		
4.89	174	4.87(1)	w+	4.90(1)	w-
4.45	392	4.42(1)	m	4.47(1)	m
4.33	4			4.34(1)	w
4.14	99	4.15(1)	w-	4.15(1)	w-
4.06	119	4.07(1)	w-	4.07(1)	w-
3.95	13			3.93(1)	w-
3.85	273	3.85(1)	m	3.85(1)	m
3.65	17			3.61(1)	w-
3.51	19			3.52(1)	w-
3.41	235	3.43(1)	w+	3.43(1)	w
3.31	131	3.31(1)	w-	3.31(1)	w-
3.24	129	3.25(1)	w-	3.25(1)	w-
3.17	155	3.17(1)	w	3.17(1)	m
3.10	227	3.10(1)	w	3.10(1)	w

(a)Calculated values obtained from the crystal structure.[1b] (b) Adjacent lines combined where 2θ values are less than 0.50° apart. (c) The number in brackets is the estimated error in the least significant digit. (d) estimated relative intensity.

$K_2[Ca(C_8H_8)_2]$ - top.

$K_2[Yb(C_8H_8)_2]$ - bottom.

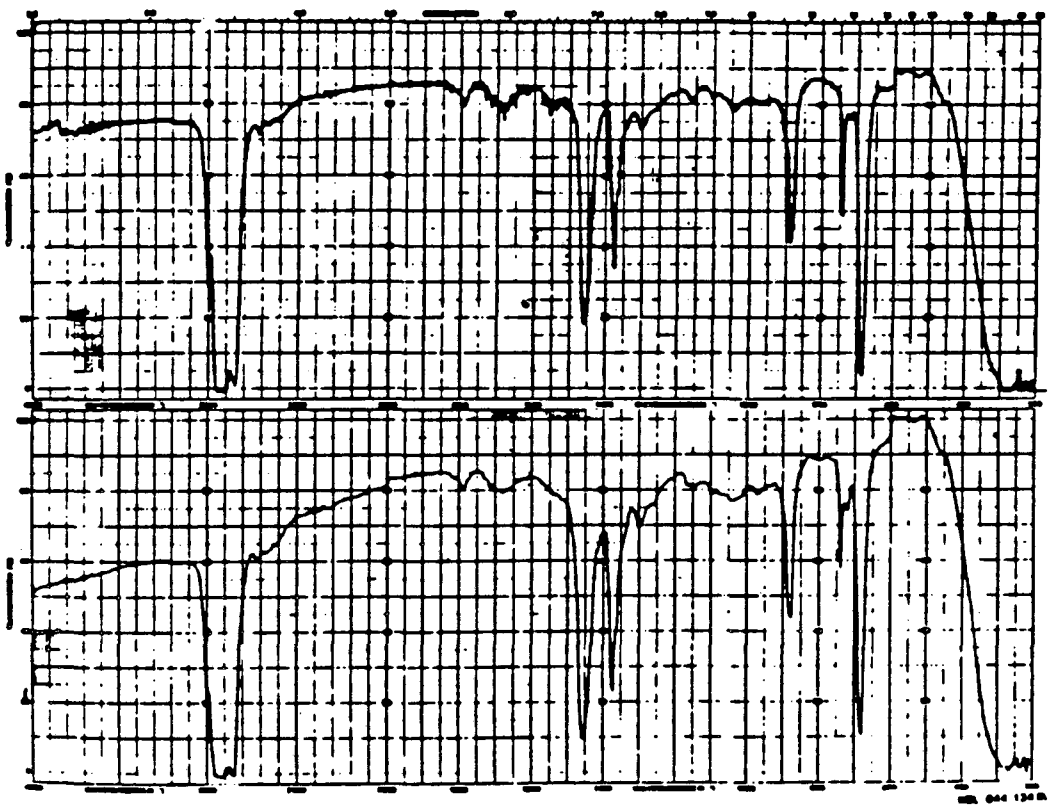

Figure 2.1: Infrared Spectra (nujol mull) of $K_2[Yb(C_8H_8)_2]$ and $K_2[Ca(C_8H_8)_2]$[1b]

cooling of an ether solution of the divalent and trivalent compounds. Crystals of the ytterbate(III) could be obtained by liquid diffusion of hexane into a glyme solution.

Electron Exchange

While taking an NMR of a mixture of the divalent and trivalent ytterbium compounds (which does not have an observable proton NMR although the *t*-butyl protons of the *t*-butyl derivative are observable) it was discovered that the NMR resonance of the diamagnetic divalent compound disappeared. When the solution was cooled to -50 ^{o}C, however, a sharp singlet at 5.5 ppm appeared. As the NMR tube was warmed, the signal at 5.5 ppm broadened and disappeared at 0 ^{o}C (Figure 2.2). These results are indicative of some exchange process between the divalent and trivalent ytterbium compounds, either ligand exchange or electron exchange. These two types of exchange were distinguished by using potassium bis([8]annulene)calcate(II).

If the ytterbium (II-III) exchange were ligand exchange, then one would also expect ligand exchange between potassium bis([8]annulene)-calcate(II) and potassium bis([8]annulene)ytterbate(III). If the exchange in the ytterbium system is electron exchange, however, then exchange between the calcium compound and the ytterbium(III) compound could not occur. A mixture of the ytterbium(III) and calcium(II) compounds was dissolved in THF-d_8 and proton NMR spectra were recorded at a series of temperatures. The sharp resonance due to the bis([8]-annulene)calcate(II) was observable at 5.47 ppm at a variety of temperatures (Figure 2.3) thus supporting the electron exchange mechanism

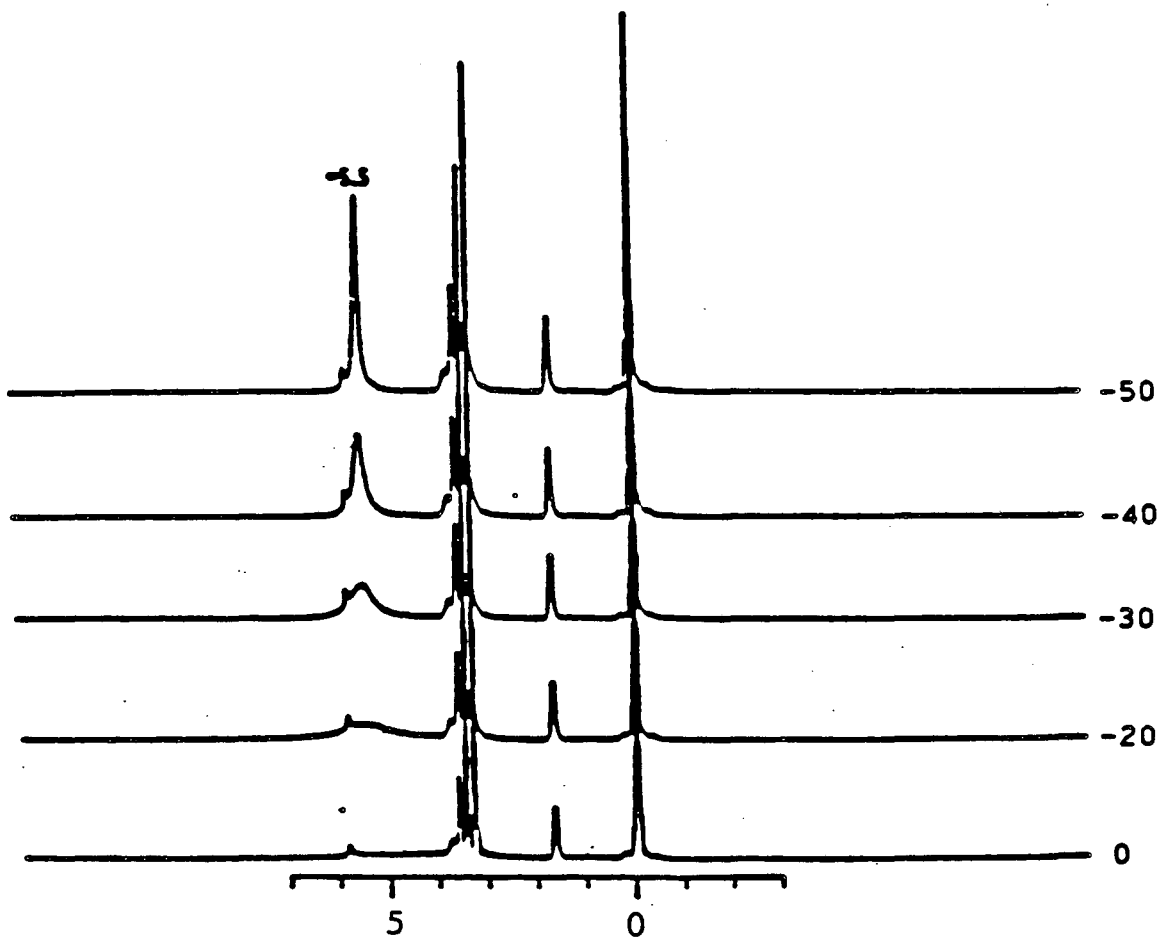

Figure 2.2: Temperature dependent ^1H NMR of glyme adducts of potassium bis([8]annulene)ytterbate(II-III) in THF-d_8. The peak at 5.5 ppm is due to the ytterbate(II) ring protons.

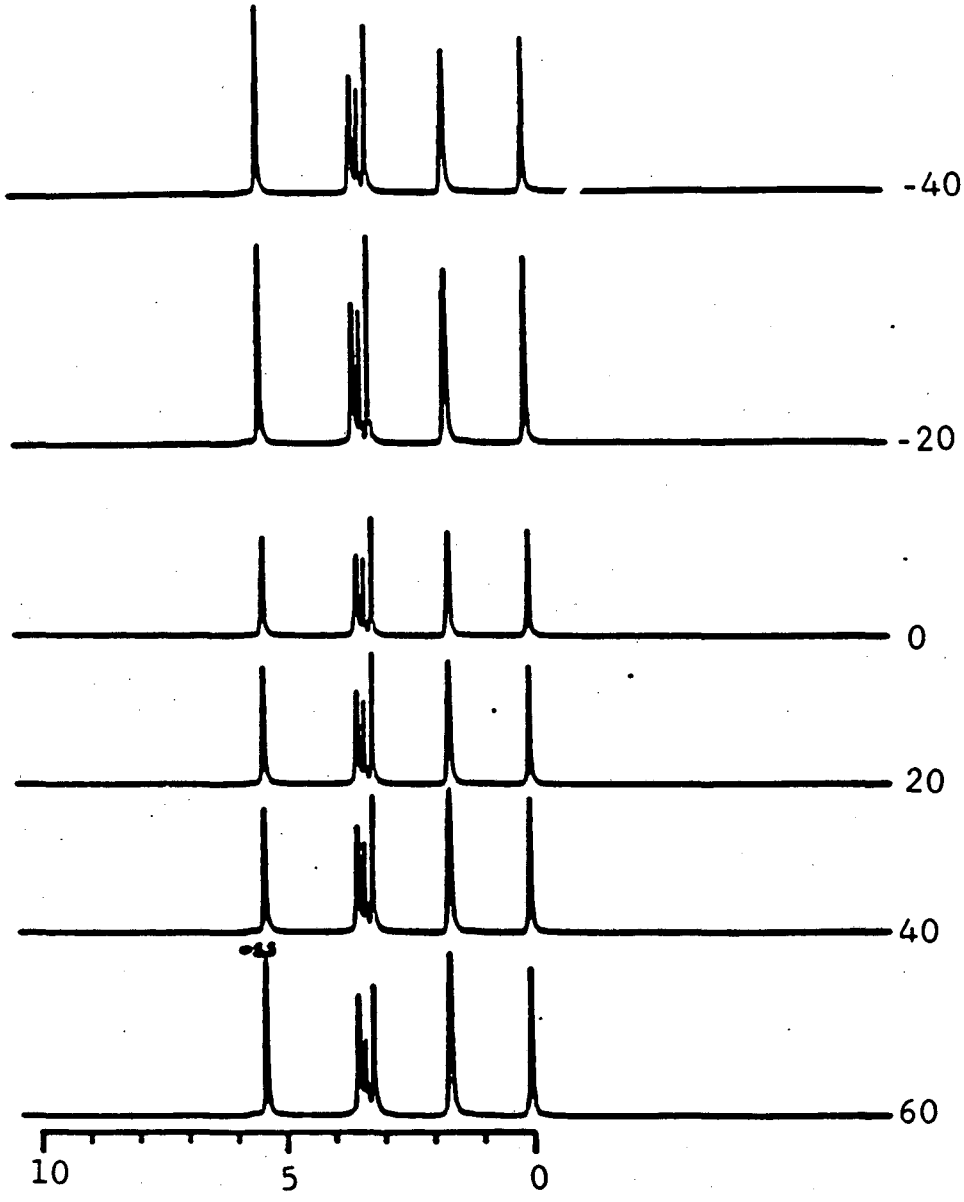

Figure 2.3: Temperature Dependent ^1H NMR Spectra of a Mixture of $[K(DME)]_2[Ca(C_8H_8)_2]$ and $[K(DME)][Yb(C_8H_8)_2]$ in THF-d_8

in the ytterbium (II-III) system.

This exchange is thus analogous to the electron exchange between ferrocene and ferricenium ion studied by Wahl and coworkers[3] and described in the first chapter of this thesis. We used the same equation that they used to relate the NMR linewidth of the exchanging species to the natural linewidths of the pure paramagnetic and diamagnetic compounds and the rate of exchange:

$$W_{dp} = f_p W_p + f_d W_d + f_p f_d 4\pi(\delta\nu)^2/kc$$

In this equation W_{dp}, W_p, and W_d are the linewidths of the exchanging species, the natural line width of the pure paramagnetic species, and the natural line width of the pure diamagnetic species, respectively, at the appropriate temperature; f_p and f_d are the mole fractions of the paramagnetic and diamagnetic species, $\delta\upsilon$ is the separation of chemical shifts in hz between the pure diamagnetic and paramagnetic species at the appropriate temperature; k is the second order rate constant; and c is the total concentration of ytterbium species.

The *t*-butyl derivatives were used in the exchange study because the NMR resonance of the *t*-butyl protons of the paramagnetic ytterbium compound is observable whereas the ring protons are not.

Preparation of *t*-Butyl Analogues of Ytterbate(II) and (III).

Potassium bis(*t*-butyl[8]annulene)ytterbate(III) (1) was prepared in high purity by addition of *t*-butylcyclooctatetraene dianion to a slight excess of ytterbium trichloride in THF. If a slight excess of the dianion is used, a mixture of the divalent and trivalent ytterbium compounds results. The unsubstituted cyclooctatetraene dianion is not

a strong enough reducing agent to reduce the unsubstituted ytterbium(III) complex; the reduction potential of the ytterbium(III) complex must therefore be between that of cyclooctatetraene dianion and *t*-butylcyclooctatetraene dianion.

Use of a large excess of ytterbium trichloride, however, results in formation of significant amounts of a violet, air sensitive, THF-insoluble compound which is also formed on partial exposure of the trivalent compound to oxygen (possibly the triple decker sandwich complex[4]). This compound can be reduced with sodium potassium alloy to potassium bis(*t*-butyl[8]annulene)ytterbate(II) (**2**). **2** was prepared by Steve Kinsley in liquid ammonia from a mixture of ytterbium, *t*-butylcyclooctatetraene, and potassium. The trivalent complex can be reduced conveniently to the divalent complex with potassium and the divalent complex can be oxidized to the trivalent complex with benzyl bromide, benzyl chloride (the complex is not stable to excess benzyl bromide or benzyl chloride), or ytterbium trichloride; thus, mixtures of different relative concentrations of the divalent and trivalent complex could be obtained for NMR line width measurements.

Determination of the Rates and Mechanism for Electron Exchange.

^{1}H NMR spectra were taken for a mixture of **1** and **2** at several different temperatures (Figure 2.4). At -70 ^{o}C the exchange is frozen out on the NMR time scale as evidenced by the sharp peak at 1.55 ppm due to *t*-butyl protons of the diamagnetic compound. The group of ring protons centered at 6 ppm for the diamagnetic compound is also relatively sharp whereas the *t*-butyl protons of the paramagnetic compound

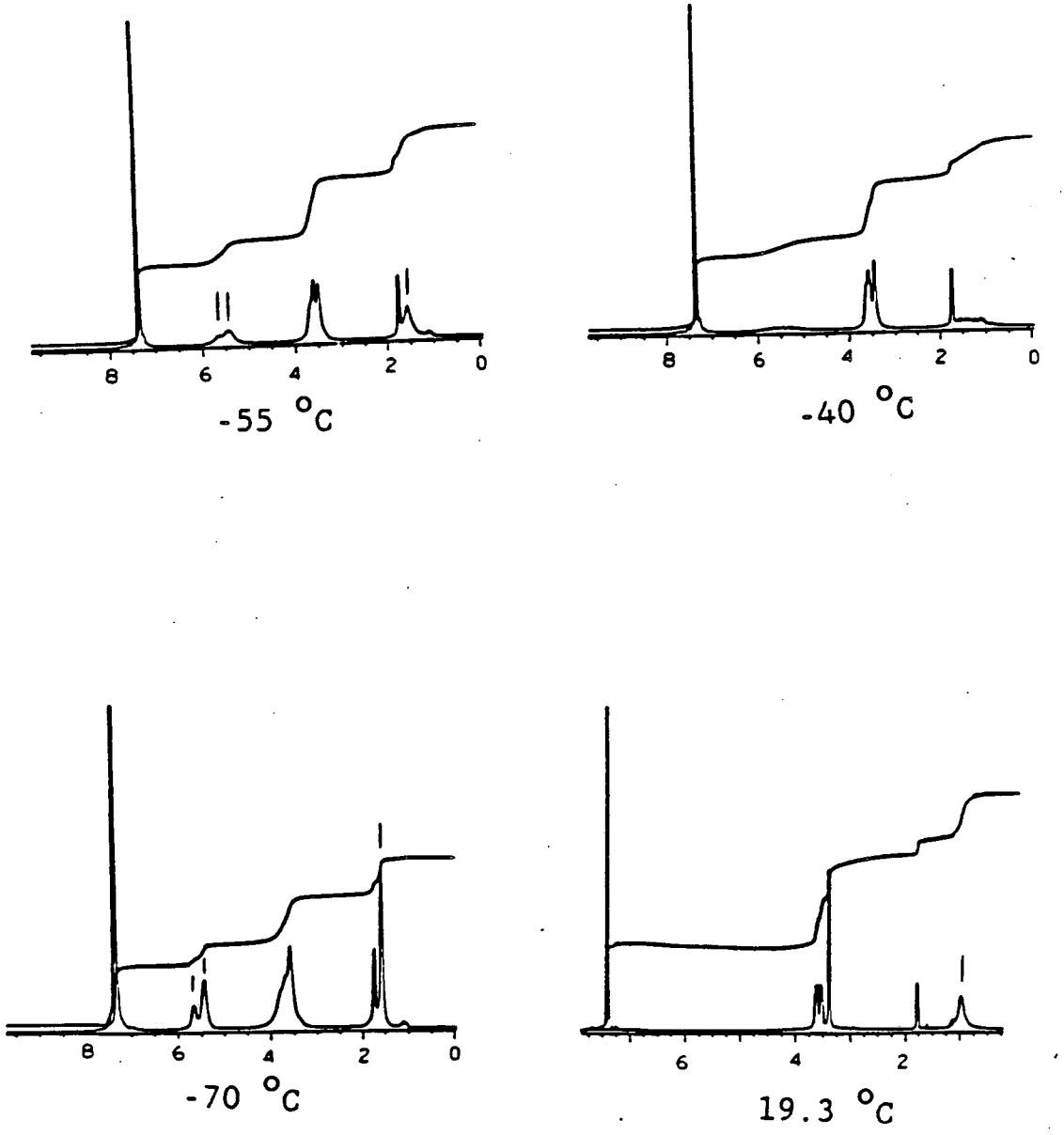

Figure 2.4: Temperature Dependent ^{1}H NMR of diglyme adducts of *t*-butyl Derivatives of Yb(II-III) in THF-d_8

have a resonance which is too broad to observe at this temperature. As the temperature is lowered, the peak at 1.55 ppm broadens and disappears at -40 °C. Between -10 and 20 °C the peak due to exchange involving the *t*-butyl protons is sufficiently sharp to get a reproducible line width measurement and broad enough that effects of shimming on the observed line width are insignificant. Rates of exchange were therefore determined in this temperature region.

The results for the rate of exchange as a function of temperature in THF-d_8 in the presence of diglyme (the initial NMR studies were performed starting with crystals of the diglyme adduct of the divalent complex which was oxidized in THF-d_8 with benzyl bromide to obtain varying mixtures of the divalent and trivalent complex) are listed (Table 2.1) and a plot of the log of the rate of exchange vs inverse temperature with the determined activation parameters is shown (Figure 2.5)

Table 2.1

Rates of Exchange in THF/Diglyme

T, °C	10^{-6} k $M^{-1}s^{-1}$
-10.0	1.7 ± 0.3
0.0	2.9 ± 0.4
10.0	7.2 ± 1.0
19.3	9.6 ± 2.0

$\Delta H^{\ddagger} = 9.0 \pm 1.4$ Kcal mol^{-1}

$\Delta S^{\ddagger} = 4 \pm 5$ eu

The rate of exchange (1×10^7 M^{-1} s^{-1} at 19.3 °C) is quite close to typical rates determined by Wahl, *et. al.*[3] in the ferrocene-ferricenium ion case (for example 4.3×10^6 M^{-1} s^{-1} for the unsubstituted system

in dichloromethane with PF_6^- as the counterion). The high rate of exchange rules out ligand exchange and confirms the initial conclusion that the exchange is electron exchange. Nevertheless, these rates are lower than those expected for diffusion-control (approximately 10^9) and some activating process is required.

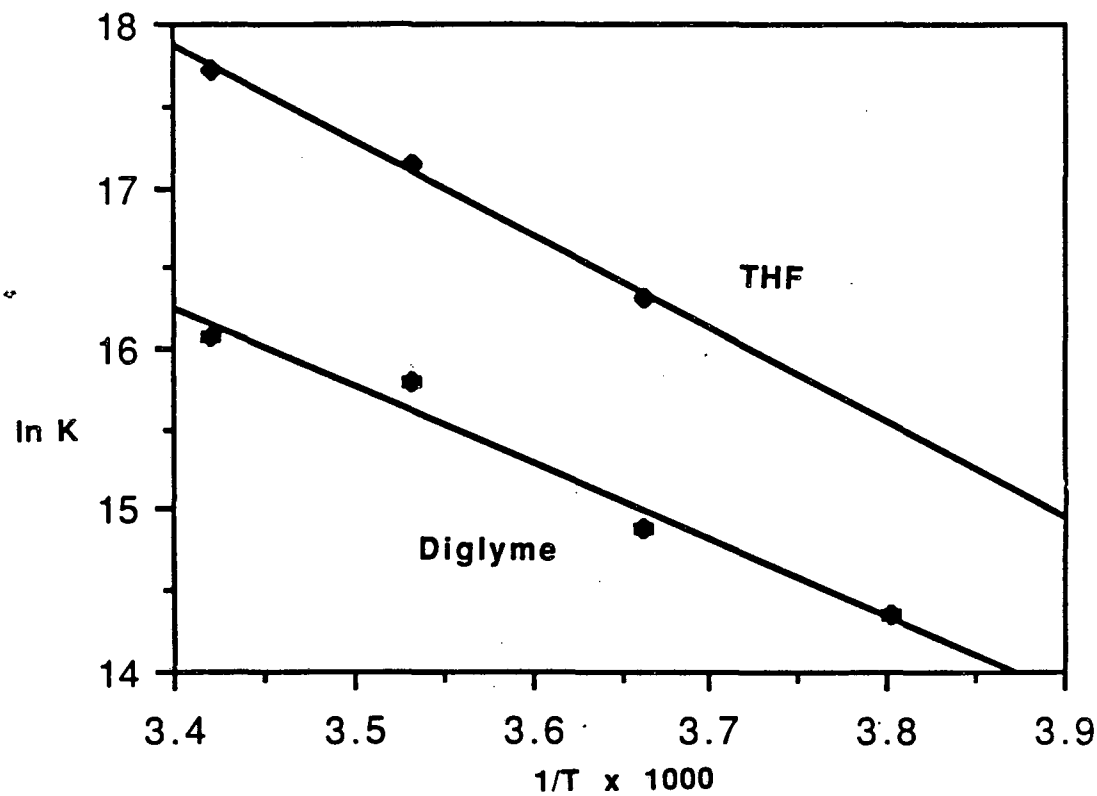

Figure 2.5: Plot of the natural log of the rate constant for electron exchange in THF-d_8 (in the presence and absence of diglyme) vs inverse temperature

A reasonable exchange mechanism involves encounter of two contact ion pairs with transfer of both an electron and a potassium counterion (Scheme 2.1) However, this mechanism does not appear to be consistent with the small entropy of activation found. A reasonable modification of such a mechanism would involve prior dissociation of solvating diglyme from one potassium cation in 2 (Scheme 2.2); with coordination sites at this potassium now available, reaction with 1 would be facilitated and the entropy gained by loss of the diglyme would compensate for that required in the bimolecular reaction step. The central structure in Scheme 2.2 is either a short-lived intermediate or a transition state. Evidence that the ytterbium complexes are solvated by diglyme even when only a small amount of diglyme is present in THF solution includes the observations that the chemical shift

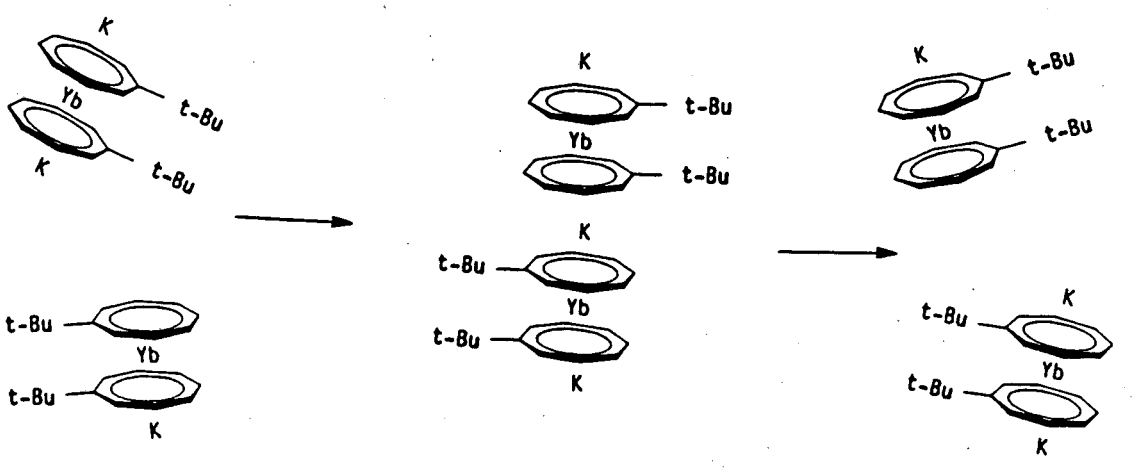

Scheme 2.1

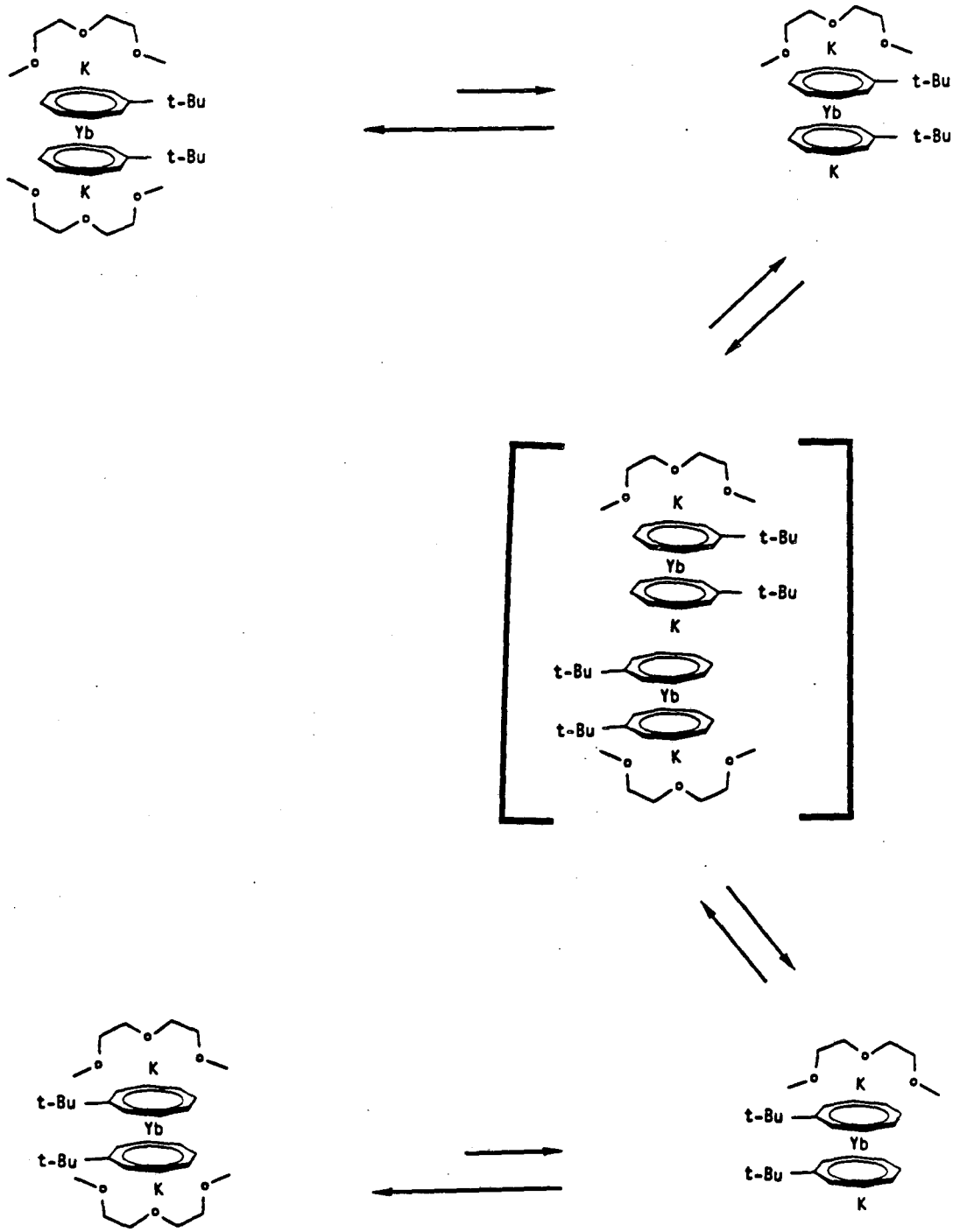
K
t-Bu
Yb
t-Bu
K
K
t-Bu
Yb
t-Bu
K
K
t-Bu
Yb
t-Bu
K
t-Bu
Yb
t-Bu
K
K
t-Bu
Yb
t-Bu
K
K
t-Bu
Yb
t-Bu
K

Scheme 2.2

of diglyme changes and the resonance broadens when the paramagnetic ytterbium(III) complex is added to a THF-diglyme solution whereas the THF resonance is essentially uneffected.

To test this revised mechanism a large excess of diglyme was added to the NMR tubes. If loss of diglyme is required for electron exchange then excess diglyme should lower the rate. However, we found no significant change in the exchange rate. Alternatively, sufficient coordination space around the central potassium may be created if the diglyme loosens from η^3 to η^1 coordination in the rate determining step as shown in Scheme 2.3. This mechanism predicts that electron transfer will be faster in THF in the absence of diglyme because THF coordinates potassium cation more weakly than does diglyme. The rates of exchange in THF-d_8 in the absence of diglyme are summarized in Table 2.2 and are plotted as a function of temperature in Figure 2.5: Again there is scatter in the results but the rates are generally about five times faster than in the presence of diglyme. The activation parameters, although containing a considerable uncertainty, do show a more positive entropy of activation than in the diglyme case as expected for the proposed mechanism in Scheme 2.3; more entropy

Table 2.2

Rates of Exchange in THF

T, °C	$10^{-7}\ k\ M^{-1}s^{-1}$
0.0	1.2 ± 0.3
10.0	2.8 ± 0.7
19.3	4.9 ± 1.6

$\Delta H^{\ddagger} = 11 \pm 2$ Kcal mol^{-1}

$\Delta S^{\ddagger} = 14 \pm 6$ eu

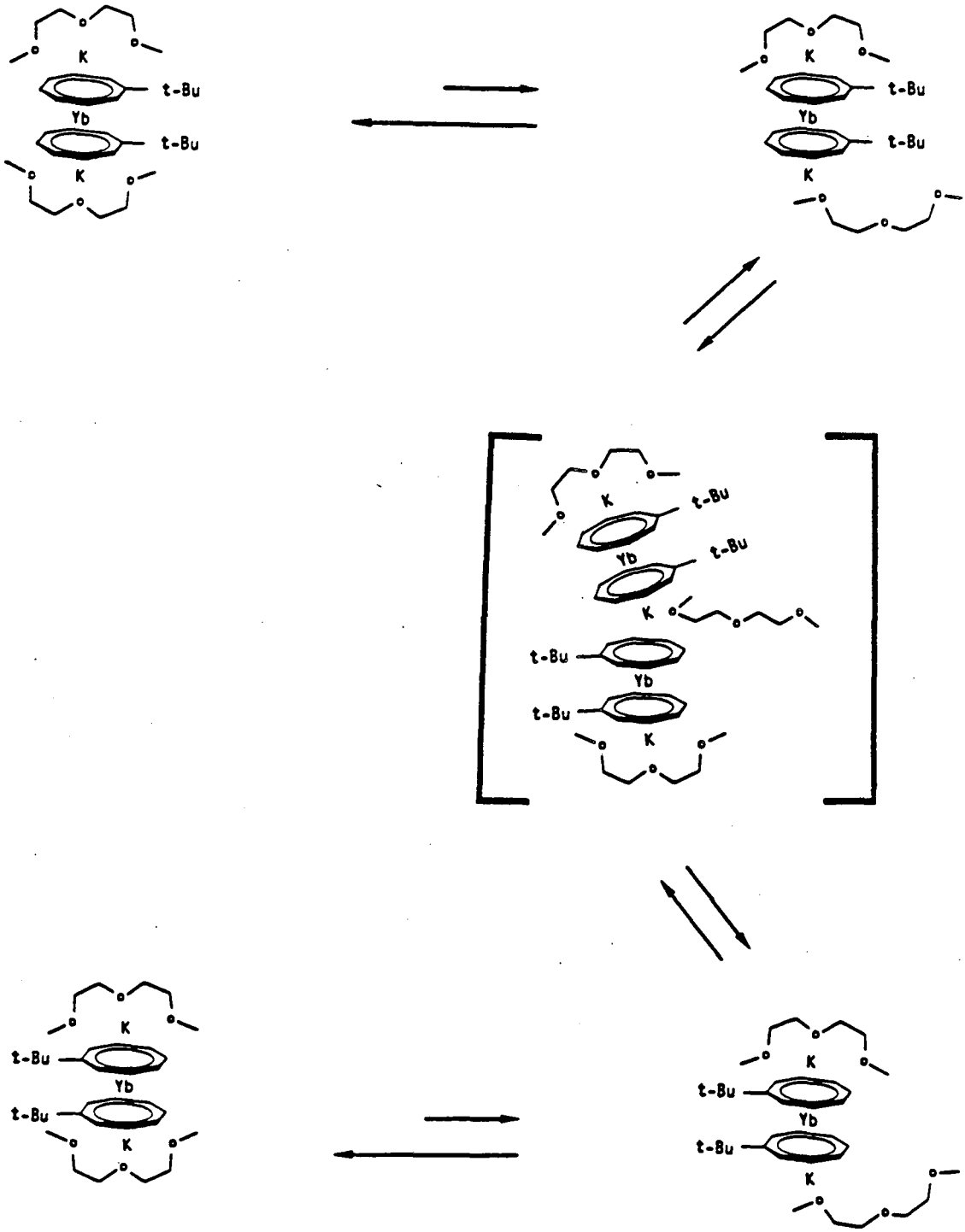
K
t-Bu
Yb
t-Bu
K
K
t-Bu
Yb
t-Bu
K
K
t-Bu
Yb
t-Bu
K
t-Bu
Yb
t-Bu
K
K
t-Bu
Yb
t-Bu
K
K
t-Bu
Yb
t-Bu
K

Scheme 2.3

should be gained from completely freeing a coordinating THF than in converting diglyme from η^3 to η^1 coordination. The fact that exchange is slower in the presence of diglyme also proves that exchange is not occurring by conversion of contact ion pairs to solvent separated ion pairs which then undergo exchange (Scheme 2.4) because diglyme should facilitate the conversion to solvent separated ion pairs and hence lead to an increase in rate of exchange.

These results are analogous to those for electron transfer between benzene and benzenepotassium and related systems.

Ion Pair Electron Transfer

There has been extensive study of electron transfer between aromatic compounds and their radical anions under a variety of conditions.[5] From various studies (*vide infra*) it appears that the dominant factor controlling the rate of electron transfer is the type of ion pairing in these systems. It has been known for several years that in solvents of low polarity, particularly ether solvents, ions often exist as ion pairs rather than the free ions typically found in such higher polarity solvents as water, DMSO, and HMPA. In the case of delocalized anions having alkali metal counterions in ether solution the species predominantly exist as a mixture of contact ion pairs and solvent separated ion pairs, with solvent separated ion pairing being favored by greater delocalization of charge, by smaller cations (which are better solvated), by better donor solvents (in THF both types of ion pairing are found whereas in ether contact ion pairing is almost exclusive, and in tetraglyme solvent separated ion pairs predominate),

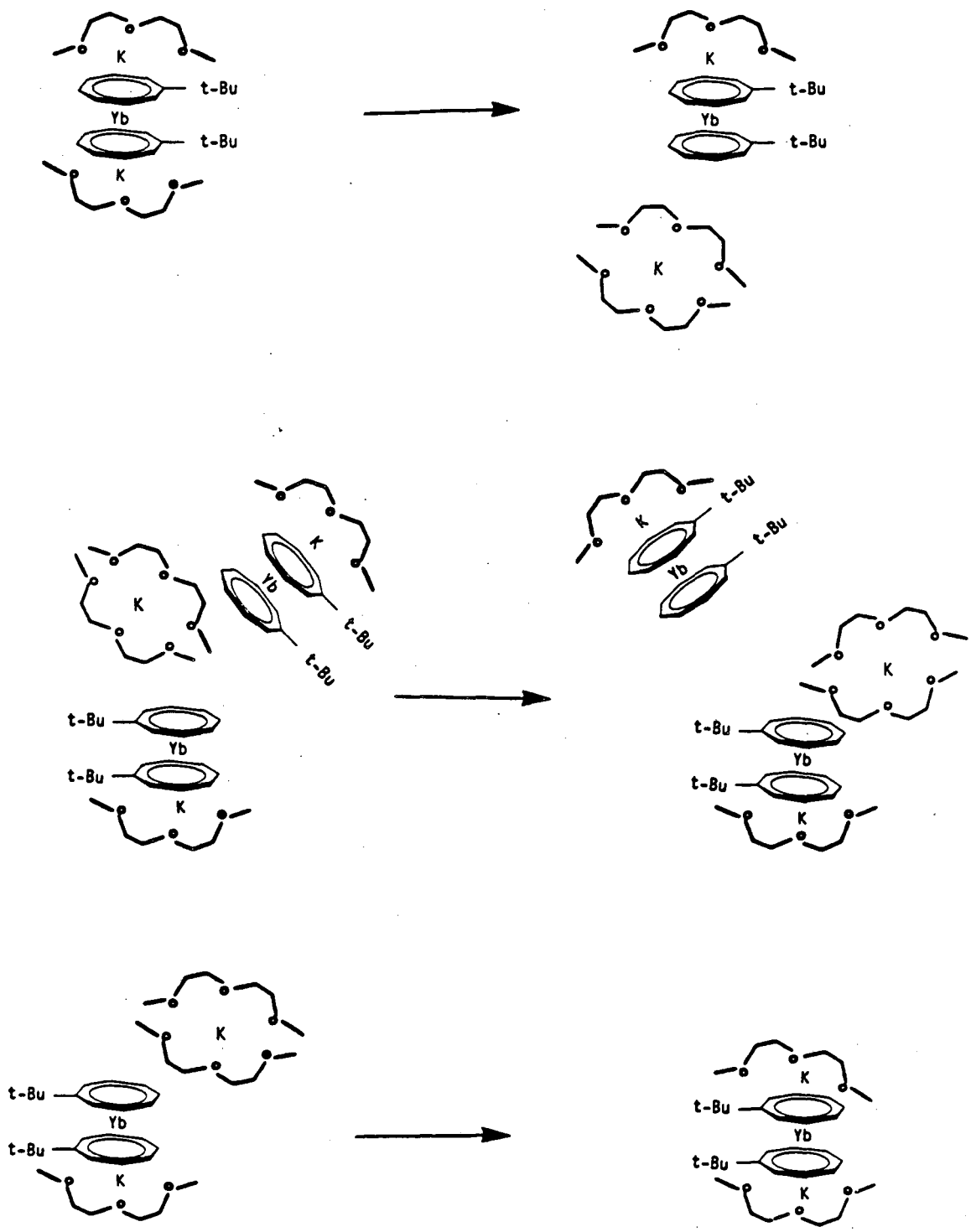
K
t-Bu
Yb
t-Bu
K
K
t-Bu
Yb
t-Bu
K
K
Yb
t-Bu
t-Bu
t-Bu
Yb
t-Bu
K
K
t-Bu
t-Bu
Yb
K
t-Bu
Yb
t-Bu
K
K
t-Bu
Yb
t-Bu
K
K
t-Bu
Yb
t-Bu
K

Scheme 2.4

and finally by lower temperature (contact ion pairing frees up coordinating solvent and hence is entropy favored and enthalpy disfavored.)

Table 2.3 lists the rates of electron transfer as measured by EPR techniques for naphthalene and benzene with their respective radical

Table 2.3

compound	solvent/counterion	ionic state	$K \times 10^{-7}$
Naphthalene	HMPA	FI	50
Naphthalene	THF/K^+	FI	300
Naphthalene	DME/K^+	FI	220
Naphthalene	THF/Na^+	ssIP	170
Naphthalene	THF/Li^+	ssIP	46
Naphthalene	DME/Na^+	ssIP	134
Naphthalene	THP + G4/Na^+	ssIP	45
Naphthalene	THP/Na^+	cIP	0.2
Naphthalene	THF/Na^+	cIP	1.3
Naphthalene	THF/K^+	cIP	3.2
Naphthalene	THF/Cs^+	cIP	8.4
Naphthalene	DME/Na^+	IP	<3.0
Benzene	THF/K^+	IP	16.3
Benzene	DME/K^+	IP	3.6

anions with varying counterion, solvent, and ion pairing type. The first thing to notice is that free ions and solvent separated ion pairs undergo electron exchange at or near the diffusion controlled limit whereas contact ion paired systems undergo exchange several orders of magnitude slower. Notice also that addition of tetraglyme to sodium naphthalenide in tetrahydropyran converts the system from a

contact ion paired system to a solvent separated ion paired system and increases the rate of exchange by more than two orders of magnitude. In contrast changing the solvent for the exchange of potassium benzene with benzene from THF to better coordinating glyme slows the rate of exchange. Apparently when replacing a poorer coordinating solvent with a better one causes a switch from contact ion pairing to solvent separated ion pairing or free ions, the rate of exchange increases several orders of magnitude, but when the better coordinating solvent does not change the ion pairing, the rate of exchange slows somewhat. This second case agrees with the results with the ytterbium system in which exchange is slower in the presence of diglyme indicating that the type of ion pairing does not change when diglyme is added. Notice also that the rate of exchange of potassium benzene in glyme is close to the rate for the ytterbium system in the presence of diglyme.

The rate determining step in the ytterbium system appears to be completely dependent on change in solvation. In the next two chapters electron exchange in other bis([8]annulene) systems is studied and an effort is made to see if the same mechanism for exchange applies.

Experimental Section

General. Air sensitive compounds were handled under argon either in a Vacuum Atmospheres model HE 243 dry lab with a HE 93A dry train or using standard Schlenk line techniques. Unless otherwise noted, materials were obtained from commercial suppliers and used without additional purification. ^{1}H NMR spectra were obtained on UC Berkeley 200 and 250 MHz superconducting FT spectrometers equipped with

Cryomagnets Inc., magnets and Nicolet model 1280 data collection systems, a Bruker 500 MHz AM 500 superconducting FT spectrometer with Aspect 3000 computer system, and a 90 MHz JEOL FX 90Q FT spectrometer. Temperatures were measured with a thermocouple mounted next to the NMR tube. Chemical shifts are reported in ppm with positive shifts reported for peaks downfield of TMS, and with peaks referenced to TMS or the upfield residual THF peak taken as 3.58 ppm. Visible spectra were taken on a Cary model 118 or IBM model 9430 spectrophotometer. Tetrahydrofuran (THF), toluene, and hexane were distilled from sodium-benzophenone or $LiAlH_4$, freeze-thawed three times, and stored with 4A sieves prior to use. Cyclooctatetraene was obtained from BASF and vacuum transferred and stored in 4A sieves prior to use. Potassium bis(t-butyl[8]annulene)ytterbate(II) was prepared as described previously, and the reactions in liquid ammonia were carried out as detailed previously.[1]

***t*-Butylcyclooctatetraene**: 100 mL of 1.7 M *t*-butyllithium in pentane (156 mmol) was added dropwise, through a dropping funnel to a solution of dry, freshly distilled cyclooctatetraene (11 g, 96 mmol) in 125 mL of dry ether at -78 ^{o}C under argon. The resulting purple solution was stirred for 1 hr. at -78 ^{o}C and then allowed to warm to 0 ^{o}C. The dianion was quenched by adding a solution of I_2 (60 g, 230) in 200 mL of dry ether dropwise. The solution first turned yellow, then green, after which the addition was halted. Ice water was added and the solution was stirred with approximately 3 g of sodium bisulfite to reduce excess iodine. The ether layer was separated, dried with anhydrous magnesium sulfate, the solvent was removed via aspirator, and

the product, distilled under full vacuum. *t*-Butylcyclooctatetraene comes over at about 50 ^{o}C affording 1.83 g (9 %), ^{1}H NMR: ($CDCl_3$) 5.8, 1.5.

Potassium bis(*t*-butyl[8]annulene)ytterbate(III) (1). Freshly cut potassium (0.74 g, 19 mmol) was added to a stirring solution of 1.42 g (8.88 mmol) of freshly distilled and dried t-butylcyclooctatetraene in approximately 50 mL of dry, degassed THF in an argon glove box. The solution immediately turned from a faint yellow to a medium brown. The solution was stirred for about 2 hours and then added dropwise, over the period of about 2 min, to a rapidly stirred suspension of 1.34 g (4.80 mmol) of ytterbium trichloride in 100 mL of dry, degassed THF. After approximately one-third of the dianion solution was added, the trichloride solution turned navy blue. In each of several preparations there was a considerable delay before the solution turned blue, probably because the first step of the reaction is reduction of ytterbium trichloride. The solution was stirred for about 1 h until a pink precipitate could be detected indicating that the ytterbium had been completely oxidized to the trivalent state. (This pink product is apparently an oxidation product of the ytterbate in which either ytterbium trichloride or small quantities of oxygen act as the oxidizing agent.) Then, 100 mL of THF was added and the solution was filtered. The THF was removed *in vacuo* and the blue residue was washed with toluene and pumped dry, yielding 725 mg (31%) of product. Vis: λ_{max} (THF) = 602 nm (ϵ=2000); ^{1}H NMR: (THF-d_8) -13.9 (395 Hz, 19.3 ^{o}C), 14.7 (456 Hz, 10 ^{o}C), -15.5 (502 Hz, 0.0 ^{o}C) -16.8 (600 Hz, -10 ^{o}C). Satisfactory analysis could not be obtained.

Electron Exchange Studies. Suitable mixtures of the 1 and 2 were prepared by oxidation or reduction of the pure compounds to produce a variety of mole fractions of the two compounds (typically between 5 and 20% of the paramagnetic compound to give manageable line widths of 50 to 200 Hz for the exchanging mixtures). NMR tubes were prepared using THF-d_8 containing a known concentration of benzene as a standard; solutions containing 0.005 to 0.1 M of total ytterbium gave useful spectra. Relative mole fractions were determined by comparing the chemical shift of the exchanging peak at a given temperature to the known chemical shifts of the pure compounds. Line widths of the exchange peaks were determined at -10.0, 0.0, 10, and 19.3 °C with the diglyme adduct and at 0.0, 10.0, and 19.3 °C in the absence of diglyme. Line widths of the two pure complexes were also determined at these temperatures.

Rate constants for electron exchange were obtained by inputting the natural linewidths of the pure paramagnetic and diamagnetic ytterbium species and the linewidth of the exchanging species into the equation of Chan, DeRoos, and Wahl[3] for determination of the second order exchange rate. Activation parameters and their uncertainties were obtained from the ACTEN program.[6]

References.

1. Kinsley, S.; Streitwieser, A., Jr.; Zalkin, A. *Organometal.* 1985, 4, 52.

2. Kinsley, S. Personal Conversation.

3. (a) Chan, M. S.; DeRoos, J. B.; Wahl, A. C. *J. Phys. Chem.* 1973,

77, 2163. (b) Yang, E. S.; Chan, M. S.; Wahl, A. C. *J. Phys. Chem.* **1980**, *84*, 3094.

4. Miller, M. J.; Lyttle, M. H.; Streitwieser, A., Jr. *J. Org. Chem.* **1981**, *46*, 1977.

5. Szwarc, M.; Jagur-Grodzinski, J. In *Ions and Ion Pairs in Organic Reactions*; Szwarc, M., Ed.; Wiley-Interscience: New York, 1974; Vol. 2.

6. Detar, D. F. "Computer Programs in Chemistry"; W. A. Benjamin: New York, 1969; Vol. 3.

Appendix: Individual Rates of Electron Exchange

Rate of Exchange in THF/Diglyme x 10^{-7} vs Conc. (Molar)

[YbIII]	[YbII]	19.3 °C	10 °C	0.0 °C	-10 °C
0.011	0.114	1.04	0.64	0.32	0.19
0.016	0.067	1.08	0.80	0.32	0.18
0.0048	0.119	0.97	0.72	0.37	0.16
0.034	0.164	0.61	0.77	0.24	0.19
0.024	0.134	0.80	0.77	0.21	0.13
0.011	0.082		0.60	0.26	0.15
0.014	0.082	1.05			
0.0016	0.023	1.50			
0.039	0.080	0.50			
0.021	0.062	1.09			
0.025	0.105	0.96			

Rate of Exchange in THF x 10^7 vs Conc. (Molar)

[YbIII]	[YbII]	19.3 °C	10 °C	0.0 °C
0.044	0.0156	2.9	3.9	1.25
0.0032	0.0088	7.8		
0.0024	0.0216	7.1	2.4	1.28
0.0047	0.0343	5.0	3.6	1.37
0.0048	0.0250	4.5	1.3	0.76
0.017	0.0879	2.6		
0.0081	0.0269	4.3	1.8	0.81
0.040	0.160		4.0	

Chapter 3: Electron Transfer in Uranium and Transuranium Systems

Introduction

Studies of electron transfer were extended to bis([8]annulene) actinide systems in order to determine how general the findings in the ytterbium system are. The systems that appeared to be the most promising were the uranium, neptunium, and plutonium systems, because there had been reports of bis([8]annulene) compounds of each of these metals in two oxidation states, and because in each system there had been something surprising about the physical properties of one of the compounds.

Concerning uranium, there are a variety of organo-uranium(III) systems, as described in the first chapter of this thesis, however, the reduction product of uranocene had never been fully characterized although its preparation was reported in 1981.[1] In that year Marquet-Ellis and coworkers reported that a reduction product of uranocene is prepared by addition of one equivalent of lithium naphthalenide to uranocene or by treating UCl_3 with COT dianion. This latter method was repeated by Kinsley who found that only uranocene was produced.[2]

Marquet-Ellis *et. al.* reported that the reduction product is brown, and it was characterized primarily by reversible oxidation to uranocene.[3] They also reported that the compound has a ^1H NMR resonance approximately 31 ppm upfield of TMS with a width at half height of 40 Hz. This resonance is surprisingly sharp for a uranium(III) compound inasmuch as that for uranocene is about 90 Hz wide, and it is expected that a uranium(III) compound, which has an

odd number of unpaired electrons, should have a considerably broader NMR resonance than a uranium(IV) compound, which has an even number.

Bis([8]annulene) compounds of plutonium III and IV and neptunium III and IV have been prepared and thoroughly characterized. Bis([8]-annulene)neptunium(IV), neptunocene, was prepared by Karraker *et. al.*[4] by addition of neptunium tetrachloride to a THF solution of COT dianion:

$$NpCl_4 + 2\ K_2COT \xrightarrow[THF]{} NpCOT_2 + 2KCl$$

The product, which was reported to appear yellow as a dilute solution and red when concentrated, was purified by toluene extraction and characterized by a uv-vis spectrum and comparison of its IR spectrum and X-ray powder pattern to that of uranocene. It is paramagnetic and its Mössbauer spectrum has been reported. Table 3.1 lists the isomer shifts of several neptunium compounds including neptunocene. Notice that the isomer shift of neptunocene is closer to that of neptunium trichloride than that of neptunium tetrachloride, indicating substantial charge donation from ring to metal that would arise from substantial covalency. Bis(1,3,5,7-tetramethyl[8]annulene)neptunium(IV) has also been prepared from reaction of the tetramethyl-COT dianion and neptunium tetrachloride.[5,6] Its ^1H NMR spectrum was also reported (*vide infra*).

Plutonium tetrachloride does not exist so bis([8]annulene)plutonium(IV), plutonocene, was prepared by addition of bis(tetraethylammonium)plutonium(IV) hexachloride to COT dianion:

$$(Et_4N)_2PuCl_6 + 2\ K_2COT \xrightarrow[THF]{} PuCOT_2 + 4KCl + 2Et_4NCl$$

The cherry red product was purified and characterized in the same way as the neptunocene, but it was reported that it exhibited an "unusual"

type of temperature dependent diamagnetism. This does not agree with theoretical predictions, based on a simple crystal field model, that plutonocene should have a J=0 ground state and hence exhibit temperature independent paramagnetism.[7] Plutonocene has also been prepared by direct reaction of the finely divided metal with COT.[8] The preparation of the bis(1,3,5,7-tetramethyl)plutonocene has been reported, but the compound is almost certainly potassium bis(1,3,5,7-tetramethyl-[8]annulene)plutonate(III).[9]

Potassium bis([8]annulene)neptunate(III) was prepared by reaction of neptunium tribromide with COT dianion in THF:[10]

$$NpBr_3 + 2K_2COT \xrightarrow[THF]{} KNpCOT_2 + 3KBr$$

The burgundy colored product was characterized by comparison of its powder pattern to that of potassium bis([8]annulene)cerate(III). Its magnetic susceptibility indicates two regions of temperature independent paramagnetism between 2.2 and 5.5 K and between 5.5 and 19 K. Above 19 K it exhibits typical temperature dependent paramagnetism (*vide infra*). Its Mössbauer spectrum has been taken and it indicates a considerable degree of covalency, although not as much as in neptunocene (Table 3.1).

Table 3.1 Isomer Shifts of Neptunium Compounds at 4.2 K relative to $NpAl_2$

NpO_2	-0.56
$NpCl_4$	-0.34
$NpAl_2$	0.00
$NpCp_4$	+0.72
$Np(COT)_2$	+1.94
$NpCl_3$	+3.54
$NpCp_3 \cdot 3THF$	+3.64
$KNp(COT)_2 \cdot 2THF$	+3.92

The preparation and characterization of potassium bis([8]annulene)plutonate(III) are the same as for the neptunate. The turquoise-green plutonium compound exhibits temperature dependent paramagnetism. Attempts to prepare the neptunate or plutonate from the chloride salts failed, presumably due to the low solubility of these salts. Both of these compounds are extremely water sensitive, in contrast to neptunocene and plutonocene which are reported to be water stable.[11] Traces of oxygen oxidize the trivalent neptunium and plutonium compounds to neptunocene and plutonocene, respectively.

Preparation of Compounds

Potassium bis([8]annulene)uranate(III) and potassium bis(methyl-[8]annulene)uranate(III) were prepared from the parent uranocenes by potassium reduction of a THF solution. This reaction does not work as well with uranocene as with substituted uranocenes due to the low solubility of the unsubstituted compound; in this case a better synthesis involves reduction catalyzed by a few milligrams of naphthalene. Both reduction products can be crystallized as their diglyme adducts by gaseous pentane diffusion into a THF-diglyme solution although X-ray quality crystals could only be obtained from the methyl compound.

The ^{1}H NMR in THF-d_8 of potassium bis([8]annulene)uranate(III) at room temperature consists of a single broad resonance of about 200 Hz at 1/2 height at -31.8 ppm. The ^{1}H NMR of potassium bis(methyl[8]annulene)uranate(III) (Fig. 3.1) consists of a 40 Hz methyl peak at -5.2 ppm and four ring peaks in the ratio of 2:1:2:2 at -29.3, -29.9,

-32.7, and -35.3 ppm which are all about 200 Hz wide. The width of these peaks agrees with expectations for uranium (III) compounds.

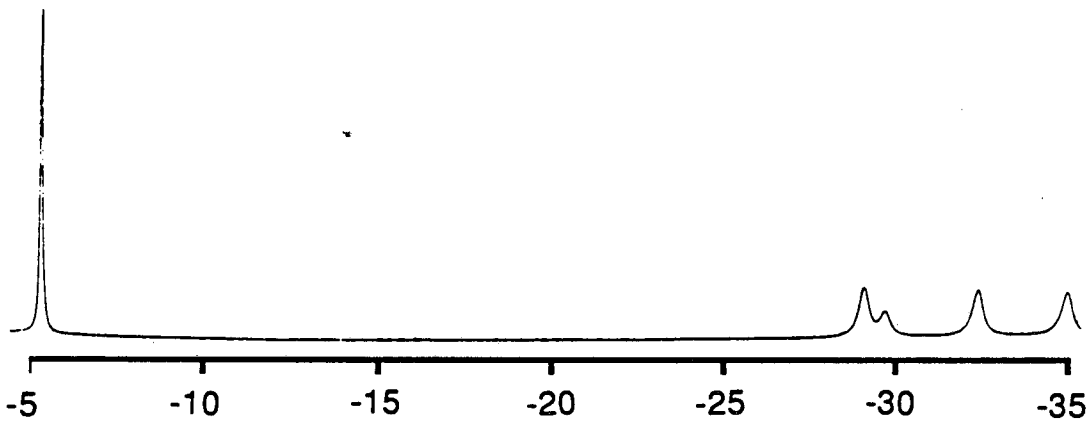

Figure 3.1: ^{1}H NMR of potassium bis(methyl[8]annulene)uranate(III)

As the halogen salts of the actinides are difficult to synthesize, particularly when combined with the hazards of working with transuranium compounds, we decided to use the bis(tetraethylammonium) hexachlorides of neptunium(IV) and plutonium(IV) to prepare neptunocene and plutonocene. These salts have the advantage of being air stable, and the bis([8]annulene) neptunium(III) and plutonium(III) compounds could then be prepared by potassium reduction of neptunocene and plutonocene. We also decided to work with the *t*-butyl derivatives of the compounds because we had found in prior work[12] that the *t*-butyl group serves as a useful NMR marker for paramagnetic compounds as well as improving their solubility.

The preparation of bis(*t*-butyl[8]annulene)plutonium(IV), di-*t*-butylplutonocene, is quite straightforward. It begins with the preparation of bis(tetraethylammonium)plutonium(IV) hexachloride by bubbling HCl into an aqueous solution of plutonium(IV) containing

tetraethylammonium chloride. The resulting yellow solid is dried and treated with *t*-butylcyclooctatetraene dianion to produce the blood-red 1,1'-di-*t*-butylplutonocene:

$$Et_4NCl + Pu(IV)_{aq} \xrightarrow[HCl]{} (Et_4N)_2Pu(IV)Cl_6$$

$$(Et_4)_2Pu(IV)Cl_6 + K_2\text{-}t\text{-BuCOT} \xrightarrow[THF]{} (t\text{-BuCOT})_2Pu(IV)$$

The ^1H NMR spectrum of the plutonocene (Fig. 3.2) consists of 3 ring peaks between 10.3 and 9.8 ppm. The first peak is a multiplet which is the superposition of the H5 and H4 resonances, next is a doublet representing H2, and at 9.8 ppm is a triplet due to H3. The *t*-butyl resonance appears at 2.15 ppm. These peaks are all sharp and have paramagnetic shifts of about 0.5 ppm for the *t*-butyl groups and 4.5 ppm for the ring protons compared to the diamagnetic 1,1'-di-*t*-butylthorocene and 1,1'-di-*t*-butylcerocene. These resonances do not shift as a function of temperature indicating temperature independent paramagnetism.

The reduction product, potassium bis(*t*-butyl[8]annulene)plutonate(III), was prepared by potassium reduction of a THF-d_8 solution of di-*t*-butylplutonocene. The lime green product was not isolated. Its ^1H NMR (Fig. 3.3) consists of a *t*-butyl resonance at -2.6 ppm and 4 ring peaks in the ratio of 2:2:2:1 between 11 and 15 ppm. The *t*-butyl peak shifts upfield as the temperature as lowered and the ring peaks shift downfield, indicative of typical paramagnetic behavior.

Preparation of 1,1'-di-*t*-butylneptunocene is more difficult than the plutonocene owing to the uncertainty of the oxidation state of neptunium in solution. In aqueous solution in the presence of oxygen

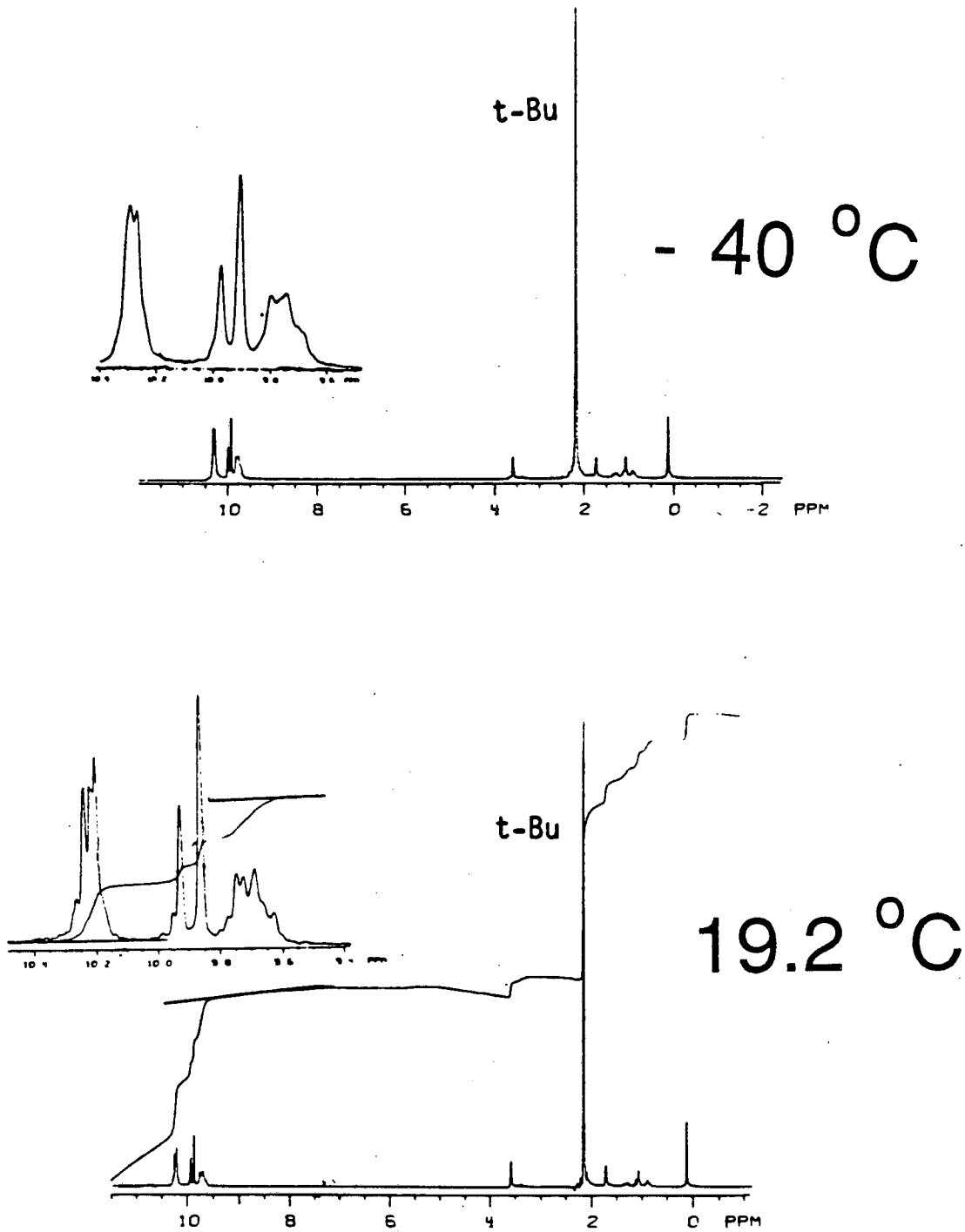

Figure 3.2: ^{1}H NMR spectra of di-*t*-butylplutonocene in THF-d_8

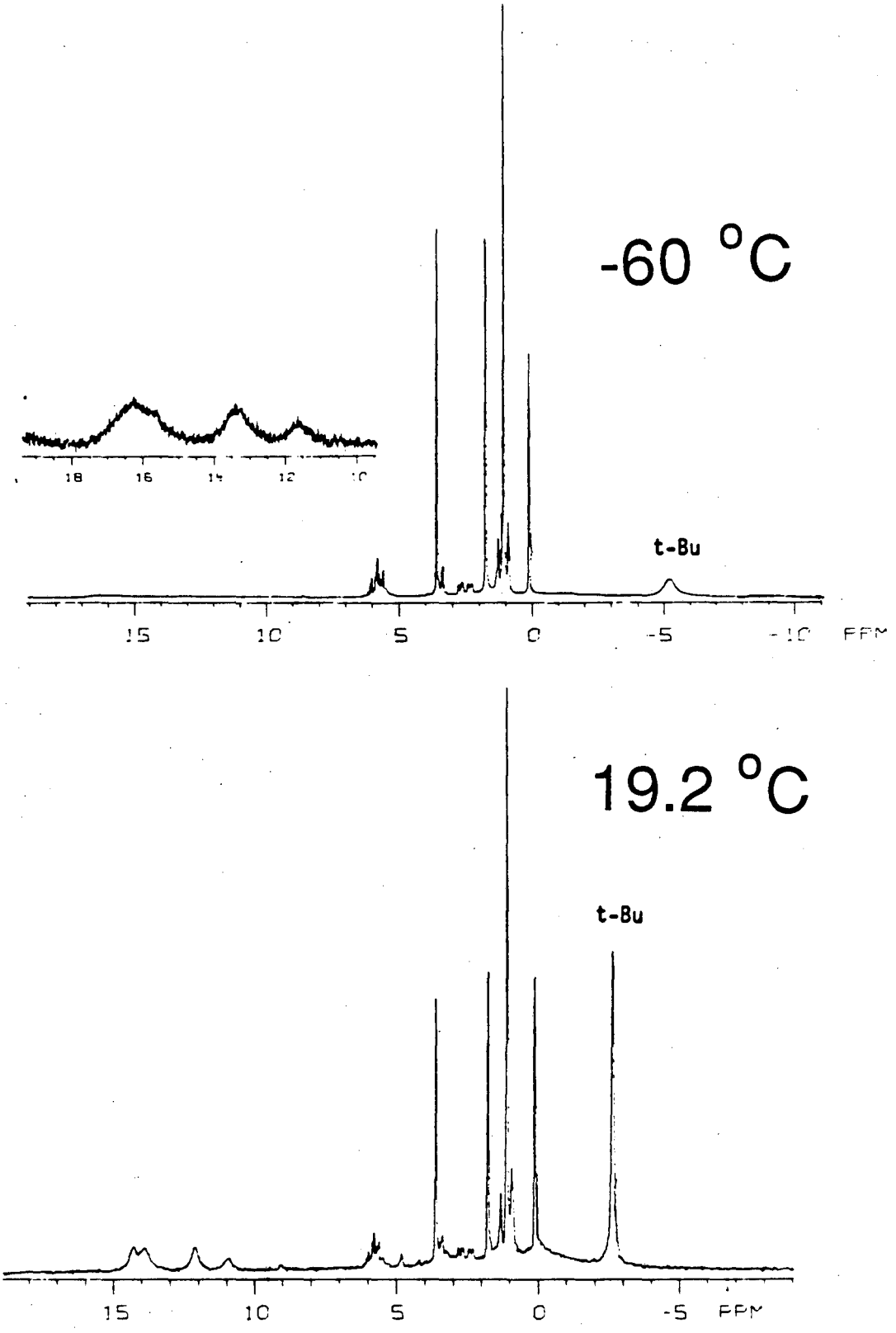

Figure 3.3: ^{1}H NMR spectra of potassium bis(*t*-butyl[8]annulene)plutonate(III) in THF-d_8

neptunium exists as Np (V) and (VI), so the first step in the preparation of the neptunocene is electrochemical reduction to the tetravalent state. The success of this reduction can be monitored by the near IR spectrum.[13] The bis tetraethylammonium hexachloride is then prepared as with the plutonium, but with neptunium traces of a different oxidation state appear to change the color and X-ray powder pattern of the perported bis(tetraethylammonium)neptunium(IV) hexachloride. In several attempts by us and others[14] several different powder patterns were obtained. In the belief that neptunocene is a thermodynamic sink in the system we continued the preparation by treating the neptunium salt with *t*-butylcyclooctatetraene dianion in THF and obtained the desired greenish-brown product.

The ^{1}H NMR spectrum of the neptunocene (Fig. 3.4) consists of a single broad peak of about 150 Hz at -5.15 ppm. This is consistent with the previously reported spectrum of octamethylneptunocene[5] which has methyl peaks 300 Hz wide at +13 ppm and ring peaks at -37 ppm of 2000 Hz. The ring peaks in the *t*-butyl compound are probably not observable because they are not symmetrical, meaning there would not be a single ring resonance as in the octamethyl compound but four different resonances necessarily having reduced intensities. This pattern of change in the direction of paramagnetic shift with each succeeding methyl group has been observed and explained with uranocenes.[15]

Potassium reduction of di-*t*-butylneptunocene produced burgundy colored potassium bis(*t*-butyl[8]annulene)neptunate(III). Its ^{1}H NMR spectrum (Fig. 3.5) consists of a sharp resonance at 4.12 ppm due to the *t*-butyl protons and a series of sharp multiplets for the ring

protons in the ratio of 1:2:2:2. At -6.0 ppm there is a triplet resulting from H5, at -7.1 ppm a triplet due to the H4, at -8.0 a doublet due to H2, and at -8.4 a triplet due to H3. The *t*-butyl resonance shifts downfield as the temperature is lowered and the ring peaks shift upfield, indicative of typical paramagnetic behavior.

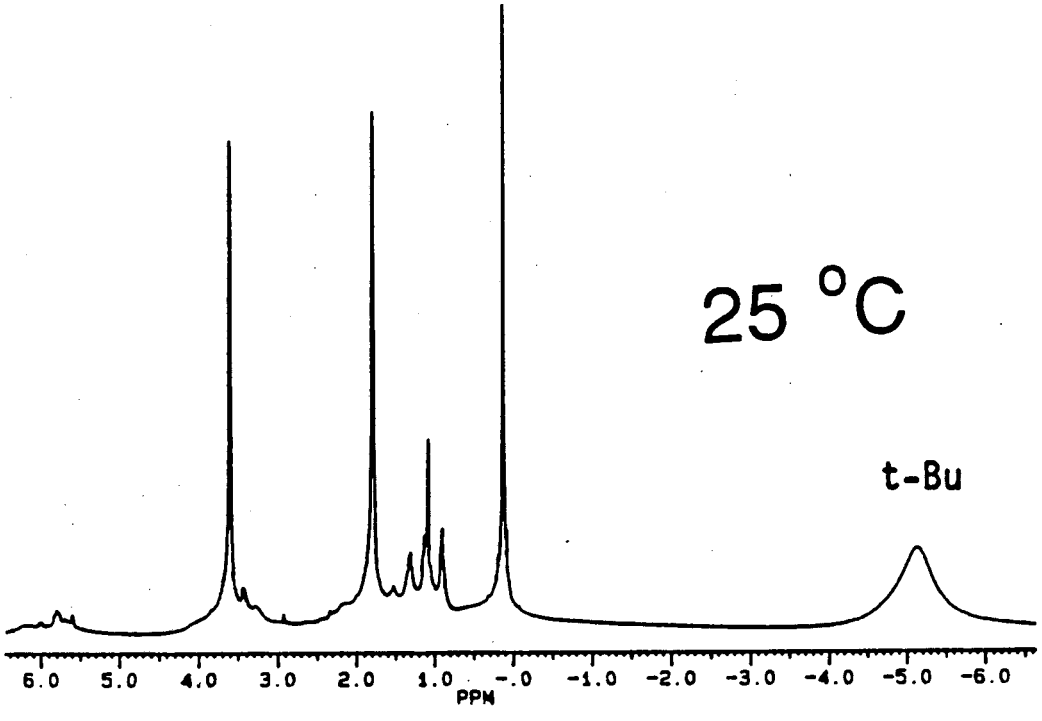

Figure 3.4: ^{1}H NMR spectrum of di-*t*-butylneptunocene in THF-d_8. The *t*-butyl resonance is marked; the peaks at 3.58 and 1.73 ppm are residual solvent, and the peak at 0.1 ppm is grease.

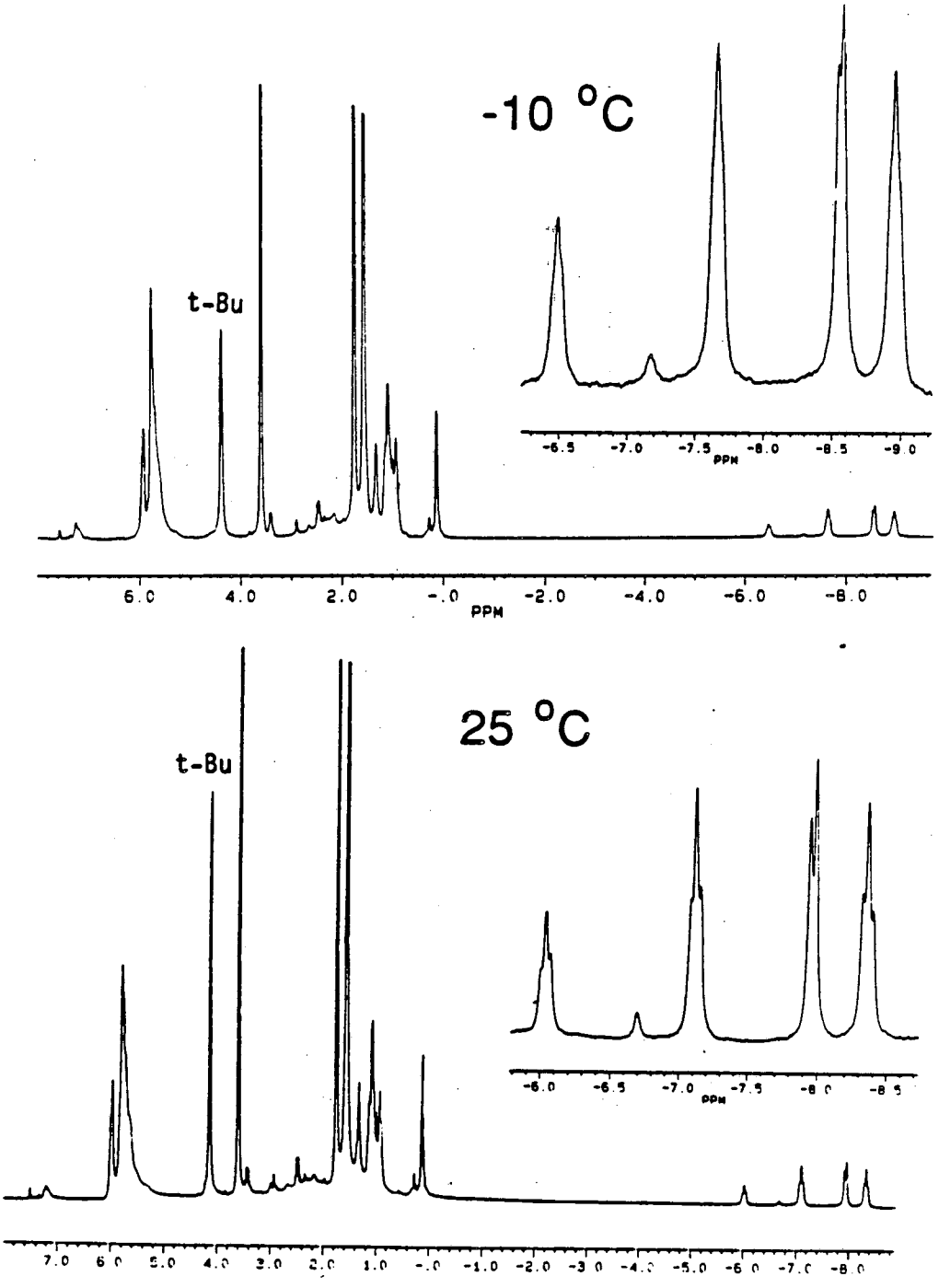

Figure 3.5: ^{1}H NMR spectra of potassium bis(*t*-butyl[8]annulene)neptunate(III) in THF-d_8

Electron Exchange

When uranocene is mixed with its reduction product, the resulting peak has a chemical shift at room temperature which is the weighted average of the chemical shifts of the two species individually. The linewidth also is approximately the weighted average of uranocene and its reduction product. When dimethyluranocene is mixed with its reduction product the same situation results. With both of these systems it has not been possible thus far to freeze out the exchange.

This is not surpising because near the coalescence temperature the linewidth varies approximately linearly with the difference in chemical shifts between the two species in Hz and with the rate constant. The exchange in the ytterbium system is in the slow exchange region at about -70 ^{o}C at 200 MHz. At this temperature the difference in chemical shifts between the two species is approximately 26 ppm. With a difference in chemical shift between uranocene and its reduction product of only about 5 ppm it will be quite difficult to freeze out this exchange.[16]

Partial reduction of di-*t*-butylplutonocene led to an NMR spectrum (Fig. 3.6) at 28 ^{o}C containing a sharp resonance at -0.12 ppm and a series of broad resonances between 11 and 14 ppm. As the temperature was lowered to -50 ^{o}C the broad ring resonances broadened further into the base line and the sharp resonance due to the *t*-butyl protons broadened and shifted upfield to -1.5 ppm. This upfield shift occurs because the *t*-butyl resonance of the trivalent plutonium compound shifts upfield as the temperature is lowered, while the tetravalent compound exhibits no change in chemical shift versus temperature so

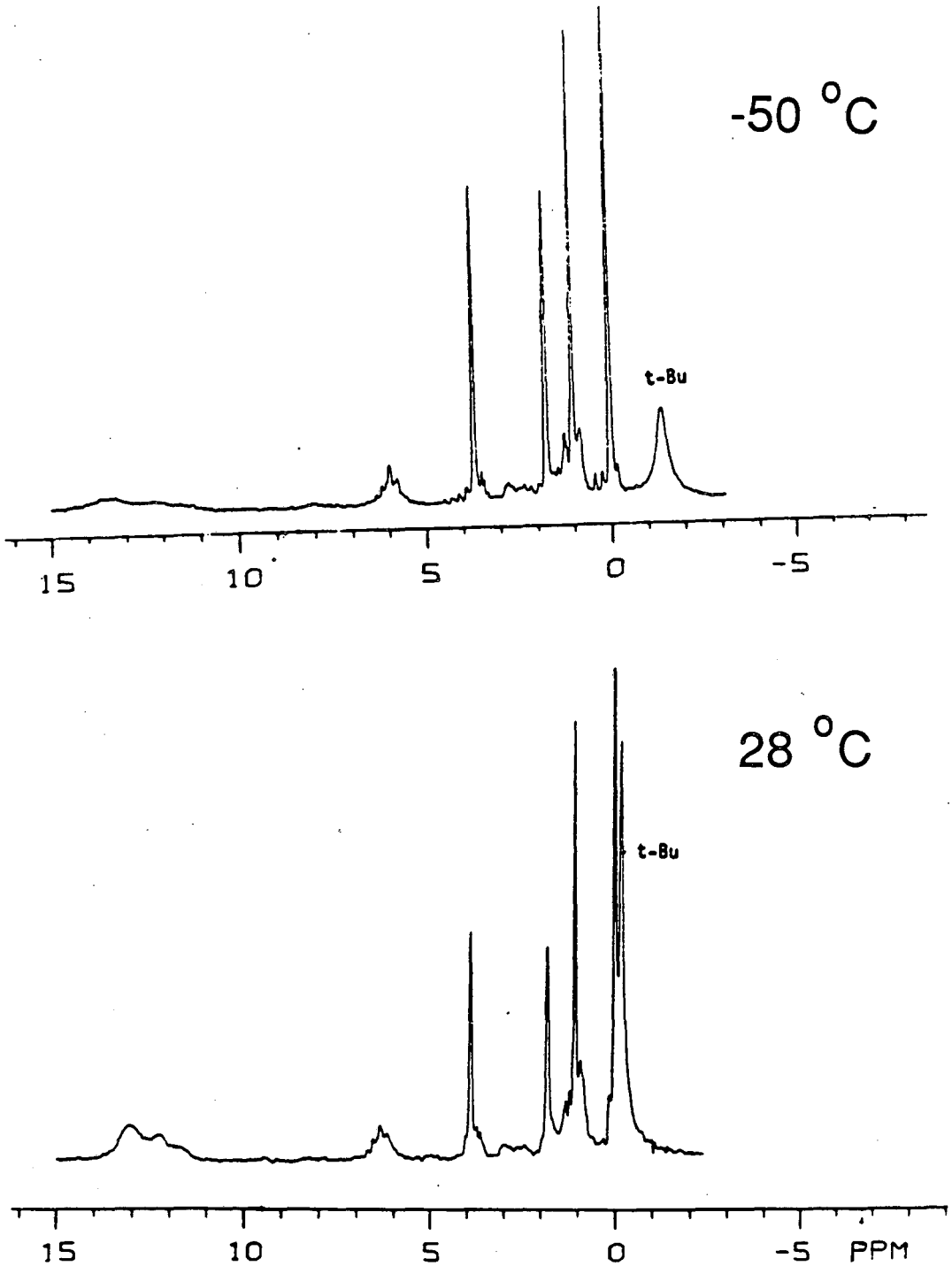

Figure 3.6: ^{1}H NMR spectra of a mixture of 1,1′ di-*t*-butylplutonocene and potassium bis(*t*-butyl[8]annulene)plutonate(III)

the net effect for the exchanging peak is an upfield shift.

Partial oxidation of the neptunate produced an NMR spectrum (Fig. 3.7) containing a broadened peak at 3.9 ppm due to the *t*-butyl protons. The ring protons broadened to the point of being barely distinguishable above the baseline. When the temperature was lowered to -20 ^{o}C the peaks sharpened considerably so that four definite peaks could be seen in the ratio of 1:2:2:2 with a width of approximately 70 Hz.

Due to the small chemical shift differences between the peaks for the plutonium(III) and (IV) compounds it was not possible to freeze out this exchange. In the neptunium system, however, the ring peaks for the tetravalent compound should be near the reported resonances for octamethyl-neptunocene at -37 ppm. Since the ring peaks for the trivalent compound appear between -6 and -8.4 ppm this gives a difference for the 300 MHz spectrometer which was available for this transuranium work of about 9000 Hz. This is almost twice as large as the difference in the previously studied ytterbium system. Unfortunately the spectrometer that was used is only equipped to go down to -20 ^{o}C, but at that temperature the ring peaks do sharpen considerably as can be seen in Figure 3.6, indicating that the slow exchange region has almost been reached.

Magnetic Properties of Plutonium(IV) and Neptunium(III):

As was mentioned in the introduction to this chapter, it has been predicted by a simple crystal field argument that plutonocene would have a J=0 ground state with low-lying excited states and thus would

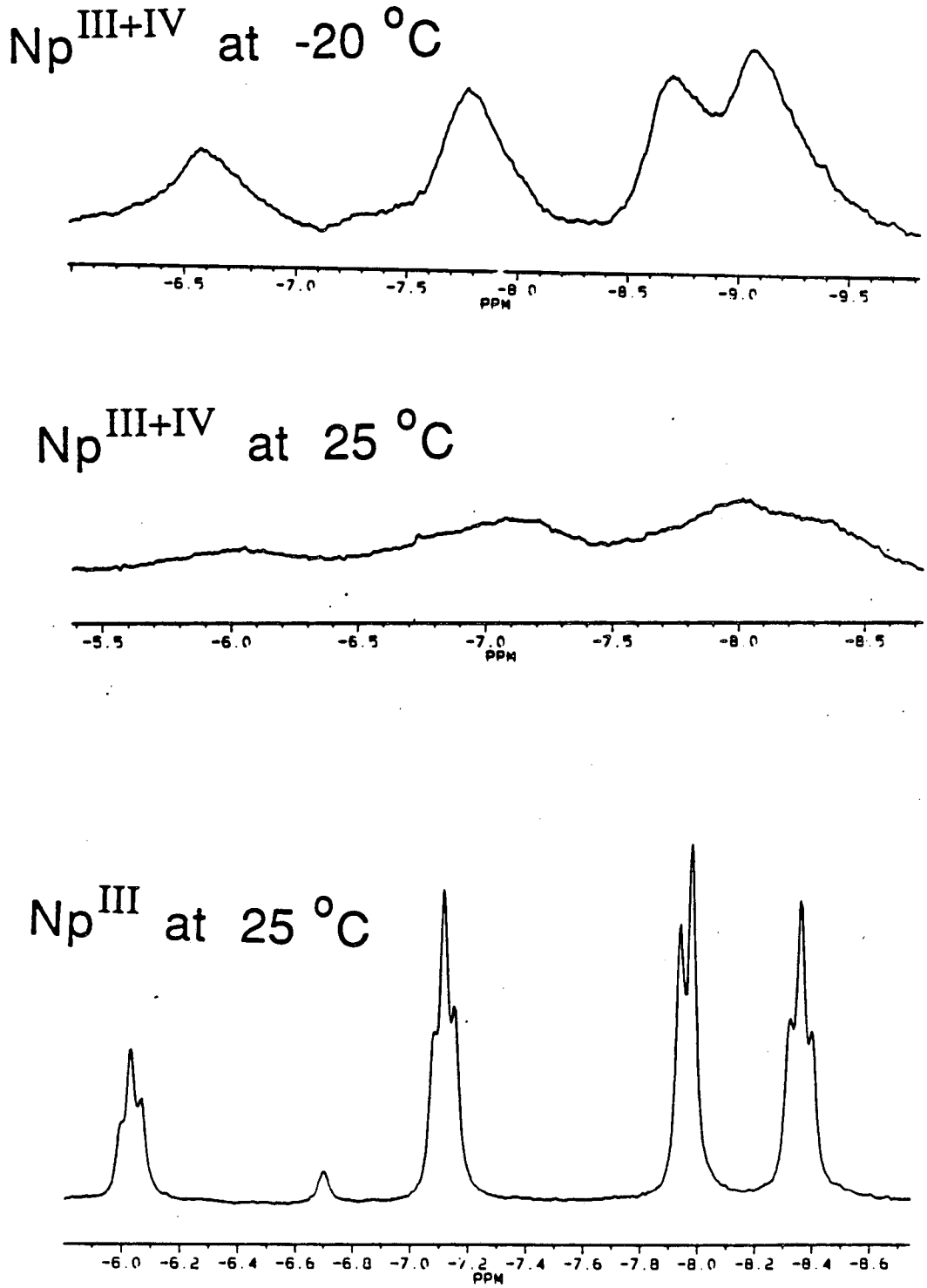

Figure 3.7 ^{1}H NMR spectra of ring protons in potassium bis(*t*-butyl-[8]annulene)neptunate(III) and its mixture with 1,1' di-*t*-butyl-neptunocene

exhibit temperature independent paramagnetism, but Karraker *et. al.* reported that plutonocene exhibited a strange temperature dependent diamagnetic susceptibility.[4] We have found by NMR that di-*t*-butylplutonocene does exhibit temperature independent paramagnetism.

Potassium bis(*t*-butyl[8]annulene)neptunate(III) is isoelectronic with di-*t*-butylplutonocene and might be expected to exhibit similar magnetic properties with differences arising from the lower symmetry, lower crystal field splitting, lower spin orbit coupling, and expected lower degree of covalency of the neptunium compound. The applicability of this approach can be tested by comparing the uranocene reduction product with neptunocene, these compounds also being isoelectronic. Both compounds have broad NMR peaks although those of the neptunium compounds are much broader (2000 Hz for ring protons compared to 200 Hz in the uranium compound). The paramagnetic shifts of the two compounds are very close for the ring protons (-37 ppm vs -32 ppm) but quite different for the methyl protons (+13 ppm vs -5 ppm).

Karraker reported that potassium bis(8]annulene)neptunate(III) exhibits two different regions of temperature independent paramagnetism below 15 K and temperature dependent paramagnetism above that temperature, possibly indicating a low lying paramagnetic electronic state that is populated at 15 K. We find that the *t*-butyl derivative exhibits a large temperature dependent shift between 25 ^{o}C and -20 ^{o}C although the resonances are reasonably sharp (ring protons about 5 Hz).

The Unidentified Uranocene Reduction Product

Studies of electron transfer in the uranocene system were initially complicated by the preparation (by reducing uranocene with potassium in THF-d_8) of a compound which was initially believed to be potassium bis([8]annulene)uranate(III). The ^{1}H NMR spectrum of the compound and uranocene is shown in Figure 3.8. Notice how sharp the peak is, and that its chemical shift is close to that of the real potassium bis([8]annulene)uranate(III). These two resonances do not broaden as the temperature is raised, indicating that no type of exchange is occurring between the unidentified compound and uranocene on the NMR time scale.

The sharpness of the NMR resonance (about 10 Hz) indicates that

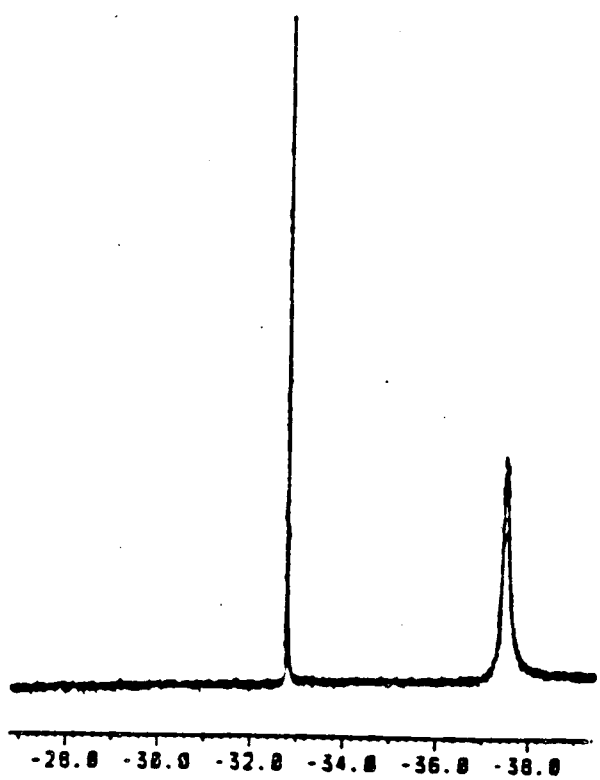

Figure 3.8: Uranocene and its Unidentified Reduction Product

the compound is a uranium(IV) compound of lower symmetry than uranocene.[17] One explanation for this compound was that it is the product of the reaction of uranocene with the enolate of acetaldehyde which can be formed by decomposition of THF. Because THF-d_8 was used, the only resonances observable would be those of the COT ring. An attempt was therefore made to synthesize the compound by preparing the enolate of acetaldehyde by butyllithium initiated decomposition of THF, and by reacting this enolate with uranocene. When this was done an immediate reaction was seen to occur as evidenced by the solution turning from green to brown. The product, however, has an NMR spectrum which bears no resemblance to that of the unidentified reduction product. The spectrum, shown in Figure 3.9, is difficult to interpret, and identification of the unidentified reduction product has not yet been possible.

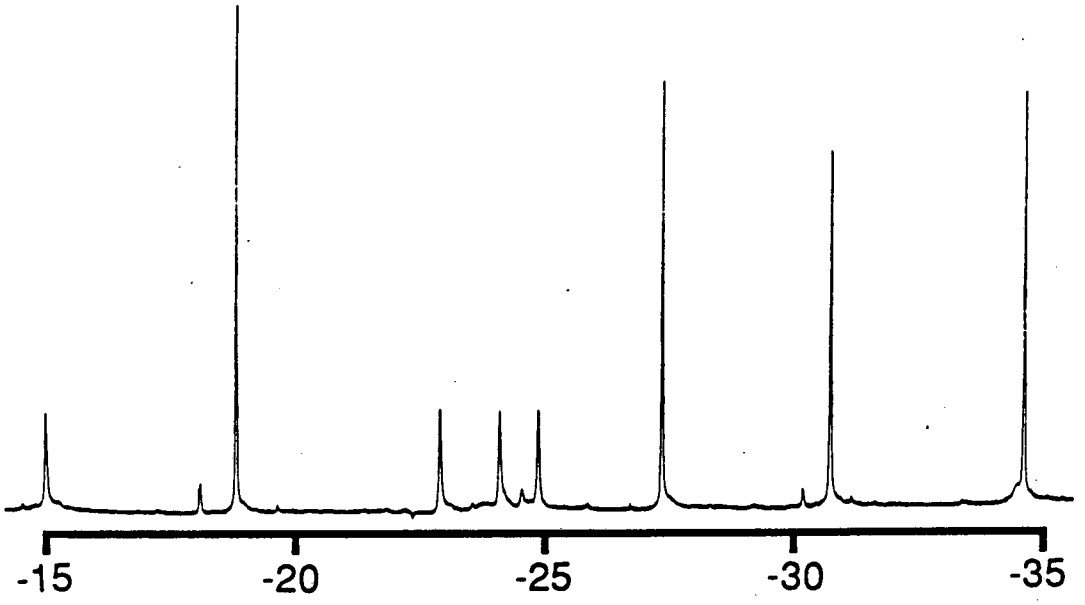

Figure 3.9: Upfield region of the ^{1}H NMR spectrum of the product formed from reaction of uranocene and the enolate of acetaldehyde

Comments on Extension of Electron Transfer Work to other Systems

At this point, it is perhaps appropriate to comment on desirable areas to which this electron transfer work might be extended. Although there are several possible systems, I believe three are of particular interest. The first is dimetallic and mixed metallic systems; biuranocenylene and other such systems are discussed in the next chapter of this thesis. Second, it would be interesting to prepare a uranium(V) compound and study its exchange with its reduction products; attempts have been made to synthesize the mixed ligand COT dianion - cycloheptatriene trianion uranium compound. These yielded some promising NMR results but it was not possible to isolate the product. The third area of interest, and the one that will be the focus of this commentary, is exchange between thorocene and its reduction product, and in particular, isolation and study of the physical properties of potassium bis([8]annulene)thorate(III).

After many years and frequent attempts there had been no thorough characterization of a thorium(III) compound. Thus, the preparation of $[(Me_3Si)_2\text{-}Cp]_3Th(III)$ and the solving of its X-ray crystal structure were significant accomplishments.[18] Of added interest was the fact that the unpaired electron in the system is a d-electron rather than an f-electron.[19] The only problem with this work is that the compounds are extremely difficult to obtain pure and so their bulk properties are not as they should be (i.e. the bulk magnetic susceptibility is much lower than expected[20] and the compound does not form base adducts with compounds that form adducts with $(TMS_2Cp)_3U(III)$).[21]

A promising system for avoiding these problems is the

bis([8]annulene) system because if potassium bis([8]annulene)thorate(III) could be prepared the bulky COT rings should hinder electrophilic attack of the thorium. The compound might also have interesting magnetic properties (it might be a Jahn-Teller ion).[22]

In preliminary attempts to prepare the thorate by potassium reduction of thorocene in the presence of catalytic naphthalene at -20 ^{o}C, some success has been achieved. A redish-purple compound was produced which appears to undergo electron exchange with thorocene (when di-n-butylthorocene is reduced its NMR resonances broaden and shift). Upon solvent removal the compound has been found to decompose, perhaps because of intermolecular proton abstraction. The best hope for this work is probably to use bulky COT ligands such as tetramethyl-COT or 1,5-di-*t*-butyl-COT which should hinder this process. Unfortunately, these ligands are difficult to synthesize,

Experimental:

General: General procedures used were the same as mentioned in chapter two.

Handling neptunium and plutonium: Owing to the hazards of handling ^{237}Np and ^{242}Pu, multiple levels of containment were used at all times. Air sensitive work was done either in a glove box or on a Schlenk line inside a reverse pressure glove box while wearing an additional pair of gloves. NMR spectra were taken in double NMR tubes containing an inner teflon tube and an outer flame sealed pyrex tube. ^{1}H NMR spectra and ^{13}C NMR spectra were obtained on a Bruker 300 MHz

superconducting spectrophotometer. Visible and near IR spectra were obtained on a Cary model 17 spectrophotometer. The samples were flame sealed in a pyrex cuvette which was mounted in a lead box containing a quartz window.

Potassium bis([8]annulene)uranate(III): In an argon glove box 0.50 g (1.1 mmol) of uranocene were dissolved in about 100 mL of THF. Approximately 2 mg (0.2 mmol) of naphthalene and 0.06 g (1.5 mmol) of freshly cut potassium were added and after several hours the solution turned from green to brown. When the solution had completely changed color, after approximately 8 hrs., it was filtered into a round bottomed flask, 10 mL of diglyme was added, and the flask was connected via U-tube to another round bottomed flask containing approximately 40 mL of pentane. After several days 0.40 g (58%) of reddish brown crystals of the diglyme adduct were obtained. These crystals were all multi-twinned and thus unsuitable for X-ray crystallography. ^{1}H NMR: (THF-d_8, 20 ^{o}C) -31.8 (s), about 200 Hz at half-height.

The procedure can be repeated for the reduction of methyluranocene; however, owing to its higher solubility, addition of catalytic naphthalene is not necessary and reduction of the substituted uranocene is complete within one hour. Typical yields are similar to that of the unsubstituted compound, and crystals suitable for crystallography were obtained. The structure is reported in chapter five of this thesis. ^{1}H NMR: (THF-d_8, 35 ^{o}C) -5.2 (s, 3H), -29.3 (s, 2H), -29.9 (s, 1H), -32.7 (s, 2H), -35.3 (s, 2H); ring peaks are about 210 Hz at half-height, and the methyl peak is about 40 Hz at half-height.

Bis(tetraethylammonium)plutonium(IV) hexachloride: Hydrogen chloride gas was bubbled into a solution reported to contain approximately 230 mg (0.95 mmol) of plutonium(IV) in about 12 mL of H_2O. A yellow precipitate formed, and it was separated from the solvent by filtration, washed with ethanol, and pumped dry at about 100 ^{o}C for two days yielding 665 mg (98%) of bis(tetraethylammonium)plutonium(IV) hexachloride.

Bis(tetraethylammonium)neptunium(IV) hexachloride: A 10 mL greenish brown, aqueous solution containing 0.27 g (1.1 mmol) of neptunium as the pentavalent and hexavalent ion was reduced electrochemically to a light green solution containing tetravalent neptunium. The ratio of peaks at 960 and 980 nm[22] indicated that over 95% of the neptunium was reduced to the tetravalent state.

Hydrogen chloride gas was bubbled into 10 mL of the aqueous solution containing 0.27 g (1.1 mmol) of neptunium (IV). The solution turned from green to yellow and a yellow powder precipitated. The product was filtered, washed with ethanol, and pumped dry for several days at about 60° to produce 0.55 g (0.78 mmol 68%) of bis(tetraethylammonium)neptunium hexachloride.

1,1'-Di-*t*-butylneptunocene: In an inert atmosphere glove box approximately 0.20 g (5 mmol) of potassium was added to a solution of 0.266 g (1.66 mmol) *t*-butylcyclooctatetraene in 30 mL of THF. The solution was stirred for several hours and added to a stirred suspension of 0.53 g (0.75 mmol) of bis(tetraethylammonium)neptunium(IV) hexachloride in 20 mL of THF. The mixture was stirred for several

hours and the solvent was removed *in vacuo*. The product was dissolved in approximately 20 mL of toluene, filtered, and the solvent was removed *in vacuo*. The resulting green-brown solid was washed with pentane yielding approximately 0.15 g (36%) of 1,1'-di-*t*-butylneptunocene. ^{1}H NMR: (THF-d_8, 25 ^{o}C) -5.15 (s, 150 Hz).

1,1'-Di-*t*-butylplutonocene: The same procedure was used as that for the neptunocene except that 0.389 g (0.54 mmol) of the hexachloride salt and 0.174 g (1.09 mmol) of *t*-butylcyclooctatetraene were used and the yield of the blood red product was approximately 0.12 g (40%). uv-vis: (THF) 412, 421, 456 nm. ^{1}H NMR: (THF-d_8) 2.15 (s, 9H), 10.2 (m, 3H, H-4 + H-5), 9.9 (d, 2H, H-2), 9.8 (m, 2H, H-3). ^{13}C NMR: (THF-d_8, DEPT 135) 95.3, 95.1, 94.0, 89.8, 35.3.

Reduction of neptunocene and plutonocene: Reduction was carried out by treating a THF-d_8 solution of the neptunocene or plutonocene with potassium and loading the resulting solution into an NMR tube which was then sealed. In the case of neptunium the reduction product is a violet-red, whereas for plutonium it is light green. ^{1}H NMR of potassium bis(*t*-butyl[8]annulene)plutonate(III): (THF-d_8, 19.3 ^{o}C) -2.55 (s), 11 (s), 12.2 (s), 13.8 (s), 14.3 (s). ^{1}H NMR of potassium bis(*t*-butyl[8]annulene)neptunate(III): (THF-d_8, 25 ^{o}C) s 4.12 (s,9H), -6.0 (t, 1H, H-5), -7.1 (t, 2H, H-4), -8.0 (d, 2H, H-2), -8.4 (t, 2H, H-3).

Electron Exchange Studies: NMR tubes for uranocene exchange were

prepared by making a THF solution of a mixture of the uranium(III) and uranium(IV) compounds. NMR tubes for plutonium exchange were prepared by partially reducing a THF solution of the tetravalent compound in THF-d_8 and loading this solution directly into the NMR tube. NMR tubes for neptunium exchange were prepared by partially oxidizing the neptunium(III) compound with teflon.

References

1. Billian, F.; Folcher, G.; Marquet-Ellis, H.; Rigney, P.; Saito, E. *J. Am. Chem. Soc.* **1981**, *103*, 5603.

2. Personal Communication with S. A. Kinsley.

3. The ESR was taken at 4 K and indicated a paramagnetic compound that was not a uranium(IV) species. The mass spectrum gave a parent ion for uranocene.

4. Karraker, D. G.; Stone, J. A.; Jones, E. R., Jr.; Edelstein, N. *J. Am. Chem. Soc.* **1970**, *92*, 4841.

5. Streitwieser, A., Jr.; Dempf, D.; La Mar, G. N.; Karraker, D. G.; Edelstein, N. *J. Am. Chem. Soc.* **1971**, *93*, 7343.

6. Solar, J. P.; Burghard, H. P. G.; Banks, R. H.; Streitwieser, A., Jr.; Brown, D. *J. Am. Chem. Soc.* **1980**, *19*, 2186.

7. The argument is described in reference 4 although it incorrectly states that a J=0 groundstate implies diamagnetism.

8. Starks, D. F.; Streitwieser, A., Jr. *J. Am. Chem. Soc.* **1973**, *95*,

3423.

9. The preparation is described in reference 6 but the green color indicates that it is the plutonium(III) compound. Presumably on preparation of the powder pattern capillary there was sufficient oxidation to produce a pattern which matched that of bis(tetramethyl)uranocene.

10. Karraker, D. G.; Stone, J. A. *J. Am. Chem. Soc.* **1974**, *96*, 6885.

11 This is mentioned in reference 4 but the stability is probably similar to that of uranocene which, although originally worked up in degassed water, does decompose with a half life of 20 hours in THF containing 1 Molar water.

12 Eisenberg, D. C.; Kinsley, S. A. Streitwieser A, Jr. Submitted for Publication *J. Am. Chem. Soc.*

13 Katz; Seaborg; Morss. *The Chemistry of the Actinide Elements*, 2nd Ed.; Chapman and Hall: New York, 1986; Vol 1. p 468.

14 In several attempts it was observed that the product resulting from bubbling HCl into an aqueous neptunium(IV) solution varies in color, usually from white to yellow, and that the x-ray powder pattern calculated contains the lines reported as well as some additional lines. Kot, W. K. Personal Communication.

15 Luke, W. D.; Streitwieser, A., Jr. In Lanthanide and Actinide Chemistry and Spectroscopy; Edelstein, N. M., Ed.; ACS Symposium Series 131; American Chemical Society: Washington, DC, 1980; pp 93-140.

16 Just below the coalescence temperature the width of the resonances is roughly directly proportional to the difference in chemical shift of the two species involved as well as to the rate of exchange. Thus if the rate of exchange is the same in the uranium system as in the ytterbium system, the coalescence temperature will be much lower in the uranium system due to the smaller difference in chemical shift between the two exchanging species.

17 Uranocene, which is a highly symmetric compound has a ^{1}H NMR resonance which is several times broader than most organo-uranium(IV) compounds including the uranium half-sandwich compound. It also has a broader NMR resonance than most substituted, and therefore lower symmetry, uranocenes.

18 Blake, P. C.; Lappert, M. F.; Atwood, J. L.; Zhang, H. *J. Chem. Soc., Chem. Commun.* **1986**, 1148.

19 Kot, W. K.; Shalimoff, G. V.; Edelstein, N. M.; Edelman, M. A.; Lappert, M. F. *J. Am. Chem. Soc.* **1988**, *110*, 986.

20 Kot, W. K.; Shalimoff, G. V.; Edelstein, N. M. Unpublished Results.

21 Personal Communication with W. K. Kot.

22 If the molecule has pseudo D_{8h} symmetry and a d ground state then the ground state should be degenerate.

Chapter 4: Reduction of Biuranocenylene

Introduction

Bis(1,1'-bicyclooctatetraenyl)diuranium, biuranocenylene (Fig. 4.1), was first synthesized by Miller in 1981.[1] The ligand was prepared by cuprous chloride coupling of cyclooctatetraenylmagnesium bromide; this method was found to be superior to the previously reported synthesis[2] involving reaction of cyclooctatetraenyllithium with bromocyclooctatetraene.

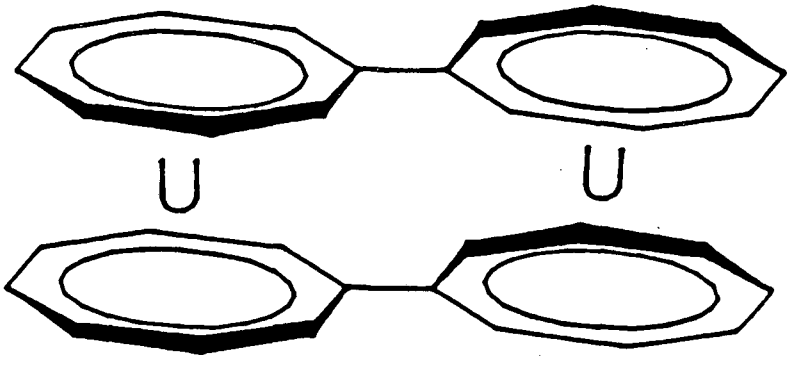

Figure 4.1: Biuranocenylene

Biuranocenylene was then prepared by addition of 2.6 mmol of uranium tetrachloride to a solution of 5.3 mmol of bicyclooctatetraenyl dianion in THF. Hexane extraction yielded 1,1'-bis(cyclooctatetraenyl)uranocene (32%) and THF extraction yielded biuranocenylene (45% yield based on UCl_4 and 22.6% yield based on bicyclooctatetraenyl). Biuranocenylene was characterized primarily by its mass spectrum, which contains the parent ion, and by its ^1H NMR spectrum

which at 30 °C contains seven peaks at -35.3, -37.1, -41.1, -41.5, -42.6, -47.2, and -97.3 ppm, indicating that the rings are twisted; the far upfield peak near -100 ppm presumably corresponds to the 2-endo protons which are pointed in toward the two uraniums. The bending of the rings is presumably due to the fact that if coplanar the hydrogens adjacent to the ring-ring juncture would be less than 1 Å apart (Fig. 4.2).

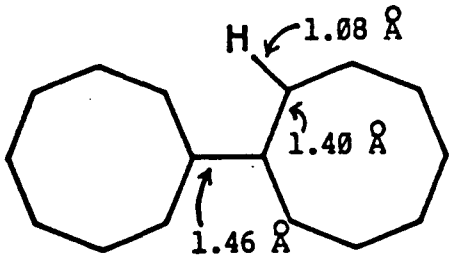

Figure 4.2: Assumed Ligand Geometry in Biuranocenylene

The synthesis of biuranocenylene was altered by Hsu-Kun Wang.[3] Her preparation involved addition of bicyclooctatetraenyl dianion to a THF solution of UCl_4 followed by hexane extraction to produce 1,1' bis(cyclooctatetraenyl) uranocene in 15% yield. Addition of potassium yielded the tetraanion of this uranocene, which was subsequently added to a THF solution of UCl_4. THF extraction yielded biuranocenylene in unreported yield. Unlike Miller, she was able to obtain satisfactory elemental analysis on the product.

Synthesis of Compounds

My attempts at synthesis of biuranocenylene began with Miller's

synthesis of bicyclooctatetraenyl using the CuCl induced coupling of COTMgBr. This reaction typically goes in moderate yield of about 40%. These moderately low yields seem to be typical of reactions with COT, although this yield could probably be improved by using high vacuum sublimation as the main method of purification. The resulting bicyclooctatetraenyl appears to be thermally unstable at room temperature over several weeks, although it is quite stable at a typical refrigerator temperature of about 5 ^{o}C.

The synthesis of biuranocenylene itself was based on the method of Hsu-Kun Wang, although a more straightforward method was used. This method involves reduction of bicyclooctatetraenyl with excess potassium to its purple dianion, followed by addition of the dianion to a THF solution of UCl_4. The resulting di(cyclooctatetraenyl)uranocene was then filtered and reduced with a slight excess of potassium to the brown tetraanion. This solution was then added to UCl_4 in THF to produce biuranocenylene.

One attempt was made at using Miller's method of synthesis; this was unsuccessful. With both methods the yield of biuranocenylene is highly dependent on the quality of the UCl_4.

Purification of the product is difficult owing to its low solubility and reluctance to crystallize. The present method involves washing the product with hexane to remove excess ligand, grease, and di(cyclooctatetraenyl)uranocene. Excess UCl_4 and UCl_3 was removed by washing the remaining solid with a mixture of THF and hexane with THF soxhlet extraction yielding biuranocenylene. Although it has been reported that biuranocenylene is thermally unstable, I have never found this to be so. It should be noted that addition of LAH or KH to

a THF solution of UCl_4 and bicyclooctatetraenyl produces biuranocenylene in one step but containing several organometallic impurities.

Reduction of Biuranocenylene

The ^1H NMR spectrum of biuranocenylene with peaks at -36.3, -38.0, -42.0, -42.3, -43.5, -48.0, and -99.4 is shown in A of Figure 4.3. Its partial reductions by potassium in THF-d_8 gave the ^1H NMR spectra shown in B-E of Figure 4.3. The first reduction gave spectrum B with six relatively sharp resonances at -34.8, -37.6, -38.8, -40.1, -42.6, -46.5, and a broad far upfield resonance at -85.3 ppm. The appearance of only seven peaks different from those in A demonstrates a rapid intermolecular electron exchange between biuranocenylene and its reduction product in close analogy to the other bis([8]annulene) f-element systems mentioned in this thesis. The broadening of the far upfield resonance relative to the other resonances is attributed to the greater chemical shift difference between the biuranocenylene 2-endo proton and the reduced biuranocenylene 2-endo proton compared to other ring hydrogens.

Further reduction results in spectrum C which consists of 6 broad peaks at -37.3, -38.0, -42.7, -43.5, and -48.6 ppm in an approximate ratio of 1:1:2:1:1 with the far upfield resonance now being too broad to observe. D is a spectrum of C at higher temperature; the broad resonances in C have sharpened considerably indicating exchange in the in the near fast region to have increased. Further reduction results in spectrum E. The far upfield resonance is seen to have reappeared

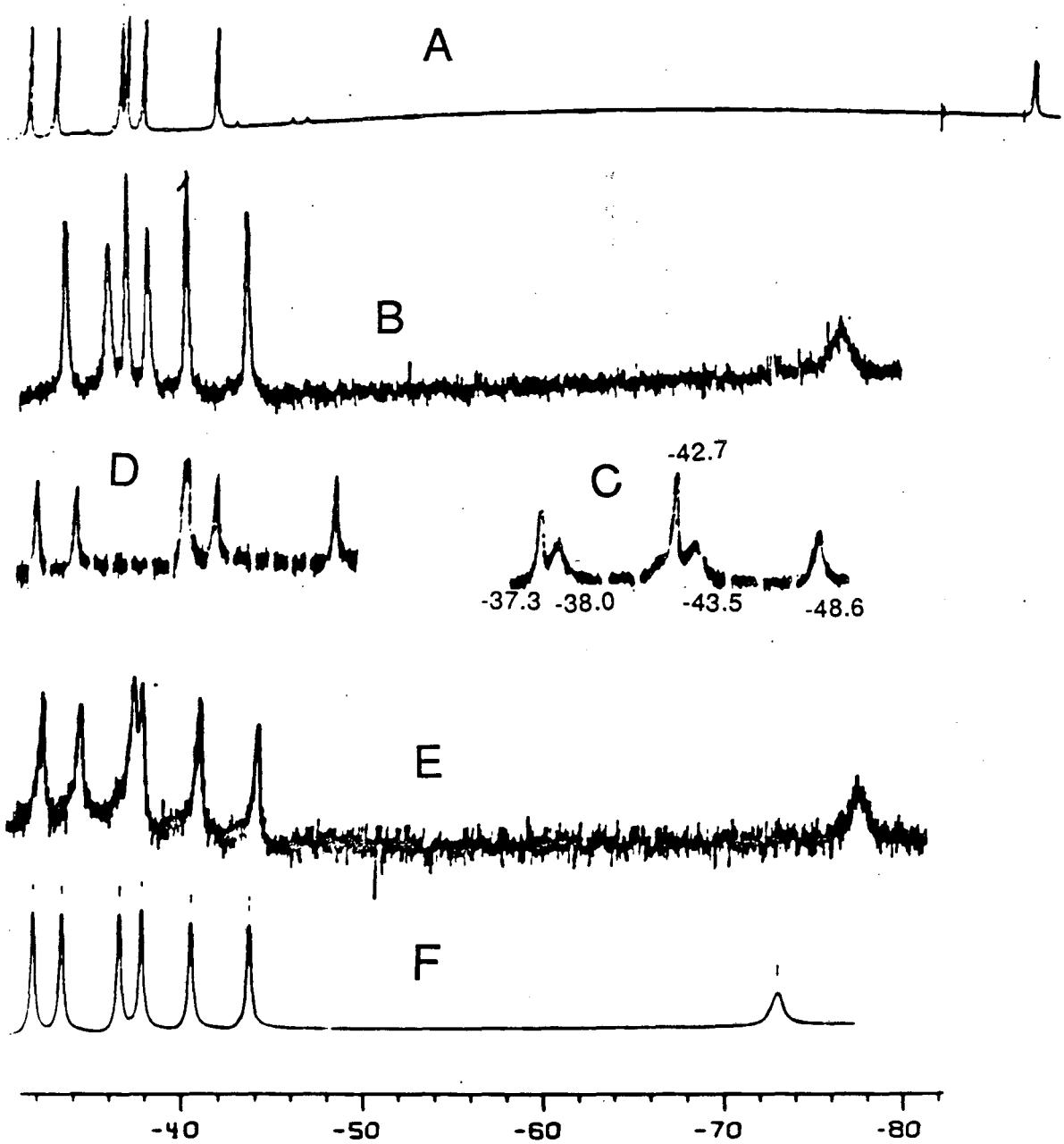

Figure 4.3: ^{1}H NMR Spectra of the Reduction of Biuranocenylene (the scale at the bottom is only approximately correct)

and shifted over 20 ppm downfield from the far upfield resonance of biuranocenylene. The downfield peaks have sharpened and the third peak in C which integrates at twice the area of the other peaks has begun to split.

Complete reduction results in spectrum F, which still shows only seven resonances, six sharp peaks at -31.9, -33.5, -36.6, -37.8, -40.4, -43.5, and a slightly broader far upfield peak at -71.8 ppm. The two joined cyclooctatetraene rings are still equivalent, meaning that intramolecular electron exchange is fast on the NMR time scale. This reduction product is the 1-electron product as evidenced by the fact that the peaks are relatively sharp (on the order of 70 Hz in contrast to reduced uranocene and reduced methyluranocene, both of which have resonances for the ring peaks of about 200 Hz at 1/2 height). This narrowness of the peaks also indicates that the uraniums are equivalent on the electronic time scale. (If the uraniums are not equivalent electronically, the width of the reduced biuranocenylene resonance should be the average of the width for a substituted uranocene, approximately 90 Hz, and that of previously mentioned reduced uranocene resulting in an average of approximately 150 Hz.) The visible spectrum of reduced biuranocenylene was examined to check this conclusion.

The visible spectrum of biuranocenylene (B in Fig 4.4) is similar to that of dimethyluranocene (A in Fig 4.4). If the reduction product were valence localized on the visible time scale then the visible spectrum of the reduction product would be expected to resemble a superposition of the visible spectrum of uranocene and that of the uranocene reduction product, which has a long UV tail into the

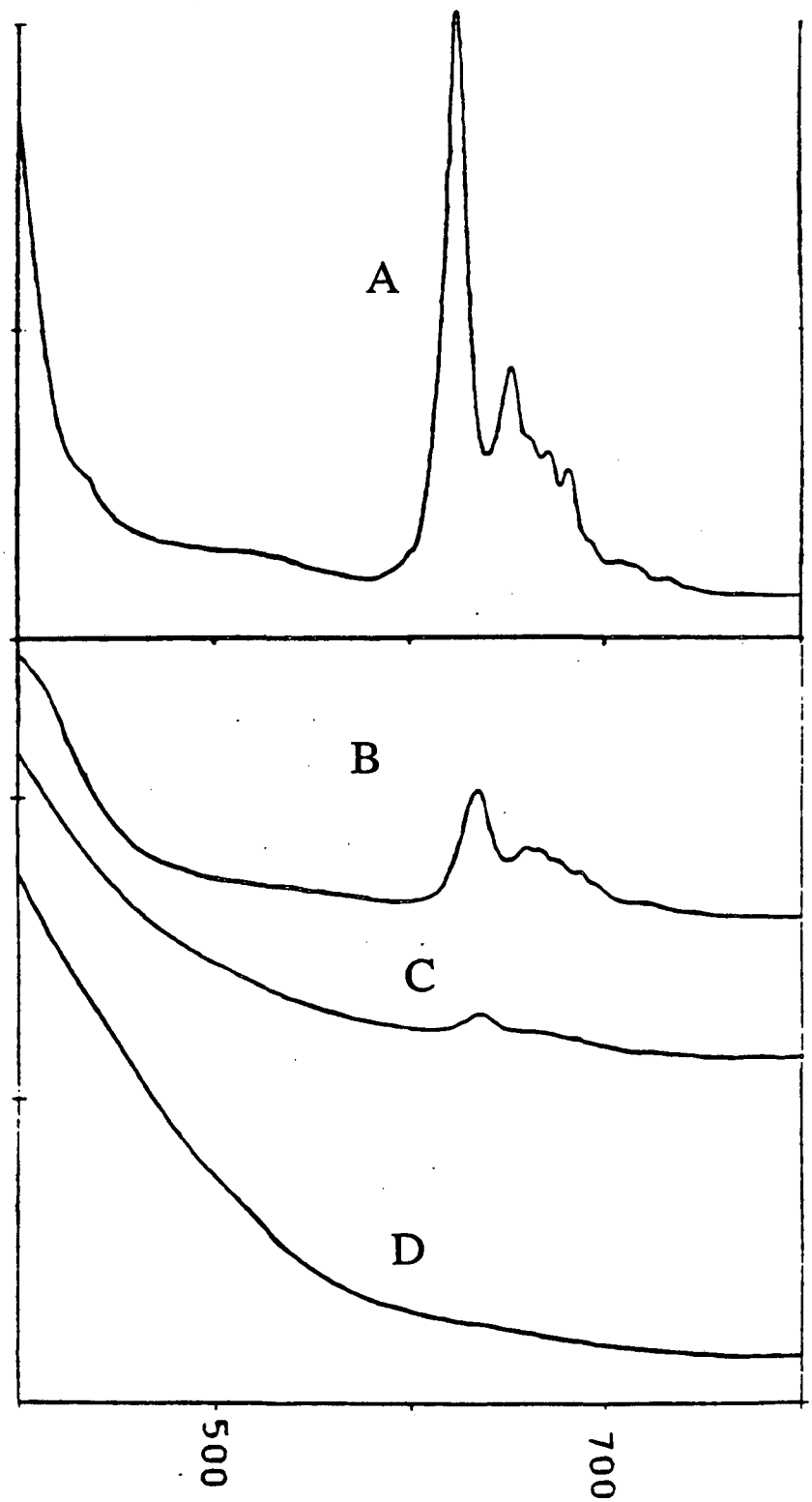

Figure 4.4: Visible spectra of dimethyluranocene (A), and reduction of biuranocenylene (B, C, and D)

visible region. The reduction of biuranocenylene is shown in C, D, and E of Figure 4.4 where spectrum C represents partial reduction and spectrum D represents complete reduction. The characteristic uranocene cascade of peaks is seen to diminsh and finally disappear, and the tail in the visible is seen to increase, indicating that the mixed valence compound is not valence localized on the visible time scale. That is, we conclude that the reduction product has electronically equivalent uraniums in which the five 5f electrons are delocalized such that each uranium has an intermediate oxidation state of 3 1/2.

Perspective on Biuranocenylene

A great deal of interesting work remains to be done with biuranocenylene or some similar bis([8]annulene) dimetalic f-element system, such as obtaining a crystal structure of the mixed metal compound, examining its electrochemical characteristics, preparing mixed-metal compounds, preparing bimetallic cerium compounds, etc. The work thus far, however, has been very difficult for several reasons. First, I have not been able to obtain pure biuranocenylene in good yield. The key to improving this reaction may be to use Miller's method of preparation using purified UCl_4 (probably by refluxing with thionyl chloride followed by THF extraction). Unfortunately this method is not useful in obtaining mixed metal systems. On that front, my attempts at obtaining a mixed metal uranium-cerium compound met with some success although I was not able to isolate the product; attempts at obtaining a uranium-ytterbium compound were unsuccessful.

The second major problem with biuranocenylene is its very low

solubility which makes it quite difficult to work with. One might consider making a substituted biuranocenylene, but only the 5,5′ substituted compound would be of interest (nonsymmetric substitution of bicyclooctatetraenyl would lead to a plethora of biuranocenylene isomers), and that is quite difficult to make. In his thesis Miller suggested several other ligand systems but these require rather extensive syntheses and the eventual yield of the ligands is generally less than 10%.

A final difficulty with this system is the instability of the biuranocenylene reduction product. In a sealed NMR tube it decomposed overnight. One might hope that further purification of it would lead to greater stability, but the NMR sample was prepared from microcrystals of the reduction product which should be relatively pure.

I do have a suggestion for this system, although it would be difficult to extend to mixed metal systems. If UCl_4 were added to a solution containing bicyclooctatetraenyl dianion and cyclooctatetraene

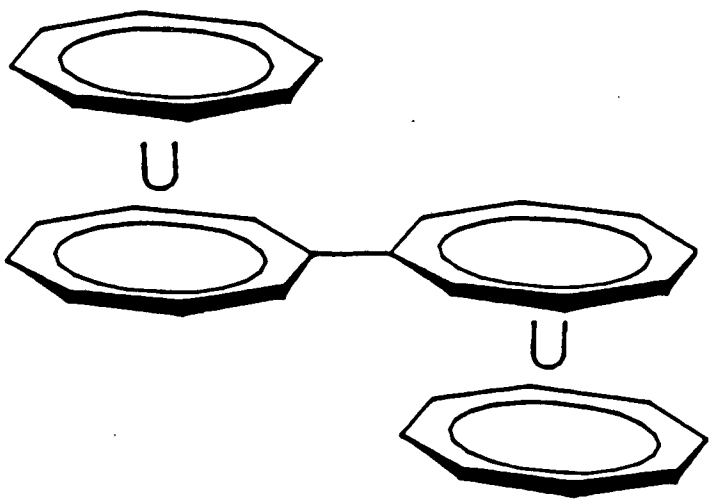

Figure 4.5: Biuranocene

dianion in some optimized ratio, the compound in Figure 4.5, which by analogy to the ferrocene sytem would be called biuranocene, might be obtained. Unfortunately, uranocene and biuranocenylene would probably also be obtained, but the desired product, having lower symmetry, might be considerably more soluble than uranocene or biuranocenylene and thus not that difficult to separate from those side products. In addition to greater solubility, its reduction product might be more stable because the steric interactions between the endo hydrogens of the rings would be significantly diminished.

Experimental

Synthesis of BrCOT: A predried 500 mL, 3-necked flask containing a magnetic stir bar and fitted with a dropping funnel and gas inlet was connected, via gauche tubing, to a predried Schlenk flask containing 50 g (0.45 mol) of potassium t-butoxide and flushed with argon. COT (43.5 g, 0.418 mol) was syringed in to the flask, and 180 mL of dry CH_2Cl_2 was added via cannula. The resulting solution was stirred at -78 ^{o}C. Br_2 (72 g, 0.45 mol) in 180 mL of dry CH_2Cl_2 was added dropwise over 20 min, and then stirred an additional 10 min. The solution was then allowed to warm, and a small portion of potassium t-butoxide was added through the gauche tubing. Upon initiation of the reaction, as indicated by the white t-butoxide turning brown, the flask was placed in a -35 ^{o}C calcium chloride-water-dry ice bath. The remaining *t*-butoxide was added in portions over the period of 2 hrs while making sure the resulting mixture did not warm up. After the addition was complete the reaction mixture was stirred an additional 1 hr and

allowed to warm to 0 ^{o}C. (If the flask heated up at this time it was again placed in the $CaCl_2$ bath and stirred an additional hour.) The reaction mixture was stirred for 30 min at 0 ^{o}C and cold water was added. The mixture was then poured into an erlenmeyer flask along with several ether washings from the 3-necked flask. This mixture was stirred and allowed to stand until the solid had collected at the bottom. The organic solution at the top was decanted into another flask, and more ether was added to the initial erlenmeyer. The stirring and decanting procedure was repeated for two portions of ether. The decantant liquid was separated using a seperatory funnel, dried by anhydrous magnesium sulfate, and filtered. Solvent was removed from this solution using a rotovap, making sure that the solution did not warm above 30 ^{o}C. When the volume was reduced to about 75 mL, the solution was fractionally distilled at about 10 microns, affording 52.75 g (69%) of BrCOT. It is possible to partially separate the COT from the BrCOT, but the BrCOT fraction usually contains about 10% COT. The two are generally separated by the next reaction, and their ratio can be determined by NMR integration with the COT peak appearing at 5.73 ppm in acetone-d_6. ^{1}H NMR: (acetone-d_6, 400 Mhz) 6.23 (s), 5.88 (m), 5.84 (m), 5.67 (m).

Preparation of bicyclooctatetraenyl: A predried 300 mL 3-necked flask containing a magnetic stir bar was fitted with a septum, a dropping funnel, and a gas inlet. Magnesium turnings (5 g, 0.2 mol) were added and the system was evacuated and back filled with argon. The flask was charged with 125 mL of dry THF and a few drops of ethylene dibromide were added to initiate the grignard. The dropping

funnel was charged with 24.0 g (0.13 mol) of COTBr in 75 mL of dry THF. The flask was cooled to 0 ^{o}C and 5 mL of the solution was added. Upon initiation of the Grignard as indicated by a change in color, the remaining COTBr solution was added dropwise over the period of 15 min. The resulting brown solution was stirred for 1 hr, allowed to warm to room temperature, and stirred an additional 15 min. The stirring was stopped, the solid was allowed to settle, and the solution was added dropwise, via cannula, to a Schlenk flask containing a stirred suspension of 26 g (0.26 mol) predried CuCl in 200 mL of dry THF at -78 ^{o}C. About 75 mL of THF was then added to the 3-necked flask, and the mixture was stirred, allowed to settle, and the solution was added dropwise to the Schlenk flask. This mixture was stirred for 2 hrs, allowed to warm to 0 ^{o}C, stirred an additional 30 min., and quenched with water. The resulting mixture was filtered, hexane was added, and the organic layer was isolated using a separatory funnel. The orange solution was dried by anhydrous magnesium sulfate, filtered, and the solvent was removed by rotovap, and later vaccum line, making sure the temperature of the solution did not rise above 30 ^{o}C. The orange solid was recrystalized from ether. Pure product could be obtained by vacuum sublimation affording 2.98 g (6%) of product, mp 124.5-125.5 ^{o}C, NMR: (acetone-d_6, 400 MHz) 5.85 (m).

Preparation of Biuranocenylene: In an inert atmosphere glove box potasssium (about 0.25 g, 6.4 mmol) was added to a solution of 0.50 g of bicyclooctatetraenyl (2.4 mmol) in 50 mL of dry THF. The solution was stirred for 2 hr and it turned purple. The resulting solution was added dropwise, by pipette, to a stirred solution containing 0.5 g of

UCl_4 (1.3 mmol) in 50 mL of THF. The solution turned brownish green and was stirred an additional hour. This solution was filtered, and to the resulting dark green solution was added 0.2 g (5 mmol) of potassium. The solution was stirred for several hours and eventually turned brown. This solution was added dropwise to a stirred solution containing 0.6 g of UCl_4 (1.6 mmol) in 50 mL of THF. The resulting greenish brown solution was stirred overnight, the solvent was removed *in vacuo*, and the resulting solid was washed with hexane to remove excess ligand, grease, and di(cyclooctatetraenyl)uranocene. The remaining green solid was soxlet extracted for several days with THF. The extractant was washed with a mixture containing 20 mL of dry THF and 100 mL of dry hexane in order to remove any UCl_4 still present. Yield of the remaining green biuranocenylene was 0.15 g (14%). NMR: (THF-d_8, 20 ^{o}C) -36.3 (s), -38.0 (s), -42.0 (s), -42.3 (s), -43.5(s), -48.0 (s), -99.4 (s); peaks are all approximately 90 Hz at half-height.

Reduction of Biuranocenylene: THF-d_8 solutions of biuranocenylene were reduced by stirring with potassium and then loading and sealing the NMR tube, or by melting potassium onto the top of the NMR tube and adding the biuranoceneylene solution. In the latter case reduction was carried out by inverting the tube for a given length of time and monitoring the reduction by NMR. Complete reduction of biuranocenylene was obtained by potassium reduction of a THF solution containing approximately 50 mg of biuranocenylene and also containing a few drops of diglyme. The brown product was filtered and slow diffusion of liquid hexane yielded microcrystals of the product. A ^{1}H NMR was obtained, but within two days the product in the NMR tube and the

remaining crystals were no longer soluble in THF. ^{1} NMR of biuranocenylene reduction product: (THF-d_8, 20 ^{o}C) -31.9 (s), -33.5 (s), -36.6 (s), -37.8 (s), -40.4 (s), -43.5 (s), -71.8 (s). The first six peaks are approximately 90 Hz at half-height; the far upfield peak is about 120 Hz.

References

1. Miller, M. J.; Streitwieser, A., Jr. *J. Organomet. Chem.* **1981**, *209*, C52.

2. Edwards, J. D.; Howard, J. A. K.; Knox, S. A. R.; Riera, V,; Stone, F. G. A.; Woodward, P. *J. A. Chem. Soc., Dalton Trans.* **1976**, 75.

3. Wang, H-K unpublished results.

Chapter 5: Structures of Organo-f-Element Compounds Differing in the Oxidation State of the f-Element: Crystal Structures of Bis([8]annulene) Complexes of Ytterbium(III), and Uranium(III)

Introduction

The X-ray crystal structure of uranocene was solved in 1969;[1] it was the first crystal structure of an organo-f-element compound. At that time the referees were even skeptical that positions of carbon atoms could be determined in a uranium compound because carbon diffracts X-rays so much weaker than uranium does. Three years later the structure of thorocene was solved,[2] its main difference between the uranocene structure being a slightly larger metal-carbon distance.

The first bis([8]annulene)lanthanide structure solved was that of potassium bis([8]annulene)cerate(III).[3] For quite a few years this was the only bis([8]annulene)lanthanide structure solved, and the only additional actinide structures were those of substituted uranocenes. Of these, the structure of bis(1,3,5,7-tetramethyl)uranocene[4] is of particular note because each of the methyl groups is bent in toward the uranium by about 4°. It was argued that this bending was to orient the carbon π orbitals toward the uranium atom (Fig. 5.1).

In two articles[5] Raymond *et. al.* noted that if the metal ionic radius for the ten coordinate metal was subtracted from the metal carbon distance, then the difference obtained, the COT dianion ionic radius, did not vary significantly (Table 5.1). This was contrasted with the fact that in transition metals the metal carbon distance can not be divided into a metal ionic radius and a ligand ionic radius.

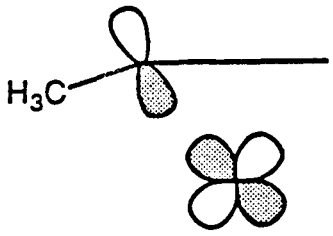

Figure 5.1: Effect of Bending the Methyl Group on the Metal-Ligand π Overlap

Table 5.1: Metal-Carbon Distances for COT Complexes (Table of Raymond and Eigenbrot)[5b]

compound	R(M-C) Å	metal ionic radius Å	Calc. COT^{-2} ionic radius Å
$U(COT)_2$	2.647	1.06	1.59
$U(Me_4COT)_2$	2.658	1.06	1.60
$Th(COT)_2$	2.701	1.13	1.57
$K(dig)Ce(COT)_2$	2.742	1.25	1.49
$[Ce(COT)Cl*2THF]_2$	2.710	1.20	1.51
$Nd(COT)_2THF_2$	2.68	1.18	1.50
$Nd(COT)_2$	2.79	1.18	1.61
	2.68	1.16	1.52
$Zr(COT)_2*THF$	2.461	0.89	1.57
Ti(COT)Cp	2.323	0.76	1.56
$[K(dig)]_2(Me_4COT)$	3.003	1.46	1.54
$K_2(COT)(dig)$	2.98	1.38	1.60
	3.05	1.46	1.59
$Rb_2(COT)(dig)$	3.10	1.52	1.58
	3.15	1.56	1.59

This is particularly true of ferrocene in which oxidation of the compound results in a slightly longer metal carbon bond even though the ionic radius of iron(III) is significantly shorter than that of iron(II). On the basis of the results from these bis([8]annulene)f-element compounds as well as results from other organo-f-element compounds, Raymond *et. al.* argued that the metal ligand distance could be estimated to a high degree of accuracy from summing the metal and ligand ionic radii. They also concluded that "within the limits of our structural criteria the bonding in organoactinides and -lanthanides is ionic."

In the last few years several more [8]annulene and bis([8]annulene) structures have been solved including the structure of potassium bis([8]annulene)ytterbate(II),[6] 1,1'-dimethylcerocene,[7] and the uranium half-sandwich, [8]annuleneuranium(IV) dichloride bis(THF).[8] In this chapter the structures of potassium bis([8]annulene)ytterbate(III) and potassium bis(methyl[8]annulene)uranate(III) are also reported. With the solution of these new structures it is now possible to compare compounds which differ in oxidation state of the central metal but do not differ in coordination to the central metal. This comparison highlights the effect of oxidation state on structure; such a comparison had only been possible with the metalocenes.

Also, with the new structures that are available it is appropriate to reexamine the argument of Raymond *et. al.* in order to determine how successful the ionic model is in describing the bonding in additional [8]annulene-f-element compounds.

The new crystal structures mentioned in this chapter were solved by Alan Zalkin.

Comparison of Structures: Bis([8]annulene) compounds of divalent and trivalent ytterbium

In Table 5.2 some pertinent data are listed for potassium bis([8]-annulene)ytterbate(III), 1, and for its reduction product potassium bis([8]annulene)ytterbate(II), 2. The structures of 1 and 2 are compared in Figure 5.2. The difference in the potassium-to-ring distance is probably due to the fact that the structure of 1 is of the diglyme adduct which is a better chelating agent than the glyme which coordinates 2, and results in the longer potassium-to-ring distance. An alternative explanation involves the greater anion polarizing capability of Yb(III) (*vide infra*).

The difference in metal-to-ring distance in the two compounds is more significant. Notice that there are two different metal-to-ring distances in 1 presumably because there is effectively more negative charge on the ring without the potassium than the one with the potassium. This effect is also seen in the uranium(III) compound (*vide infra*). The difference in the metal-to-ring distances in 1 and 2 is significant and can be explained primarily as a result of the difference in ionic radius of trivalent and divalent ytterbium; this subject is discussed more thoroughly in the discussion.

Bis([8]annulene) compounds of trivalent and tetravalent uranium

We were not able to obtain X-ray quality crystals of the uranocene reduction product, but the methyl group apparently provides a sufficient perturbation on the crystal packing of the system to promote

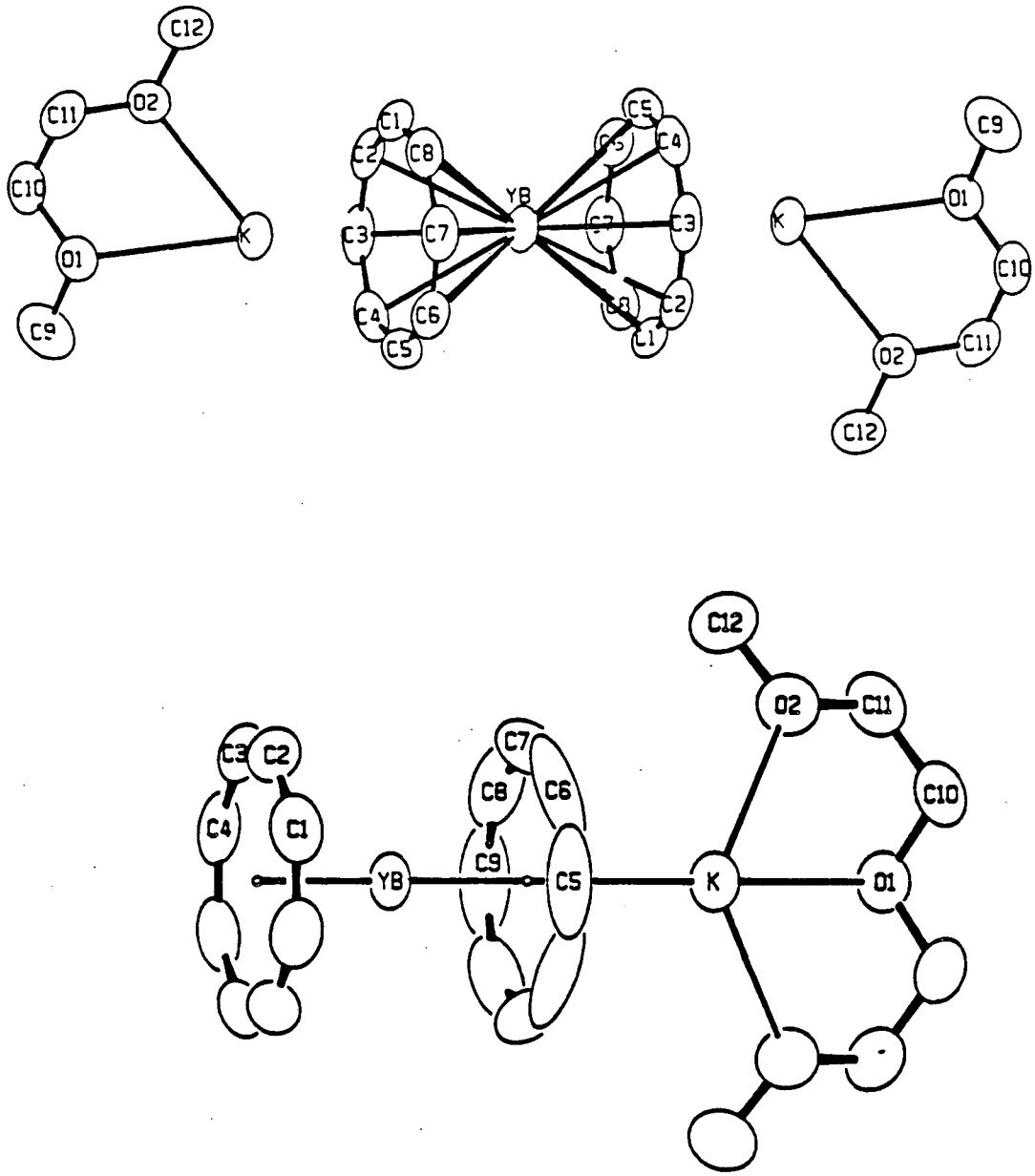

Figure 5.2: Comparison of X-ray Crystal Structures of Potassium Bis([8]annulene)ytterbate(II) (2) (above) and Potassium Bis([8]-annulene)ytterbate(III) (1)

growth of good crystals. This effect has also been seen in the cerocene system in which it was possible to grow crystals of dimethylcerocene but not of the unsubstituted compound.

The methyl group should be a minor perturbation on the metal-to-ligand distances in potassium bis(methyl[8]annulene)uranate(III), 3, as judged by the octamethyluranocene which has very similar metal-to-ligand distances to that of uranocene itself (Table 5.2). The angle of the methyl group can be compared to that of the previously solved structure of octamethyluranocene and 1.

Again, the ring with the coordinated potassium is 0.05 Å farther from the central uranium than is the other ring in 3. The difference in metal-to-ring distance between 3 and uranocene is slightly smaller than in the ytterbate system; this may be due to a greater difference between a divalent and trivalent central metal than between a trivalent and tetravalent central metal, or it may simply be due to small errors in the determined bond distances. Notice also how similar the uranium and cerium compounds of the same oxidation state are in terms of metal carbon bond distances with the cerium to ring distances being slightly longer than the uranium to ring distances (Table 5.2). The structures of 3 and uranocene are compared in Figure 5.2.

Discussion of the Ionic Bonding model

As mentioned in the Introduction, Raymond *et. al.* have used structural data to probe the relative degree of covalent bonding in structurally related metal complexes. By their method, an effective "ligand

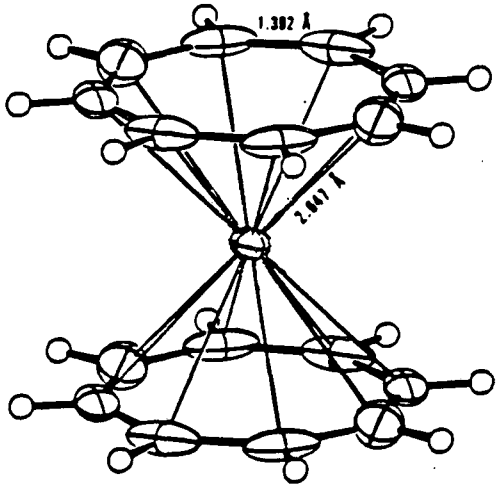

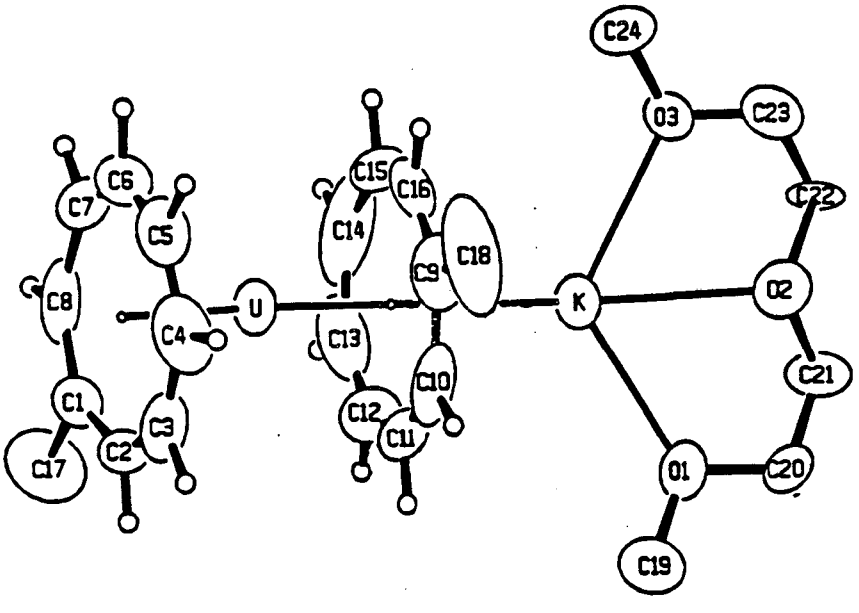

Figure 5.3: Comparison of X-ray Crystal Structures of Uranocene (above) and Potassium Bis(methyl[8]annulene)uranate(III)

radius" was calculated by subtracting the metal ionic radius (corrected for charge and coordination number) from the metal-ligand bond length. Based on the structures that were available at that time Raymond *et. al.* concluded that an ionic model based on the additivity of cation and anion radii was sufficient to rationalize the bonding in these complexes.

In the ten years since Raymond presented his argument, structural analyses of several additional cyclooctatetraene complexes have been obtained. We have updated his analysis to include these additional structures. Data from representative structures are summarized in Table 5.2.

With the addition of several structures as well as correction of some of the results in Table 5.1 it becomes apparent that there is a wider variation in the calculated COT dianion ionic radius than previously supposed. For values calculated from f-element-COT distances the calculated radius varies from 1.64 to 1.48 Å, and the radius calculated from the potassium-COT distance in #5 goes up to 1.75 Å. A good way of noticing the inadequacy of the simple ionic model is to compare COT ionic radii calculated from potassium-to-COT carbon distances for 8-coordinate diglyme adducts. The values vary from 1.48 Å to 1.75 Å, a considerable range.

If covalency in the bonding were responsible for these variations one would expect those compounds that are expected to have the highest degree of covalency in their bonding (i.e. the bis([8]annulene)-actinide(IV) compounds) to have shorter than predicted metal-carbon bonds resulting in smaller calculated COT ionic radii. This trend does not occur, but several trends in the data are apparent.

Table 5.2 Comparison of M-C Bond Lengths and COT Ionic Radii for Several Cyclooctatetraene Complexes

	Compound		Average M-C bond Length[a]	Formal Metal Ion C.N.	Metal Ionic Radius[b]	Effective COT Ionic Radius
1.	$U(C_8H_8)_2$		2.647(4)	10	1.08*	1.57
2.	$U(Me_4C_8H_4)_2$		2.658(4)	10	1.08*	1.58
3.	$(C_8H_8)UCl_2(NC_5H_5)_2$[c]		2.683	9	1.05	1.63
4.	$(C_8H_8)U(acac)_2$[c]		2.694	9	1.05	1.64
5.	$[K(diglyme)][U(MeC_8H_7)_2]$[c]	U	2.732	10	1.22*	1.51
		U	2.707	10	1.22*	1.49
		K	3.263	8	1.51	1.75
6.	$Th(C_8H_8)_2$		2.701(4)	10	1.13	1.57
7.	$(C_8H_8)ThCl_2(thf)_2$[c]		2.72	9	1.09	1.63
8.	$[K(diglyme)][Ce(C_8H_8)_2]$	Ce	2.747	10	1.25	1.50
		Ce	2.733	10	1.25	1.48
		K	3.166	8	1.51	1.66
9.	$[Ce(C_8H_8)Cl(thf)_2]_2$		2.710(2)	9	1.20	1.51
10.	$Ce(MeC_8H_7)_2$[c]		2.692(9)	10	1.07	1.62
11.	$[K(diglyme)][Yb(C_8H_8)_2]$[c]	Yb	2.614	10	1.10*	1.51
		Yb	2.598	10	1.10*	1.50
		K	3.191	8	1.51	1.68
12.	$[K(glyme)]_2[Yb(C_8H_8)_2]$[c]	Yb	2.741	10	1.26*	1.48
		K	3.017	7	1.46*	1.56
13.	$[Nd(C_8H_8)(thf)_2][Nd(C_8H_8)_2]$[d]		2.68(1)	10	1.19*	1.49
			2.79(1)	10	1.19*	1.60[e]
			2.68(1)	9	1.12	1.56
14.	$Zr(C_8H_8)_2 \cdot (thf)$		2.461(7)	9	0.90*	1.56
15.	$[(C_8H_8)TiCl(thf)]_2$[c]		2.382	8	0.77*	1.61
16.	$(C_8H_8)Ti(C_5H_5)$		2.323(4)	8	0.77*	1.55
17.	$[K(diglyme)]_2(Me_4C_8H_4)$		3.003(8)	8	1.51	1.49
18.	$K_2(C_8H_8)(diglyme)$[d]		2.98(2)	6	1.38	1.60[e]
			3.05(2)	7	1.46	1.59[e]
19.	$Rb_2(C_8H_8)(diglyme)$[d]		3.10(1)	6	1.52	1.58[e]
			3.15(1)	7	1.56	1.59[e]

Superscripts a-e and the * are explained in referenece 15.

First, similar structures yield similar COT radii. For example, uranocene in #1, thorocene in #6 and cerocene in #10, yield values of 1.57, 1.57, and 1.62 Å, respectively. Also, the uranium(III) in #5, the cerium(III) in #8, and the ytterbium(III) in #11 give values of 1.51 and 1.49 (for the inequivalent rings), 1.50 and 1.48, and 1.51 and 1.50 Å. This trend is also true for uranium and thorium half-sandwich compounds which give values of 1.63 Å in #4, 1.64 Å in #5, and 1.63 Å in #7.

Second, notice that the bis([8]annulene) tetravalent structures give values as just mentioned that average almost a tenth of an angstrom longer than those for the trivalent structures, and that the divalent structure in #12 gives a slightly smaller value. If covalency in the bonding were causing discrepancies in the calculated COT radius, then it would be expected that this trend would go in the opposite direction with the more covalent tetravalent structures having shorter, rather than longer bonds. We believe that the reason for this reverse trend is that repulsion between the COT rings becomes an important factor with the tetravalent metals, which, being smaller than the trivalent metals, forces the rings to be closer together.[7] Thus the ring-ring repulsion prevents the rings from getting closer to the central metal.

Also, notice the disparity between compound types. For example, when the COT ring in uranocene in #1 is replaced with two chlorine and two nitrogen ligands in #3, or four oxygen ligands in #4, the coordination around the uranium formally decreases from ten to nine, but the metal-COT carbon distance increases. This also occurs on going from thorocene in #6 to the nine-coordinate thorium half-sandwich in

#7. Apparently, although COT dianion is formally a ten-electron donor, in terms of ligand-ligand repulsions it is better considered to be a three-coordinate ligand. Similarly, cyclopentadienyl itself is perhaps better considered as a two-coordinate ligand as far as steric factors are concerned, although bulky cyclopentadienyl ligands act differently.

Next, notice that the bis([8]annulene) structures that have a coordinating potassium counterion give larger values for the COT ionic radius as calculated from the potassium-carbon distance than as calculated from the f-element carbon distance. This effect can be rationalized in the following manner. Highly charged cations such as U(III), Ce(III) and Yb(III) would tend to polarize the electron cloud of the cyclooctatetraene dianion to a greater degree than the univalent potassium. The dipole induced in the cyclooctatetraene dianion by the central metal would reduce the attraction to the coordinating potassium and result in a lengthened K-C bond distance. This is substantiated by the observation that the K-C distance, or more generally the r_{COT} derived from the potassium, is related to the polarizing capability of the central metal atom.[10] Complexes containing central metal atoms with the highest formal charge to ionic-radius ratio tend to have the largest K-based r_{COT}'s.

Finally it should be mentioned that there is some inconsistency in the metal ionic radii. These radii were either taken directly from Shannon's tables,[11] or, for those coordination numbers that are not listed in the tables, the data were obtained from linear interpolation using the coordination numbers that are listed in the tables.[12] The most obvious example of this inconsistency is in comparison of the

bis([8]annulene) compounds of cerium and uranium. The ionic radius for ten-coordinate cerium(III) is 0.03 Å longer than that of uranium(III), and as expected, the cerate has a metal-carbon distance 0.02 Å longer than its uranium counterpart. However, the ionic radius of ten-coordinate cerium(IV) is listed as being almost 0.05 Å shorter than that of uranium(IV) even though the metal-carbon bond in dimethylcerocene is almost 0.05 Å longer than that in uranocene. Obviously the ionic radius of cerium(IV) should be greater than that of uranium(IV).

In conclusion, the ionic model, as established by Raymond *et. al.*, is not capable of accurately predicting metal-carbon bond lengths in [8]annulene f-element compounds, but when the effects mentioned in this paper are taken into account, i.e. ligand repulsion, anion polarization, lower effective coordination number of COT dianion, the model does give reasonably good predictions of metal-carbon bond distances. Furthermore, we confirm the supposition of Raymond *et. al.* that covalency in the bonding does not manifest itself in metal-ligand bond distances, although it does in a wide variety of other physical properties.[13]

Experimental Section

Crystals of $(C_8H_8)Yb(III)(C_8H_8)K^*$ $(CH_3OCH_2CH_2OCH_2CH_2OCH_3)$ are orthorhombic, Pbca, with a = 16.1611(4), b = 14.219(5), c = 9.257(4) Å, at 23°C. For Z = 4 the calculated density is 1.539 g/cm^3. The structure was refined by full-matrix least-squares to a conventional R factor of 0.036, [2183 data, $F^2 > \sigma(F^2)$]. Yb-ring (centroid) distances are 1.84 and 1.90 Å.

Crystals of $(CH_3C_8H_7)U(III)(CH_3C_8H_7)K^*$ $(CH_3OCH_2CH_2OCH_2CH_2OCH_3)$ are monoclinic, $P2_1/c$, with a = 13.833(4), b = 9.989(3), c = 17.581(3) Å, β = 95.87(3)^o at 22°C. For Z = 4 the calculated density is 1.780 g/cm^3. The structure was refined by full-matrix least-squares to a conventional R factor of 0.038, [2209 data, $F^2 > 2\ \sigma(F^2)$]. U-ring (centroid) distances are 2.00 and 2.05 Å.

X-ray Diffraction. The air sensitive crystals were sealed inside quartz capillaries. A modified Picker FACS-I automated diffractometer equipped with a graphite monochromator and a Mo X-ray diffraction tube ($\lambda/(\Lambda\alpha/_1)$ 0.70930 Å) was used to collect sets of $\theta - 2\theta$ scanned X-ray diffraction intensities; the experimental details are given in the Appendix. The metal atom positions were deduced from three dimensional Patterson functions, and after least-squares refinement of the metal atoms, carbon and oxygen atoms were located from subsequent Fourier maps. The positional and anisotropic thermal parameters of all of the non-hydrogen atoms were adjusted with the use of a full-matrix least-squares refinement procedure. Hydrogen atom parameters were included with isotropic thermal parameters, but not all of them could be refined. In the Yb complex, the hydrogen atom locations were estimated when they were not observed in the difference electron density maps, and with the exception of five hydrogen atoms (on the ring between the Yb and K atoms), were allowed to refine with no restrictions; the five hydrogen atoms were included with fixed atomic parameters and not refined. In the U complex, all of the hydrogen atoms were included with fixed parameters and were not varied; some 55 low-angle data, whose $\sin\theta/\lambda < 0.15$, were all deleted from the U complex data set, as

a few of them exhibited large discrepancies between the observed and calculated values which were attributed to an imperfect absorption correction on an irregularly shaped crystal. With the exception of ORTEP, all computer programs are our own; scattering factors and anomalous dispersion terms were taken from International Tables.[14]

References

1. Zalkin, A.; Raymond, K. N. *J. Am. Chem. Soc.* **1969**, *91*, 5667.

2. Avdeef, A.; Raymond, K. N.; Hodgson, K. O.; Zalkin, A. *Inorg. Chem.* **1972**, *11*, 1083.

3. Hodgson, K. O.; Raymond, K. N. *Inorg. Chem.* **1972**, *11*, 3030.

4. Hodgson, K. O.; Raymond, K. N. *Inorg. Chem.* **1973**, *12*, 450.

5. (a) Baker, E. C.; Halstead, G. W.; Raymond, K. N. *Structure and Bonding* **1976**, *25*, 23. (b) Raymond, K. N.; Eigenbrot, C. W., Jr. *Accts. Chem. Res.* **1980**, *13*, 276.

6. Kinsley, S. A.; Streitwieser, A., Jr.; Zalkin, A. *Organometal.* **1985**, *4*, 52.

7. Boussie, T. R.; Eisenberg, D. C.; Rigsbee, J. T.; Zalkin, A.; Streitwieser, A., Jr. in preparation.

8. Boussie, T. R.; Moore, R. M., Jr.; Brennan, J. T.; Zalkin, A.; Streitwieser, A., Jr. Submitted for Publication in *J. Am. Chem. Soc.*

9. The problem with this argument is that ytterbium(III), being much smaller than uranium(III) and cerium(III), should give a larger COT ionic radius than is found with cerium and uranium, but it does not.

10. Although, just as in reference 10, ytterbium(III) does not have a greater effect than uranium(III) and cerium(III)

11. Shannon, R. D. *Acta Cryst., A.* **1976**, 751.

12. The procedure was carried out by T. R. Boussie; see reference 7.

13. See the perspective section of chapter one of this thesis.

14. *International Tables for X-ray Crystallography*, Kynoch: Birmingham, 1974; Vol. 4.

15. (a) All values listed in Å. (b) From tables of Shannon and Prewitt, values marked with an * are interpolated values. (c) Structures added since Raymonds articles. (d) Multiple coordination sites. (e) Bridging ring.

Appendix: Crystallographic Data

Table 1. Crystallographic Summary and Data Processing for

	$(C_8H_8)Yb(C_8H_8)K\cdot C_6H_{14}O_3$	$(CH_3C_8H_7)U(CH_3C_8H_7)K\cdot C_6H_{14}O_3$
a, Å [a]	16.611(4)	13.833(4)
b, Å	14.219(5)	9.989(3)
c, Å	9.257(4)	17.581(3)
β °,	90.00(0)	95.87(3)
cryst syst	orthorhombic	monoclinic
space group	Pbca	$P2_1/c$
volume, $Å^3$	2186.4	2416.6
d(calcd),g/cm^{-3}	1.539	1.780
Z	4	4
temp (°C)	23	22
empirical formula	$C_{22}H_{30}O_3KYb$	$C_{24}H_{34}O_3KU$
f(000)	1004	1252
fw	506.63	647.67
color	blue	red
crystal size	0.18x0.21x0.25	0.20x0.25x0.26
abs coeff, cm-1	44.56	65.59
abs corr range	1.74-2.52	2.71-4.30
$\sin\theta/\lambda$, min,max	0.06,0.65	0.15,0.60
$hk\ell$ limits	h 0,21;k±18;ℓ-12,0	h±16;k 0,11;l-20,20
scan width, °2θ	1.30 + 0.693tanθ	1.50+0.693tanθ
no. of standards	3	3
no. reflctns between stds	250	200
standards corr range	0.98-1.04	0.97-1.06
no. scan data	5052	8544
no. unique reflections	2628	4279
no. non-zero wtd data	2183 ($F^2>\sigma$)	2209 ($F^2>2\sigma$)

p[b]	0.06	0.05
extinction k[c]	1.48×10^{-7}	1.75×10^{-7}
max % extinction corr	16.5%	16.5%
no. parameters	174	262
R (non-zero wtd dat)[d]	0.036	0.038
Rw[e]	0.043	0.043
R (all data)	0.046	0.109
Goodness of fit[f]	1.12	1.13
max shift/esd	0.006	0.003
max/min, diff map (e/Å^3)	0.83,-0.83	1.77,-2.39

(a) Unit cell parameters were derived by a least-squares fit to the setting angles of the unresolved MoKα components of 43 reflections ($20<2\theta<36$) for the Yb complex and 20 reflections ($22<2\theta<33$) for the uranium complex.

(b) In the least-squares, the assigned weight $w = 4F^2[\sigma^2(F^2)+(pF^2)^2]^{-1}$ F^2 is the observed structure amplitude and p is an assigned value that adjusts the weighted residuals of the strong reflections to be comparable to the weak ones.

(c) Simple extinction correction has the form $(Fobs)corr = (1+kI)Fobs$, where I is the uncorrected intensity and Fobs is the observed scattering amplitude.

(d) $R = \sum|(Fobs-Fcal|/\sum|Fobs|$

(e) $Rw = \sqrt{(\sum[\ w\ (|Fobs|-|Fcal|)]^2\ /\ \sum(w\ Fobs^2))}$

(f) σ_1 = error in observation of unit weight = $\sqrt{(\sum w[|Fobs|-|Fcal|]^2 /(no-nv))}$, where no is the number of observations and nv is the number of variables.

Table 2. Positional Parameters with Estimated Standard Deviations

$(C_8H_8)Yb(III)(C_8H_8)K\cdot(CH_3OCH_2CH_2OCH_2CH_2OCH_3)$

Atom	x	y	z
Yb	0.00992(2)	1/4	0.12447(3)
K	0.18141(9)	1/4	0.50650(15)
O1	0.24203(27)	1/4	0.7904(5)
O2	0.20094(26)	0.0838(3)	0.6510(4)
C1	0.0141(3)	0.2010(6)	-0.1478(6)
C2	-0.0299(4)	0.1313(4)	-0.0768(6)
C3	-0.0935(4)	0.1309(4)	0.0233(6)
C4	-0.1388(3)	0.2004(5)	0.0931(6)
C5	0.1656(6)	1/4	0.1573(12)
C6	0.1416(6)	0.1628(10)	0.1909(10)
C7	0.0847(8)	0.1232(5)	0.2783(12)
C8	0.0265(6)	0.1586(8)	0.3703(10)
C9	0.0036(5)	1/4	0.4083(10)
C10	0.2882(3)	0.1672(5)	0.8072(6)
C11	0.2341(4)	0.0848(4)	0.7924(6)
C12	0.1499(5)	0.0071(5)	0.6269(7)

$(CH_3C_8H_7)U(III)(CH_3C_8H_7)K\cdot(CH_3OCH_2CH_2OCH_2CH_2OCH_3)$

Atom	x	y	z
U	0.25530(4)	0.12337(5)	0.00889(2)
K	0.26172(19)	0.48195(28)	0.18729(15)
O1	0.0901(6)	0.6018(9)	0.2077(4)
O2	0.2570(6)	0.7528(9)	0.2376(4)
O3	0.4257(6)	0.6425(10)	0.1904(5)

C1	0.1845(9)	-0.1321(15)	-0.0119(6)
C2	0.1187(8)	-0.0436(14)	-0.0564(7)
C3	0.1251(10)	0.0554(14)	-0.1106(7)
C4	0.2011(14)	0.1193(17)	-0.1438(6)
C5	0.3025(14)	0.1010(17)	-0.1373(7)
C6	0.3669(10)	0.0220(19)	-0.0943(9)
C7	0.3636(10)	-0.0732(18)	-0.0422(8)
C8	0.2834(13)	-0.1421(16)	-0.0070(7)
C9	0.2640(13)	0.3960(17)	0.0130(6)
C10	0.1641(12)	0.3582(18)	0.0350(8)
C11	0.1319(9)	0.2711(17)	0.0864(9)
C12	0.1694(14)	0.1893(20)	0.1386(11)
C13	0.2554(22)	0.1438(16)	0.1659(9)
C14	0.3554(22)	0.1788(24)	0.1484(11)
C15	0.3913(9)	0.2664(19)	0.0968(10)
C16	0.3546(11)	0.3511(15)	0.0423(8)
C17	0.1398(12)	-0.2216(19)	0.0429(8)
C18	0.2602(21)	0.4893(19)	-0.0573(10)
C19	-0.0035(11)	0.5664(18)	0.1709(9)
C20	0.0878(10)	0.7267(14)	0.2467(7)
C21	0.1845(10)	0.7547(16)	0.2899(7)
C22	0.3492(9)	0.7888(14)	0.2728(7)
C23	0.4201(10)	0.7765(16)	0.2132(7)
C24	0.4969(10)	0.6245(18)	0.1388(9)

Table 3. Selected Distances (Å)

$(C_8H_8)Yb(C_8H_8)K\cdot C_6H_{14}O_3$		$(CH_3C_8H_7)U(CH_3C_8H_7)K\cdot C_6H_{14}O_3)$	
Yb - Ct1[a]	1.843	U - Ct1	1.999
Yb - Ct2	1.915	U - Ct2	2.045
Yb - C1	2.616(6)	U - C1	2.745(14)
Yb - C2	2.601(5)	U - C2	2.689(11)
Yb - C3	2.588(5)	U - C3	2.710(12)
Yb - C4	2.587(5)	U - C4	2.713(11)
		U - C5	2.725(12)
		U - C6	2.697(13)
		U - C7	2.680(14)
		U - C8	2.699(15)
Yb - C5	2.603(10)	U - C9	2.727(17)
Yb - C6	2.589(7)	U - C10	2.725(14)
Yb - C7	2.614(6)	U - C11	2.725(13)
Yb - C8	2.635(6)	U - C12	2.757(15)
Yb - C9	2.630(9)	U - C13	2.767(15)
		U - C14	2.746(13)
		U - C15	2.716(13)
		U - C16	2.691(13)
K - Ct2	2.670	K - Ct2	2.717
K - O1	2.814(5)	K - O2	2.849(10)
K - O2	2.734(4)	K - O1	2.715(9)
		K - O3	2.774(9)

[a] Ct represents the centroid of the atoms in the cyclooctatetraene rings.

Table 4. Selected Angles (•)

$(C_8H_8)Yb(C_8H_8)K\cdot C_6H_{14}O_3$				$(CH_3C_8H_7)U(CH_3C_8H_7)K\cdot C_6H_{14}O_3)$			
Ct1	- Yb	- Ct2	172.22	Ct1	- U	- Ct2	176.07
Yb	- Ct2	- K	163.93	U	- Ct2	- K	173.83
Ct2	- K	- O1	168.82	Ct2	- K	- O2	159.59
Ct2	- K	- O2	118.50	Ct2	- K	- O1	118.60
				Ct2	- K	- O3	114.57
O1	- K	- O2	60.05(9)	O1	- K	- O2	59.48(25)
				O2	- K	- O3	59.31(26)
O2	- K	- O2	119.56(17)	O1	- K	- O3	117.82(28)
K	- O1	- C10	107.3(3)	K	- O2	- C21	104.6(8)
				K	- O2	- C22	109.3(7)
K	- O2	- C11	119.3(3)	K	- O1	- C19	126.4(8)
K	- O2	- C12	121.6(4)	K	- O1	- C20	120.8(7)
				K	- O3	- C23	119.3(7)
				K	- O3	- C24	122.3(8)

Supplemental Table 3a. C-C, C-O and C-H distances (Å) in $(C_8H_8)Yb(C_8H_8)K\cdot(CH_3OCH_2CH_2OCH_2CH_2OCH_3)$

O1 - C10	1.412(6)	C7 - C8	1.387(16)	H8 - C8	0.97
O2 - C11	1.421(6)	C8 - C9	1.397(15)	H9 - C9	1.00
O2 - C12	1.400(8)	C10 - C11	1.484(09)	H10 - C10	0.99(4)
C1 - C1	1.394(16)	H1 - C1	0.89(5)	H11 - C10	0.98(5)
C1 - C2	1.395(11)	H2 - C2	0.91(10)	H12 - C11	0.93(6)
C2 - C3	1.407(9)	H3 - C3	0.86(6)	H13 - C11	1.02(4)
C3 - C4	1.400(9)	H4 - C4	0.75(7)	H14 - C12	0.98(6)
C4 - C4	1.414(14)	H5 - C5	1.01	H15 - C12	0.96(8)
C5 - C6	1.339(16)	H6 - C6	0.99	H16 - C12	0.95(5)
C6 - C7	1.366(15)	H7 - C7	0.97		

Supplemental Table 3b. C-C, C-O and C-H distances in $(CH_3C_8H_7)U(CH_3C_8H_7)K\cdot(CH_3OCH_2CH_2OCH_2CH_2OCH_3)$

C20 - O1	1.425(15)	C13 - C12	1.317(27)	C20 - H15	0.98
C19 - O1	1.431(16)	C14 - C13	1.49(3)	C20 - H16	0.98
C22 - O2	1.406(13)	C15 - C14	1.39(3)	C21 - H17	0.98
C21 - O2	1.428(14)	C16 - C15	1.339(22)	C21 - H18	0.98
C23 - O3	1.402(17)	C21 - C20	1.496(18)	C22 - H19	0.98
C24 - O3	1.417(16)	C23 - C22	1.513(17)	C22 - H20	0.98
C8 - C1	1.366(20)	C2 - H1	0.98	C23 - H21	0.98
C2 - C1	1.442(19)	C3 - H2	0.98	C23 - H22	0.98
C17 - C1	1.493(18)	C4 - H3	0.98	C17 - H23	0.98
C3 - C2	1.382(18)	C5 - H4	0.98	C17 - H24	0.98
C4 - C3	1.406(21)	C6 - H5	0.98	C17 - H25	0.98
C5 - C4	1.408(22)	C7 - H6	0.98	C18 - H26	0.98
C6 - C5	1.361(22)	C8 - H7	0.98	C18 - H27	0.98
C7 - C6	1.324(22)	C10 - H8	0.98	C18 - H28	0.98
C8 - C7	1.492(23)	C11 - H9	0.98	C19 - H29	0.98
C16 - C9	1.381(21)	C12 - H10	0.98	C19 - H30	0.98
C10 - C9	1.520(22)	C13 - H11	0.98	C19 - H31	0.98
C18 - C9	1.544(22)	C14 - H12	0.98	C24 - H32	0.98
C11 - C10	1.362(22)	C15 - H13	0.98	C24 - H33	0.98
C12 - C11	1.297(24)	C16 - H14	0.98	C24 - H34	0.98

Supplemental Table 4. C-C and C-O angles (•) in

$(C_8H_8)Yb(C_8H_8)K\cdot C_6H_{14}O_3$		$(CH_3C_8H_7)U(CH_3C_8H_7)K\cdot C_6H_{14}O_3$	
C10 - O1 -C10	112.8(6)	C21 - O2 - C22	112.2(9)
C11 - O2 - C12	112.9(5)	C19 - O1 - C20	111.7(10)
		C23 - O3 - C24	111.5(11)
C1 - C1 - C2	135.3(4)	C2 - C1 - C8	130.7(12)
C1 - C2 - C3	135.0(6)	C1 - C2 - C3	137.0(12)
C2 - C3 - C4	134.9(6)	C2 - C3 - C4	135.6(12)
C3 - C4 - C4	134.8(3)	C3 - C4 - C5	133.5(13)
		C4 - C5 - C6	135.3(14)
		C5 - C6 - C7	137.2(14)
		C6 - C7 - C8	134.2(13)
		C1 - C8 - C7	136.3(14)
C6 - C5 - C6	135.6(12)	C10 - C9 - C16	129.7(14)
C5 - C6 - C7	136.6(9)	C9 - C10 - C11	134.0(13)
C6 - C7 - C8	134.1(8)	C10 - C11 - C12	137.6(14)
C7 - C8 - C9	133.1(8)	C11 - C12 - C13	139.1(16)
C8 - C9 - C8	136.6(10)	C12 - C13 - C14	131.9(17)
		C13 - C14 - C15	133.3(15)
		C14 - C15 - C16	137.0(15)
		C9 - C16 - C15	137.4(14)
O1 - C10 - C11	108.7(4)	O2 - C21 - C20	108.7(10)
		O2 - C22 - C23	107.3(9)
O2 - C11 - C10	109.0(5)	O1 - C20 - C21	110.2(11)
		O3 - C23 - C22	109.5(11)
		C2 - C1 - C17	115.9(12)
		C8 - C1 - C17	113.2(14)
		C10 - C9 - C18	113.3(16)
		C16 - C9 - C18	116.7(17)

LAWRENCE BERKELEY LABORATORY
TECHNICAL INFORMATION DEPARTMENT
UNIVERSITY OF CALIFORNIA
BERKELEY, CALIFORNIA 94720